Extreme Events in Pakistan: Physical Processes and Impacts of Changing Climate

Dissertation

with the aim of achieving a doctoral degree
at the Faculty of Mathematics, Informatics and Natural Sciences
Universität Hamburg

submitted by

Maida Zahid

Department of Earth Sciences
Meteorological Institute

Hamburg, 2017

Day of oral defence: 5th December, 2017

The following evaluators recommend the admission of the dissertation:

Prof. Dr. Valerio Lucarini

Prof. Dr. Johanna Baehr

Dedicated To

My Loving Parents

Abstract

The present work mainly aims to assess the returns of major extreme events occurring in southern Pakistan (Sindh province), and the degree of risks associated to them. Furthermore, a web-tool named "SindheX" is developed for the adaptation measures, using the results of this thesis. This thesis devotes special attention to Sindh due its vulnerability to recent extreme events such as heat waves (2015), heavy precipitation/floods (2010, 2011) and cyclones (2007, 2010, 2014). Sindh lacks the information regarding the recurrence of these extreme events. The local administrators, policy makers, and other stakeholders (energy sector, agriculture sector, water management authority, port authorities etc.) in Sindh need this information to plan and implement adaptations accordingly. Considering the urgency of information, three major extremes recently affecting Sindh are identified and selected for the investigation. They include (i) Temperature (air temperature T_{max} and wet-bulb temperature TW_{max}), (ii) Sea Surface Temperature/Cyclones of Arabian Sea (North Indian Ocean) at the Sindh coastline, and (iii) Precipitation. The two most popular methods of the extreme value theory i.e. (1) Block Maxima (BM) and (2) Peaks Over Threshold (POT) are applied to estimate the return levels (RLs) of extremes, since these provide more robust information than ad-hoc approaches on return times of extreme events. Additionally, the Poisson regression is used to predict the probability of cyclonic activity in the Arabian Sea.

The temperature and precipitation extremes are estimated by applying the POT approach for the period 1980 – 2010. The results of temperature extremes of station data indicate RLs of $T_{max} > 50°C$ in Jacobabad, Mohenjo-daro, Padidan, Nawabshah, and $T_{max} > 45°C$ in Rohri, Hyderabad, Chhor, Karachi, Badin in a 5 to 100 year return period. The RLs of TW_{max} exceeds $35°C$ in the entire Sindh, severely impacting the human habitability. The RLs of ERA Interim T_{max} and TW_{max} show a difference of $3°C$ to $5°C$ from a station data, for both shorter and longer return periods. However, a simple bias correction is applied to the ERA Interim data, which shows remarkable improvement in return levels, but some discrepancies remain. The results of precipitation extremes illustrate the RLs > 150 mm/day in Rohri, Nawabshah, Hyderabad, Chhor, Karachi, and Badin and > 100 mm/day in Jacobabad and Mohenjo-daro in a 5 to 100 year return period. The Arabian Sea SST extremes are assessed using the BM method during pre-monsoon (May – June) and post-monsoon (October – November) from 1891 to 2015. The results indicate RLs of SST extremes $> 29°C$ in pre-monsoon and $> 28°C$ in post-monsoon. The probability of occurrence of a cyclonic activity like tropical depression (TD), cyclonic storm (CS), and sever cyclonic storm (SCS) in the Arabian Sea is also predicted with a Poisson regression model using SST and Southern Oscillation Index (SOI) as predictors. The results exhibit that the probability of TD, CS, and SCS in the Arabian Sea is more likely during pre-monsoon rather than post-monsoon. The maps and graphs of this thesis are available on the web–tool SindheX (www.sindhex.org), and can be used by all organizations, public and private stakeholders, who are interested in the return times of extremes in Sindh.

Zusammenfassung

Der Schwerpunkt dieser Arbeit liegt in der Untersuchung der Wiederkehrperioden von Extremereignissen im südlichen Pakistan (Sindh Provinz) und der damit verbundenen Risiken. Zusätzlich wurde basierend auf den Ergebnissen dieser Arbeit ein Web-Tool namens "SindheX" für Anpassungsmaßnahmen entwickelt. Die Studie widmet der Provinz Sindh eine besondere Aufmerksamkeit, aufgrund der Vulnerabilität dieser Region gegen unterschiedliche Arten von Extremereignissen, wie z.B. Hitzewellen (2015), Starkregen/Überflutungen (2010, 2011) und Zyklonen (2007, 2010, 2014). Die lokalen Verwaltungsbehörden, sowie die politischen und andere Entscheidungsträger (Energie-, Agrarsektor, Wasserwirtschaftsverwaltung, Hafenverwaltungen), benötigen diese Informationen für die Planung und Umsetzung von Anpassungsmaßnahmen. Basierend auf der Dringlichkeit der Informationen werden drei Variablen, deren Extremwerte die Provinz Sindh häufig betreffen, identifiziert und untersucht. Diese sind (i) Temperatur (Lufttemperatur T_{max} und Feuchttemperatur TW_{max}), (ii) Meeresoberflächentemperatur/Zyklonen im Arabischen Meer (Nördlicher Indischer Ozean), die Sindh's Küstenlinie treffen, und (iii) Niederschlag. Für die Abschätzung der Wiedekehrintervalle von Extremereignissen werden die zwei wichtigsten Methoden der Extremwerttheorie, (1) die Block Maxima (BM) - und (2) die Peaks Over Threshold (POT) - Methoden angewandt, da diese verlässlichere Informationen liefern als Adhoc- Ansätze. Zusätzlich wird die Wahrscheinlichkeit von Vorkommnissen zyklonaler Aktivitäten im Arabischen Meer durch ein Poissonregessionsmodell vorausgesagt.

Die Temperatur- und Niederschlagsextreme werden mit Hilfe der POT - Methode für den Zeitraum 1980 – 2010 untersucht. Die Messstationsdaten zeigen Wiederkehrwerte von $T_{max} > 50°C$ in Jacobabad, Mohenjo-daro, Padidan, Nawabshah und $T_{max} > 45°C$ in Rohri, Hyderabad, Chhor, Karachi, Badin für Wiedekehrintervalle zwischen 5 und 100 Jahren, während TW_{max} in der ganzen Provinz Sindh 35°C und damit die Grenze der menschlichen Überlebensfähigkeit überschreitet. Die ERA Interim Wiederkehrwerte von T_{max} und TW_{max} deuten auf einen Unterschied von 3°C bis5°C im Vergleich zu Stationsdaten sowohl für kürzere und als auch für längere Wiederkehrperioden. Folglich wird eine einfache Bias-Korrektur auf die ERA Interim Daten angewandt, die eine bemerkenswerte Verbesserung der Wiederkehrdaten bewirkt, obwohl bestimmte Unstimmigkeiten erhalten bleiben. Die Ergebnisse für Niederschlagsextreme zeigen Wiederkehrwerte > 150 mm/Tag in Rohri, Nawabshah, Hyderabad, Chhor, Karachi, und Badin und > 100 mm/-Tag in Jacobabad und Mohenjo-daro fuür Wiedekehrintervalle zwischen 5 und 100 Jahren. Die extremen Meeresoberflächentemperaturen (SST) im Arabischen Meer werden mit Hilfe der Block Maxima Methode im Vormonsun (Mai – Juni) und Nachmonsun (Oktober – November) für den Zeitraum von 1891 bis 2015 untersucht. Die Ergebnisse zeigen die Rückkehr von SST > 29°C im Vormonsun und > 28°C im Post-Monsun. Die Wahrscheinlichkeit von Vorkommnissen zyklonaler Aktivitäten, wie z.B. tropische Depressionen (TD), tropische Stürme (CS), und schwere tropische Stürme (SCS), im Arabischen Meer wird ebenfalls durch ein Poissonregessionsmodell mithilfe vom SST und Süd-Oszillations-Index als Vorhersageindikatoren

vorausgesagt. Die Ergebnisse zeigen höhere Wahrscheinlichkeiten von TD, CS, und
SCS im Arabischen Meer während des Vormonsuns als während des Nachmon-
suns. Die Karten und Abbildungen dieser Arbeit sind kostenlos über dem Web-
Tool "SindheX" (www.sindhex.org) verfügbar und können von all den öffentlichen
und privaten Betroffenen genutzt werden, welche an den Wiederkehrperioden von
Extremereignissen in Sindh interessiert sind.

Contents

Chapter 1

Introduction

1.1 Background and Motivation

Extreme events are now perceived as a major threat to human civilization, and a very intense research activity aims at understanding more accurately the processes and reasons behind these events and climate variability. Researchers are analyzing the socio-economical and environmental impacts related to extremes, and planning suitable strategies for adaptation and mitigation. A great deal of work has been devoted to investigate extreme events (IPCC, 2014), as they can cause massive environmental damages, economic losses and social disruption by overcoming the local coping abilities. Extremes differ in duration, spatial extent, nature of the process, and include events as heat waves, droughts, floods, dry and cold spells, and intense atmospheric motions, i.e. mid-latitude and tropical cyclones. It is of great interest and urgency to investigate that how extremes are going to be impacted by climate change.

This thesis devotes special attention to the southern part of Pakistan (Sindh province) because of the obvious impacts of extreme events (Zahid and Rasul, 2012; Sheridan and Allen, 2015). This region is considered as one of the most vulnerable regions in Pakistan due to the extreme temperature events and high rate of mortality associated to them (Zahid and Rasul, 2010). An example of the potential impact of maximum temperatures is the recent heat wave in Sindh, which occurred between June 17th and June 24th, 2015 and broke all the records with a death toll of 1400 people, and over 14000 people were hospitalized. The temperatures in different cities of the Sindh region were in the range of 45°C – 49°C during the event (Imtiaz and Rehman, 2015). Karachi had the highest number of fatalities (1200 people approximately). The Pakistan Meteorological Department (PMD) issued a technical report stating a very high heat index (measuring the heat stress on humans due to high temperature and relative humidity) during this heat wave (Chaudhry et al., 2015).

In summer, Sindh becomes very hot and with the arrival of a monsoon the humidity increases in the region (Chaudhry and Rasul, 2004). The extremely hot and humid

conditions can have lethal effects, and can impact the human habitability of a region (Pal and Eltahir, 2015). The human body generally maintains the temperature around 37°C. However, the human skin regulates at or below 35°C to release heat (Sherwood and Huber, 2010). Under high levels of the moisture content in the atmosphere, the human body cannot maintain the skin temperature below 35°C and can develop ailments like hyperthermia, heat strokes and cardiovascular problems. Hyperthermia is a condition where an extremely high body temperature is reached, resulting from the inability of the body to get rid of the excess heat. It occurs mostly when temperature and relative humidity levels are extremely high at the same time. Hyperthermia can occur even in the fittest human beings, if exposed to an environment where wet-bulb temperature is greater than 35°C for at least six hours.

Sindh receives precipitation mostly during summer monsoon from June to September, which fulfills the need of water for irrigation. But, Sindh is becoming wetter and experience more intense precipitation events (>100 mm/day) than before during monsoon, which causes urban flooding almost every year (Zahid and Rasul, 2011). Such an extreme precipitation events may significantly reduce the crop yields, and cause huge economic losses to the country Islam et al. (2009); IPCC (2012, 2014). Sindh is affected mostly with urban flooding caused by extreme precipitation, and also with riverine and coastal flooding produced by the tropical cyclones and storm surges in Arabian Sea. (Paulikas and Rahman, 2015). The highest flooding fatalities occur in 2010 alongwith a damage of 3 million houses, 5.3 million acres cropped area, and 20 million people were affected and displaced (Jonkman, 2005; Ahmad, 2011; Provincial Disaster Management Authority - Sindh, 2013).

The intensification of Sea Surface Temperature (SST) in the Arabian Sea is also linked with the extreme rainfall events during the summer monsoon (Shukla, 1975; Izumo et al., 2008; Schott et al., 2009; Levine and Turner, 2012). High SST of the Arabian Sea intensifies the process of convection, initiating the transport of moisture-laden air towards land, and thus increasing the likelihood of extreme precipitation. The changing trends of the Arabian Sea SST are investigated by (Khan et al., 2008; Muhammad et al., 2016). Collectively these studies project a rise of SST > 2°C in the Arabian Sea, contributing to the sea level rise. A climate-shift in the Arabian Sea after 1995 accompanied by an increase in the number of cyclones has been identified by Kumar et al. (2009).

Tropical cyclones and storm surges in the Arabian Sea have also caused a lot of damage in the coastal areas of Sindh, for instance two cyclones Gonu (02A) and Yemyin (03B) developed in the Arabian Sea in June 2007 are the worst storms recorded so far. They affected 2.5 million people and made thousands of people homeless (Tariq and Van de Giesen, 2012). Moreover, they aggravate the problem of saline intrusion inland and in the coastal aquifers, which are already under stress due to over exploitation, changes in the Indus hydrology and water usage, locally and upstream. The coastal communities are at a great risk due to an increase in

frequency and intensity of tropical cyclones in the Arabian Sea (Pelling and Blackburn, 2014). The most populous cities in Sindh are Karachi and Hyderabad are located near the coast and have to bear the brunt of heavy flooding and strong winds during the intense cyclonic activity in the Arabian Sea (Paulikas and Rahman, 2015). Sindh is also prone to other disasters such as sea level rise, droughts, saline water intrusion, coastal erosion, increased crop water requirement, decline in fisheries, changes in biodiversity, and decrease in mangroves forests.

Sindh has great importance due to the port activities, which is the hub of logistics and acts as a bridge for trading with the European and Non-European Union countries. Therefore, the trade and country's economy is at great risk due to the recent climate extremes. Hence, there is a strong need of risk assessment in Sindh to prioritize the regions for adaptations. Moreover, planners and policy makers have several questions regarding the occurrence of extremes in Sindh. They want to know that these extremes will occur every year or is it a one-time event, which areas will be most affected by extremes. Hence, in order to help the planners and to improve the planning and adaptive capacity in Sindh, we have investigated the return levels and return periods of major climatic extremes (temperature, wet-bulb temperature, precipitation, sea surface temperature, and cyclones) in Sindh for the first time, as it is highly relevant to the public and economic interest.

1.2 Study Area

1.2.1 Geography

Sindh stretches from 23.5°N – 28.5°N and 66.5°E – 71.1°E, and is bounded on the west by the Kirthar Mountains, to the north by the Punjab plains, to the east by the Thar Desert and to the south by the Arabian Sea (Indian Ocean) and in the center fertile land around Indus River (Figure 1.1). The Indus River is the source of water for the agriculture lands . Cotton, wheat and sugar cane are grown on the left bank of the Indus and rice, wheat and gram on the right bank (Chaudhry and Rasul, 2004). Cotton is the cash crop of the country.

1.2.2 Climatology

The climate in Sindh is arid and subtropical with less than 250 mm annual rainfall. The temperature frequently exceeds 45°C in summer (May – September) and the minimum average temperature recorded during winter (December – January) is 2°C. Table 1.1 shows the mean monthly climatic characteristics of the region from 1980 – 2010. High population density, limited resources, poor infrastructure and high dependence of the local agriculture on climatic factors, mark this region as highly vulnerable to the impacts of climate change.
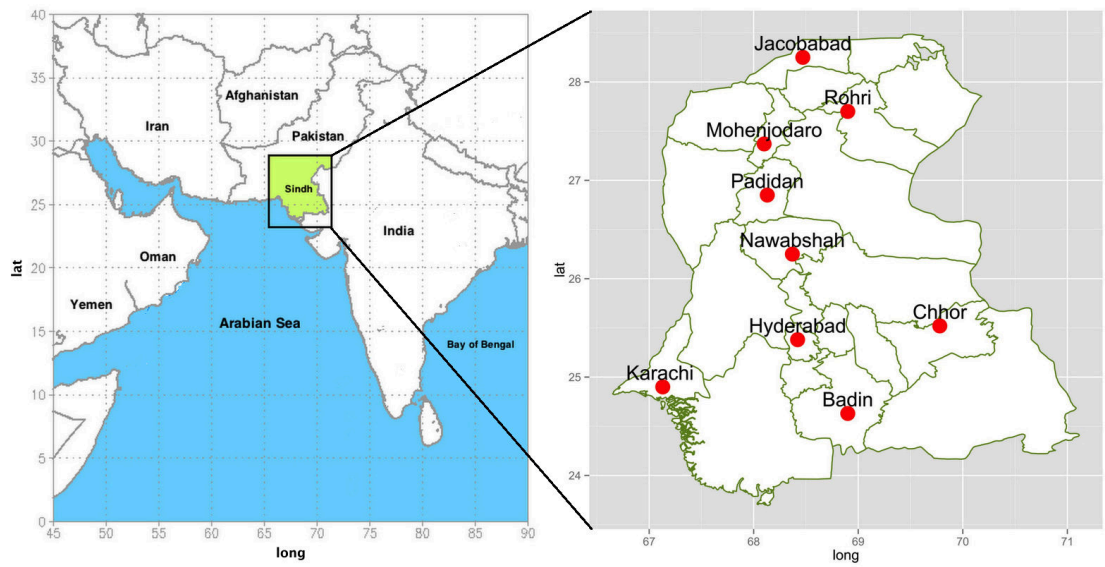
Figure 1.1: Study domain Sindh (23.5°N – 28.5°N , 66.5°N – 71.1°E) in South Asia. The red dots show the areas focused within Sindh.

1.3   Objectives

This thesis belongs to the adaptation services platform of Climate–KIC, European Institute of Technology (EIT). Therefore, its prime focus is to provide information on extremes, which planners need when, e.g., designing infrastructures that are deemed to last a very long time. Lately, three types of devastating extreme events such as heat waves, cyclones, and extreme precipitation/floods are more evident in Sindh, and caused huge economic losses as discussed earlier. It is crucial to know about the return levels and return periods of such events in order to improve planning in Sindh. Therefore, this thesis primarily focus on three variables: (1) Temperature, (2) Sea Surface Temperature/Cyclones in Arabian Sea, and (3) Precipitation. The main objectives of the thesis are listed below.

1. To estimate the return levels of maximum temperature, and maximum wet-bulb temperature extremes in Sindh, Pakistan.

2. To assess the return levels of the sea surface temperature extremes in the Arabian Sea and their link to cyclogenesis.

3. To analyze the return levels of precipitation extremes in Sindh , Pakistan.

4. A web-tool named as "SindheX" (Sindh extremes) is developed, which contains all information of above mentioned extremes in the form of temporal and spatial maps (www.sindex.org).

1.4   Introduction to Extreme Value Theory

Extreme Value Theory (EVT) provides a robust theoretical framework to analyze the extreme events, it was first introduced by Fisher and Tippett (1928). Later, Gnedenko (1943) discovered three types of limiting distributions, based on the shape parameter ξ of the known probability distribution. The three types are called as Gumbel ($\xi = 0$) the exponential tail, Fréchet ($\xi > 0$) the fat tail, and Weibull ($\xi < 0$) the upper bound tail or finite end point. EVT has emerged as an important statistical modeling technique to assess the risks in all disciplines over the last 50 years. The distinguishing feature of the EVT is to quantify the behaviour of the stochastic variable at large or small level. In particular, EVT provides information of the probability of events that are larger than the ones that have already been observed by computing the return times of the unobserved events. EVT represents an increasingly widespread approach in climate studies (Coles, 2001; Zhang et al., 2004; Brown et al., 2008; Faranda et al., 2011; Acero et al., 2014) to estimate the occurrence of the extreme events. EVT comprises two different approaches: [1] Block Maxima, and [2] Peaks over Threshold. The two methods are asymptotically equivalent, although they have different selection procedures and different ways of classifying events as extremes (Pickands, 1975; Lucarini et al., 2016).
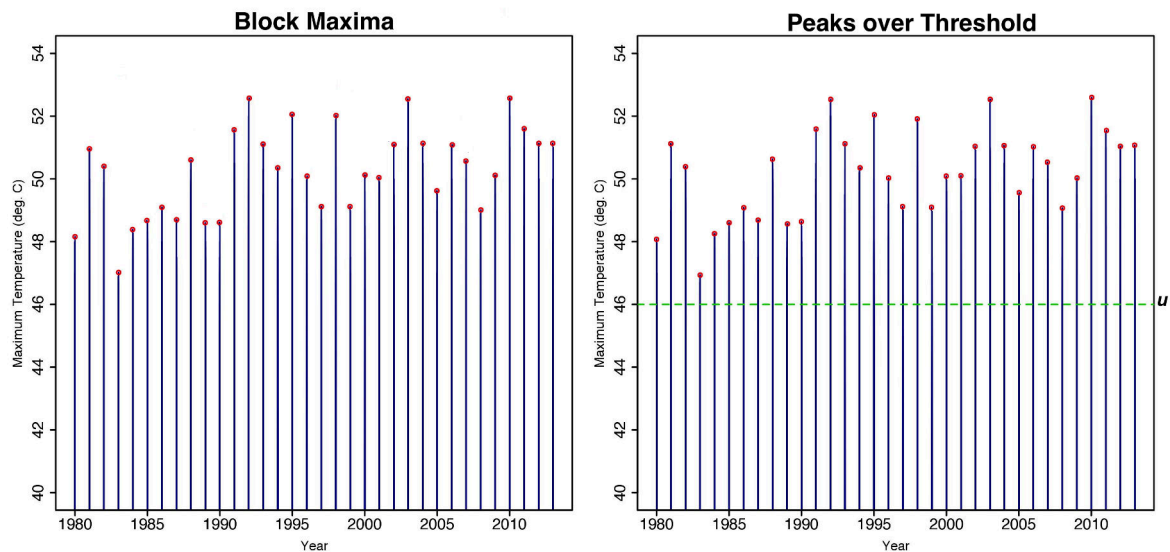
Figure 1.2: Concept of the Block maxima and Peaks over threshold

Block Maxima (BM) determines the statistical properties of extremes in a period (Block), typically daily or annual intervals are used. The data is basically divided into a blocks of size N $\geq$ 1, and the maxima M_n retrieved from each block are independent identically distributed random variable (i.i.d.r). The empirical distribution of the maxima is then fitted according to the best matching type of generalized extreme value distribution (GEV), which is a limiting distribution of BM in most of the cases (Gnedenko, 1943). The GEV fitted data implies the estimation of three

parameters (1) the location parameter μ, (2) scale parameter σ, and (3) the shape parameter ξ,and can be described by the distribution function given by Coles (2001).

$$G(z) = \begin{cases} \exp\left\{-\left[1 + \xi\left(\frac{z-\mu}{\sigma}\right)\right]^{-1/\xi}\right\} & \text{for } \xi \neq 0, \\ \exp\left\{-\exp\left[-\left(\frac{z-\mu}{\sigma}\right)\right]\right\} & \text{for } \xi = 0, \end{cases} \tag{1.1}$$

where $-\infty < \mu < \infty$, $\sigma > 0$, $1 + \xi(z - \mu)/\sigma > 0$ for $\xi \neq 0$ and $-\infty < z < \infty$ for $\xi = 0$.

GEV is a single representation of three types of distributions: Gumbel $\xi = 0$, Fréchet $\xi > 0$, and Weibull $\xi < 0$. In GEV distribution the large block sizes provides a more accurate estimation of the block maxima, with a low bias in parameter estimates. Note that for the dependent data larger block size are better, as dependence in data cause slow convergence to the GEV distribution.

BM is preferable when only the information on block maxima is available like yearly maxima in a long historical records (Kharin et al., 2007), or when the data is not exactly independent and identically distributed (i.i.d.) for example, sea surface temperature, where short range dependence is more likely. The short range dependence may exist within the block, but not between the blocks (Katz et al., 2002). BM is more often used in practice, as it is easier to apply since the blocks appear naturally in many cases according to Naveau et al. (2009). The main drawback of BM is that there might be more than one large extreme events in a single year, corresponding to actual extremes, but in BM only high values from each block is taken discarding the others. Therefore, the BM may not fully capture all extreme events (Lucarini et al., 2016).

Peaks Over Threshold (POT) determines the distribution of the exceedances over a threshold u, which has to be carefully selected. The exceedances are asymptotically distributed according to the Generalized Pareto Distribution (GPD). GPD has remarkable properties of universality when the asymptotic behaviour is considered (Lucarini et al., 2016), while one can expect that the threshold level above which the asymptotic behaviour is achieved depends on the specifics of the analyzed time series. In particular, when looking at spatial fields, it will depend on the geographical location. GPD is characterized by two parameters, the shape ξ, and the scale σ, the distribution function of GPD is given by Coles (2001).

$$H(y) = \begin{cases} 1 - \left(1 + \frac{\xi y}{\tilde{\sigma}}\right)^{-1/\xi} & \text{for } \xi \neq 0, \\ 1 - \exp\left(-\frac{y}{\tilde{\sigma}}\right) & \text{for } \xi = 0, \end{cases} \tag{1.2}$$

where $1 + \xi y/\tilde{\sigma} > 0$ for $\xi \neq 0$, $y > 0$ and $\tilde{\sigma} > 0$.

GPD also represents three types of distribution based on the shape parameter ξ. For a negative shape parameter, $\xi < 0$, the distribution is bounded (Beta distribution), for vanishing shape parameter, $\xi = 0$, the distribution is exponential, and for a positive shape parameter, $\xi > 0$, the distribution has no upper bound (Pareto distribution).

POT provides a more efficient use of data and has better properties of convergence when finite datasets are considered (Coles, 2001), therefore, it is mostly preferred over block maxima method in different disciplines. But, one has to compromise with the setting of a threshold, as in POT the choice of the threshold should be high enough to get the sufficient number of data for fitting with the GPD, and to remain in the asymptotic regime. In such an asymptotic regime the shape parameter ξ does not depend on threshold u, but the scale parameter σ vary with the threshold, thus instead a modified scale ($\sigma* = \sigma - \xi\ u$) is used which does not depend on threshold u. A successful fit can be obtained when the modified scale $\sigma*$, and shape ξ parameters are stable and compatible within the asymptotic regime.

1.5 Thesis outline

This thesis starts with an introductory chapter which gives an overview of the background and motivation, study area, objectives and introduction to extreme value theory approaches used for the analysis. The main part of the thesis is split into four Chapters 2, 3, 4, 5, and each chapter is constructed with its own Introduction, data, methods, results, and conclusions, therefore can be easily read independently from others. First three objectives are achieved in Chapter 2, 3, and 4, while the fourth objective is described in Chapter 5. The conclusion and outlook of this thesis is stated in Chapter 6. Note that repetition of the contents is possible for the clarity. Brief description of each chapter is given as follows.

Chapter 2

This chapter completes the first objective by estimating the return levels of the daily maximum temperature T_{max}, as well as maximum wet-bulb temperature TW_{max} extreme events during summer (May – September) in southern Pakistan. Peaks over threshold (POT) method is adopted, which have not yet been used for similar studies in this region. Two main datasets are analyzed: temperatures observed in nine meteorological stations in southern Pakistan from 1980 to 2013, and the ERA Interim (ECMWF re-analysis) data for the nearest corresponding locations. The analysis provides the 2, 5, 10, 25, 50, and 100 years Return Levels (RLs) of temperature extremes.The RLs of the observed T_{max} are above 50°C in northern stations, and above 45°C in the southern stations. The RLs of the observed TW_{max} exceed 35°C in the region, which is considered as a limit of survivability. The RLs estimated from the ERA Interim data are lower by 3°C to 5°C than the RLs assessed for the nine meteorological stations. A simple bias correction applied to ERA Interim data improves the RLs remarkably, yet discrepancies are still present. The

results have potential implications for the risk assessment of extreme temperatures in Sindh.

Chapter 3

This chapter fulfills the second objective by analyzing the Sea Surface Temperature (SST) extremes in the Arabian Sea, as it is very important for many aspects of the marine climate system and coastal communities. Even the changes of a few degrees in SST can influence large-scale weather phenomena, such as tropical cyclones, El Nino episodes, and south Asian monsoons. Robust warming over the Arabian Sea is evident in recent decades, thereby increasing the risk of frequent cyclonic activity in the pre-monsoon (May – June) and post-monsoon (October – November) periods. Two main data sets used are: SST data of the Hadley Center UK Met office and annual frequency of tropical depressions TD, cyclonic storms CS, and severe CS obtained from the Indian Meteorological Department (IMD), for a period 1891 – 2015. This chapter has two parts; firstly the block maxima approach is applied to the SST dataset in a stationary and non-stationary climate, to investigate the return levels of SST extremes in the Arabian Sea during pre and post monsoon. The results show that the return levels of SST extremes in the pre-monsoon ($>29°$C) are slightly higher than the return levels of the post-monsoon ($>28°$C) for shorter (2, 5, 10, 20) and longer return periods (50, 100, 200). Secondly, a Poisson regression is applied on the IMD dataset to do the probabilistic prediction of TD, CS, and severe CS using SST and SOI as predictors. The results indicate positive correlation between SST and cyclogenesis, and higher probability of the SCS iduring the pre-monsoon period in the Arabian Sea.

Chapter 4

This chapter analyzes the return levels of precipitation extremes in southern Pakistan (Sindh) and achieved the third objective. This region did not receive substantial amount of precipitation earlier, but now experiencing urban flooding due to heavy precipitation almost every year causing loss of life, property, crops and infrastructure. Most of the extreme precipitation occurs during summer monsoon (JJAS). Therefore, daily precipitation data of JJAS measured at nine weather stations of Pakistan Meteorological Department over the period 1980 – 2013 is used. The POT approach is applied to compute the return levels (RLs) of precipitation extremes, and to identify the regions most prone to them. The results show higher probability of the precipitation events >100 mm/day and >150 mm/day in 5 to 50 years return period in Rohri, Nawabshah, Hyderabad, Chhor, Karachi, and Badin.

Chapter 5

This chapter completes the last objective of this thesis by introducing SindheX, a freely available web-tool (www.sindhex.org). It contains all the temporal and spatial maps of the return levels analyzed in this thesis. The text used in the website is taken from the thesis.

Table 1.1: Monthly mean climatic characteristics of Sindh from 1980-2013

Stations	Mean Temperature (°C)												
	Jan	Feb	Mar	Apr	May	Jun	Jul	Aug	Sep	Oct	Nov	Dec	Annual
Jacobabad	15.2	18.2	24	30.5	35.6	37	34.8	33	31.4	27.8	22.3	16.7	27
Mohenjo-daro	13.9	16.7	23	29.1	34.1	35	33.9	32.9	30.9	26.7	21.1	15.9	25.9
Rohri	15.6	18.2	23.6	29.8	34.5	35.6	33.9	32.3	31.2	27.6	22.1	16.9	26.4
Padidan	14.8	17.7	23.5	29.9	34.4	35.5	33.7	32.1	31	27.5	22.4	16.4	26.5
Nawabshah	15.4	18	24	29.8	34.5	35.6	34	32.3	31.5	28	22.4	16.9	26.7
Hyderabad	18	21	26.2	30.9	33.3	34	32.4	31.1	31	29.6	24.8	19.6	27.6
Chhor	16.5	19.5	25	30.1	33.5	33.7	31.6	30.1	30.1	28.2	22.6	17.9	26.3
Karachi	18.6	21.2	25.4	28.9	31.1	31.9	30.5	29.2	29.5	28.9	24.6	20.4	26.4
Badin	17.5	20.5	25.8	30.1	32.6	32.8	31	29.6	29.6	28.7	24	19	26.6

Stations	Minimum Temperature (°C)												
	Jan	Feb	Mar	Apr	May	Jun	Jul	Aug	Sep	Oct	Nov	Dec	Annual
Jacobabad	7.9	10.9	16.6	22.4	27.4	29.8	29.3	28.4	26.3	20.5	14.3	8.9	19.9
Mohenjo-daro	4.7	7.9	13.3	18.9	24	27.4	27.9	27	24.7	18.2	11.8	7.3	17.3
Rohri	8.3	10.8	15.9	21.7	26.1	27.7	27.1	26	24.4	19.9	14.2	9.6	18.7
Padidan	6.5	8.9	14.5	20.2	24.7	27	26.9	25.8	23.7	18.3	12.4	7.6	17.8
Nawabshah	6.3	8.7	14.2	19.4	24.6	27.3	27.2	25.9	23.8	18.4	12.4	7.8	17.9
Hyderabad	11.4	13.9	18.8	22.8	26.1	27.9	27.6	26.5	25.4	22.5	17.4	13	21.1
Chhor	5.9	8.9	14.8	20.3	24.8	26.9	26.5	25.3	23.9	18.7	11.8	7	17.6
Karachi	11.5	14	18.6	23	26.6	28.3	27.6	26.3	25.6	21.9	16.8	12.7	20.7
Badin	9.9	12.6	17.9	22.3	25.7	27.6	27.1	26	25	22.1	16.5	11.4	20.2

Stations	Maximum Temperature (°C)												
	Jan	Feb	Mar	Apr	May	Jun	Jul	Aug	Sep	Oct	Nov	Dec	Annual
Jacobabad	22.6	25.6	31.4	38.6	43.9	44.4	40.2	37.6	36.8	35.1	30.3	24.4	34.1
Mohenjo-daro	23.1	26.2	32.1	38.7	43.8	44.2	40.9	38.7	37.5	35.2	30.5	24.8	34.5
Rohri	22.6	25.6	31.2	38.1	43	43.5	40.5	38.3	37.8	35.2	30	24.3	34
Padidan	23.1	26.4	32.2	39.4	43.9	44.1	40.6	38.4	38.3	36.3	31.1	25.3	34.8
Nawabshah	24.5	27.9	33.8	40.2	44.2	43.9	40.7	38.8	39	37.7	32.3	26.1	35.5
Hyderabad	24.7	28.1	33.7	38.8	41.3	40	37.2	35.6	36.3	36.7	31.9	26.2	34.1
Chhor	26.9	29.9	35.2	40	42	40.6	36.8	34.9	36.3	37.6	33.5	28.7	35
Karachi	26.3	28.4	32.2	34.7	35.5	35.4	33.3	32.1	33.2	35.5	32.5	28.2	32
Badin	25.2	28.3	33.7	37.8	39.4	37.9	34.9	33.2	34.2	35.2	31.4	26.5	32.9

Stations	Mean Precipitation (mm)												
	Jan	Feb	Mar	Apr	May	Jun	Jul	Aug	Sep	Oct	Nov	Dec	Annual
Jacobabad	3.1	7.3	12	2.7	3.5	3.2	39	35.6	5.3	1.7	0.8	8.3	120.4
Mohenjo-daro	2.6	5.8	3.4	2.9	2.2	2.5	39.9	26.6	6.6	0.4	0.9	6.3	97.1
Rohri	4.1	5.5	6.1	4.9	4.3	6.4	39.7	24.8	3	2.5	0.2	4.1	106.5
Padidan	2.9	4.3	4.4	2.1	1.3	4.2	41.8	40.9	5.4	0.7	0.3	5.5	114.7
Nawabshah	2.5	3.3	3.5	2.8	1.5	5	58.3	48.8	16.1	3.4	0.4	3.2	153.7
Hyderabad	1.4	6.8	4.2	7	2.8	4.4	47.9	71.8	13	5.4	2.2	2.1	169.9
Chhor	0.8	4.1	1.8	2.3	5.8	16.3	82.2	81.8	39.8	9	2.2	1.2	247.6
Karachi	8.4	7.4	5.3	3	0.1	10.8	60	60.9	11	2.6	0.4	4.8	176
Badin	1.2	6.6	0.4	1.7	6.2	9.6	79.5	85.9	24.8	9.3	2.4	0.5	228.5

Stations	Rainy days (mm)												
	Jan	Feb	Mar	Apr	May	Jun	Jul	Aug	Sep	Oct	Nov	Dec	Annual
Jacobabad	0.5	1	1.2	0.7	0.9	0.5	2	1.2	0.3	0.1	0	0.3	8.6
Mohenjo-daro	0.2	0.5	0.9	0.2	0.3	0.4	1.9	1.4	0.3	0.1	0.1	0.3	6.6
Rohri	0.4	0.6	0.5	0.4	0.2	0.5	1.5	0.6	0.2	0.1	0	0.3	5.3
Padidan	0.2	0.6	0.6	0.2	0.4	0.4	2.2	1.9	0.3	0.2	0	0.3	7.3
Nawabshah	0.1	0.3	0.1	0.3	0.4	0.3	1.5	1.4	0.6	0.1	0	0.2	5.3
Hyderabad	0.3	0.7	0.4	0.6	0.4	0.6	2.1	2.2	0.6	0.3	0.2	0.3	8.6
Chhor	0.1	0.3	0.2	0.4	0.3	1	3	3.2	1.2	0.4	0.2	0.2	10.3
Karachi	0.7	0.8	0.7	0.2	0.1	0.9	3.6	3.3	0.7	0.3	0.1	0.7	12
Badin	0.3	0.3	0	0.4	0.1	0.8	2.4	2.4	0.7	0.3	0.2	0.1	7.8

Chapter 2

Return levels of temperature extremes in southern Pakistan

2.1 Introduction

Extreme maximum temperature events have received much attention in recent years, because of the associated dangerous impact on the increased risk of mortality. Additionally, climate change scenarios suggest that in most regions the probability of occurrence of extremely high temperature is very likely to increase in the future (Sheridan and Allen, 2015). The Intergovernmental Panel on Climate Change (IPCC) scenarios estimates an increase in the surface temperature of the order of 4°C by the end of 2100 in Sindh, Pakistan. This may significantly reduce crop yields, and cause huge economic losses to the country(Islam et al., 2009; Rasul et al., 2012; IPCC, 2012, 2014). Furthermore, it might increase the risks of heat strokes, cardiac arrest, high fever, diarrhea, cholera and vector borne diseases. Lately, deadly heat waves and extremely high heat index (combination of high temperature and high humidity) have become more common in southern Pakistan (Zahid and Rasul, 2010). The enhanced mortality rate related to the heat waves is a serious problem, and two obvious examples are the 1991 and the 2015 heat waves (Imtiaz and Rehman, 2015).

The analysis of extreme climatic events is a very active area of research in geoscience(Christidis et al., 2005, 2010; Tebaldi et al., 2006; Morak et al., 2011, 2013). Extreme value theory (EVT) represents an increasingly widespread approach in climate studies (Coles, 2001; Zhang et al., 2004; Brown et al., 2008; Faranda et al., 2011; Acero et al., 2014) to estimate the occurrence of the extreme events. The peaks over threshold (POT) approach determines the distribution of the exceedances above a threshold. The exceedances are asymptotically distributed according to the Generalized Pareto Distribution (GPD). GPD has remarkable properties of universality when the asymptotic behavior is considered (Lucarini et al., 2016), while one can expect that the threshold level above which the asymptotic behavior is achieved depends on the specifics of the analyzed time series. In particular, when looking at spatial fields, it will depend on the geographical location.

In this chapter, we have chosen to analyze the temperature extremes in the Sindh region taking the point of view of threshold exceedances associated to the GPD family of distributions, because the statistical inference provided by the POT method provides a more efficient use of data and has better properties of convergence when finite datasets are considered with respect to alternative methods for the analysis of extremes, such as the block maxima method, which is used to fit the observed data to the generalized extreme value (GEV) distribution (Lucarini et al., 2016). Additionally, we are here interested in investigating the actual tails of the distributions and not the statistics of e.g. yearly maxima, the POT approach is indeed more appropriate. While the POT method has been applied for studying temperature extremes in different regions of the world (Burgueño et al., 2002; Nogaj et al., 2006; Coelho et al., 2007; Ghil et al., 2011) to our knowledge, it has never been used to analyze the statistics of temperature extremes in Sindh. Thanks to the properties of universality of the GPD distribution, the POT approach can in principle provide reliable estimates of return periods and the return levels also for time ranges longer than what is actually observed (Lucarini et al., 2016). This information and this predictive power can be beneficial for policy makers and other stakeholders. Since, it is exactly the kind of information planners need when, e.g., designing infrastructures that are deemed to last a very long time. Note that commonly used, more empirical approaches to the study of extremes, as those more used for assessing the "moderate extremes" (IPCC, 2012), do not have any property of universality and might have weak predictive power.

It is useful to consider two indicators of extremely hot conditions: (1) temperature extremes T_{max}, and (2) Wet-bulb temperature extremes TW_{max}. Therefore, we estimate the return levels of T_{max} and TW_{max} over different return periods during summer (May-September) in Sindh. We apply the POT method on the observational data of the nine weather stations provided by Pakistan Meteorological Department, and the ERA Interim re-analysis data of European Center for Medium range Weather Forecast (ECMWF) model for the corresponding grid points from 1980 to 2013. ERA Interim re-analysis data are generally very good at replicating also trends in temperature percentile (Cornes and Jones, 2013). Nonetheless, it is in principle not obvious that ERA Interim data can simulate well meteorological extremes, as reanalysis are constructed in such a way that typical conditions are well reproduced. This is why we look at how well ERA Interim data performs in the target area against observations. If the ERA Interim dataset characterizes well the extremes, it could be an option for the regions within Sindh where no observational data is available. Furthermore, a standard bias correction is applied on the ERA Interim data to assess whether removing the bias in the bulk of the statistics improves substantially representation of the return levels of extremes. Given the shortness of the datasets, as we will show later, it is appropriate to analyze the extremes without taking into considerations possible long-term trends (Frei and Schär, 2001); see also the discussion in Felici et al. (2007). The provision of POT-based information on stationary extremes is already quite relevant in terms of impacts for the public and private sector as it fills a big data gap in Sindh. A possibility for investigating time dependency in the temperature extremes comes for considering

the centennial NCEP reanalysis (Compo et al., 2011) and using suitable bias correction procedures. Such an analysis is not performed at this stage as we focus on observational data.

2.2 Data and Methodology

2.2.1 Meteorological Station Data

The daily maximum temperature and relative humidity data recorded at nine meteorological stations in Sindh from 1980 to 2013 are provided by the Pakistan Meteorological Department (see Table 2.1). We select nine stations, which contain a negligible amount of missing values after 1980, and are suitable for the POT analysis (Figure 2.1). An additional criterion is that only those stations are chosen where no changes occurred in measuring instruments during the last 33 years (Brunetti et al., 2006). None of the station data shows gaps with duration longer than two days, which are treated by replacing the missing value with the average of the two previous values.

Table 2.1: Code, name, geographic coordinates and altitude of the stations.

Code	Name	PMD weather stations			ERA-Interim stations	
		Latitude	Longitude	Altitude (m)	Latitude	Longitude
JCB	Jacobabad	28°18′N	68° 28′E	55	28°4′N	68° 15′E
MJD	Mohenjo-daro	27°22′N	68° 06′E	52.1	27°5′N	67° 75′E
RHI	Rohri	27° 40′N	68° 54′E	66	27°75′N	69 °25′E
PDN	Padidan	26° 51′N	68° 08′E	46	26°8′N	68 °5′E
NWB	Nawabshah	26° 15′N	68° 22′E	37	26°25′N	68° 0′E
HYD	Hyderabad	25° 23′N	68° 25′E	40	25°5 ′N	68° 15′E
CHR	Chhor	29° 31′N	69° 47′E	5	25°3′N	69°6′E
KHI	Karachi	24° 54′N	67°08′ E	21	25°2′N	67°5′E
BDN	Badin	24° 38′N	68° 54′E	10	24°75′N	68°65 ′E

The temperature data are discretized unevenly with intervals up to 1 degree Celsius. Deidda and Puliga (2006) proposed a Monte Carlo approach for addressing this issue. They showed that finite resolution in precipitation data affects the convergence of parameter estimation in the extreme value analysis. They suggested generating many synthetic datasets by adding numerical noise to the original data, and then providing the best estimate of the parameters of the extreme value distributions by averaging over all the best fits obtained in each synthetic dataset. Following their
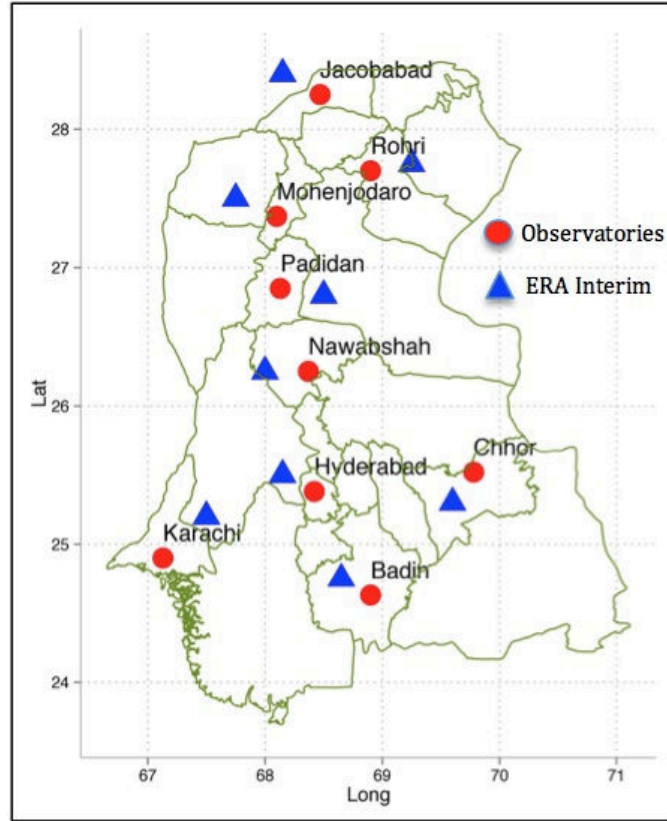
Figure 2.1: Study Domain ($23.5 - 28.5°$ N , $66.5 - 71.1°$E)

suggestion, we produce high-resolution data to compensate the effect of discretization and thus to improve the convergence of the estimator. In order to convert the temperature readings to higher resolution, we add a uniform random variable in the interval $[-0.5, 0.5]$. The main property of this noise is that $round\,(T + r) = T$, where T is the temperature with 1-degree resolution and '$round$' is the numerical function, which maps the interval $[T - 0.5, T + 0.5]$ to T. Thus, adding the noise does not perturb the information content of the observations. This procedure is applied to all temperature data, irrespective of the actual resolution, and replicated 100 times using a Monte Carlo approach. For each synthetic dataset, we perform the statistical best fit described later in the paper and then average the results. We check the influence of this noise parameterization and find no significant bias in the return level estimates. The advantage of adding a noise is to avoid the spurious statistical effects associated to the presence discrete values assigned to the temperature readings. Using the described bootstrap method we reduce such problem without biasing the data.

2.2.2   ERA Interim Reanalysis Data

The gridded daily maximum temperature and relative humidity data of ERA Interim re-analysis is obtained from the ECMWF Public Datasets web interface

(http://apps.ecmwf.int/datasets/). The ERA Interim is generated by the European Center for Medium range Weather Forecast (ECMWF) model with resolution $0.75° \times 0.75°$ (Dee et al., 2011). The gridded data are then extracted at the closest grid points of all stations, for the period 1980 – 2013 (Figure 2.1). The latitude and longitude of the ERA Interim stations are displayed in Table 2.1.

The extreme temperatures analysis is restricted to the summer season (May – September) over a period of 33 years. We have tested the datasets by applying the Mann-Kendall test; the results show that trends are not significant in such a short time interval. One of the main requirements for performing the POT analysis is assuming the stationarity of the time series. Therefore, as in Bramati et al. (2014), the Augmented Dickey Fuller (ADF) test of stationarity is performed on all time series (Dickey and Fuller, 1979). In all cases we find no sign of long-term correlations in the data. Short-term correlations (daily time scale) typically lead to clusters of extreme values and are studied by computing the extremal index θ in all time series and treated using the associated standard declustering technique (see more details in Section 2.2.4).

2.2.3   Wet–bulb Temperature Calculations

The wet–bulb temperature measures the heat stress better than other existing heat indices, because it establishes the clear thermodynamic limit on heat transfer that cannot be overcome by adaptations like clothing, activity and acclimatization (Pal and Eltahir, 2015; Sherwood and Huber, 2010). Here, we use an empirical equation developed by Stull (2011) to measure the wet–bulb temperature [°C].

$$TW = T\operatorname{atan}(\alpha_1\sqrt{RH} + \alpha_2) + \operatorname{atan}(T + RH) -$$
$$\operatorname{atan}(RH + \alpha_3) + \alpha_4(RH)^{\frac{3}{2}}\operatorname{atan}(\alpha_5 RH) - \alpha_6 \tag{2.1}$$

where TW is the wet–bulb temperature [°C], T is the temperature [°C], and RH is the relative humidity [%]. This relationship is based on an empirical fit, as in Stull (2011), where the coefficient values are $\alpha_1 = 0.151977$, $\alpha_2 = 8.313659$, $\alpha_3 =$ -1.676331, $\alpha_4 = 0.00391838$, $\alpha_5 = 0.023101$, and $\alpha_6 = 4.686035$. The Eq. 2.1 covers a wide range of relative humidity and air temperatures with an accuracy of 0.3°C.

2.2.4   Peaks over Threshold

In order to determine the return levels of extreme maximum temperatures and maximum wet-bulb temperatures, the peaks over threshold (POT) approach is applied to the data obtained from the meteorological stations in Sindh, and from the ERA Interim archive. Multi-occurrence is an important characteristic of extreme climatic events and is referred to as clustering. Clusters are consecutive occurrences

of above threshold events. It is important to post process the clustered extremes in order to take into account the assumption of weak short time correlation between extreme events, which is crucial for our statistical analysis. We have treated the clusters using the concept of Extremal Index (EI) (see Loynes (1965); O'Brien (1974); Leadbetter (1983); Davison and Smith (1990)). The Extremal Index θ measures the degree of clustering of extremes. It ranges between 0 and 1, ($\theta = 0$ means strong clustering and dependence, $\theta = 1$ absence of clusters and independence). Leadbetter (1983) interprets $1/\theta$ as the mean number of exceedances in a cluster.

The extremal index θ can be estimated in two different ways. Here, we apply the intervals estimator automatic declustering by Ferro and Segers (2003). A positive aspect of this method is that it avoids the subjective choice of cluster parameters. The main ingredient is the use of an asymptotic result for the times between threshold exceedances. The exceedance times are split into two types, a set of vanishing intra-exceedance times within the clusters, and an exponentially distributed set of inter-exceedance times between clusters. The method is iterative, starting with largest return times and stops when a limit for the inter-exceedance times is reached. The standard errors of the estimated parameters is obtained by a bootstrap procedure. In this study, once we select appropriate value for the threshold (see below) the extremal index θ value is $\leqslant 0.5$ in all the considered time series. Therefore, it is necessary to decluster the extremes by choosing the largest event in each cluster, before fitting it to the GPD.

As mentioned before, we use as statistical model for the exceedances over threshold the Generalized Pareto Distribution (GPD), which is characterized by two parameters, the shape ξ and the scale σ. The GPD for exceedances $x - u$ of a random variable x reads as

$$G(x) = 1 - [1 + \xi(\frac{x - u}{\sigma})]^{-1/\xi} \qquad (x > u, \xi \neq 0) \qquad (2.2)$$

where u is the threshold. The shape parameter ξ determines the tail behavior while the scale parameter σ measures the variability. For a negative shape parameter, $\xi < 0$, the distribution is bounded (Weibull distribution), for vanishing shape parameter, $\xi = 0$, the distribution is exponential, and for a positive shape parameter, $\xi > 0$, the distribution has no upper bound (Pareto distribution).

In particular, for a negative shape parameters $\xi < 0$ the GPD has an upper bound

$$A_{max} = u - \frac{\sigma}{\xi} \qquad\qquad (2.3)$$

$$G(x) = 0 \qquad (x > A_{max}, \xi < 0)$$

where A_{max} is an absolute maximum (Lucarini et al., 2014). In general, the best estimate for the two parameters shape ξ and scale σ depend on the threshold u (Coles, 2001). The choice of the optimal threshold for performing statistical inference from a time series is crucial. Choosing a very large value for u reduces the number of exceedances to a few values, inflating the variance of the estimators, so that the analysis is unlikely to yield any useful results. On the other hand, choosing a too small value for u would violate the asymptotic nature of the model, with a possible biased estimation and wrong model selection (Coles, 2001), see details later in Section 2.3.1. The shape ξ, the scale σ and the return levels are estimated using the Maximum Likelihood Estimator (MLE) using the R software (R Development core team 2015), which also provides an estimate of the standard error of the estimates.

Additionally, we wish to investigate the N - years return levels x_N, which are exceeded on the time scale of N years (Coles, 2001) and can be expressed as

$$x_N = u + \frac{\sigma}{\xi}[(Nn_y\zeta_u)^\xi - 1] \tag{2.4}$$

where N represents the return period, n_y is the number of observations per year , ζ_u is the probability of an individual observation exceeding the threshold u, the shape parameter is ξ and the scale parameter is σ.

2.2.5   Bias Correction Method

A simple bias correction is applied to each ERA Interim time series through a rescaling that adjust the first two moments (mean and variance) to the sample moments calculated on the corresponding observations (Acharya et al., 2013). Therefore, the bias correction is applied to the entire time series and it is not tailored to the extreme events only. The idea is to check whether by adjusting the properties of the bulk of the statistics we improve the skill of the ERA Interim dataset considerably in describing extreme events. The bias corrected ERA Interim time series x is

$$x = \bar{z} + \frac{y_{ERA} - \bar{y}}{\sigma_y}.\sigma_z \tag{2.5}$$

where y_{ERA} is the ERA Interim time series, $\bar{y}$ and σ_y its mean and standard deviation, whereas $\bar{z}$ and σ_z are the mean and standard deviation of the meteorological station temperatures. The properties of extremes are commonly assumed to be closely controlled by the first two moments of the underlying distribution e.g. the IPCC (2012) relates changes in the properties of extremes to changes in the mean

and in the standard deviation of the underlying distributions - EVT clarifies that, in fact, only a loose link exists between true extremes and the bulk of the events. Note that the proposed method of bias corrections has no impact on the estimates of the shape parameter, while it affects the scale and location parameters, thus impacting at any rate the return levels.

2.3   Results and Discussion

2.3.1   Threshold Selection

The threshold selection is the first step in a POT analysis. One needs to test whether the asymptotic regime is reached, i.e. whether we are choosing true extremes. It must be noted that EVT does not predict where (in terms of quantiles) one should expect the asymptotic regime to start. This can be investigated by checking whether the best fits of the shape parameter ξ and the modified scale parameter $\sigma^* = \sigma_u - \xi u$ are stable with respect to increases in the chosen value of u (Scarrott and Macdonald, 2012). The optimal threshold u is selected as the lowest value where the two parameters are invariant in order to reach the asymptotic limit (Coles, 2001; Furrer et al., 2010).
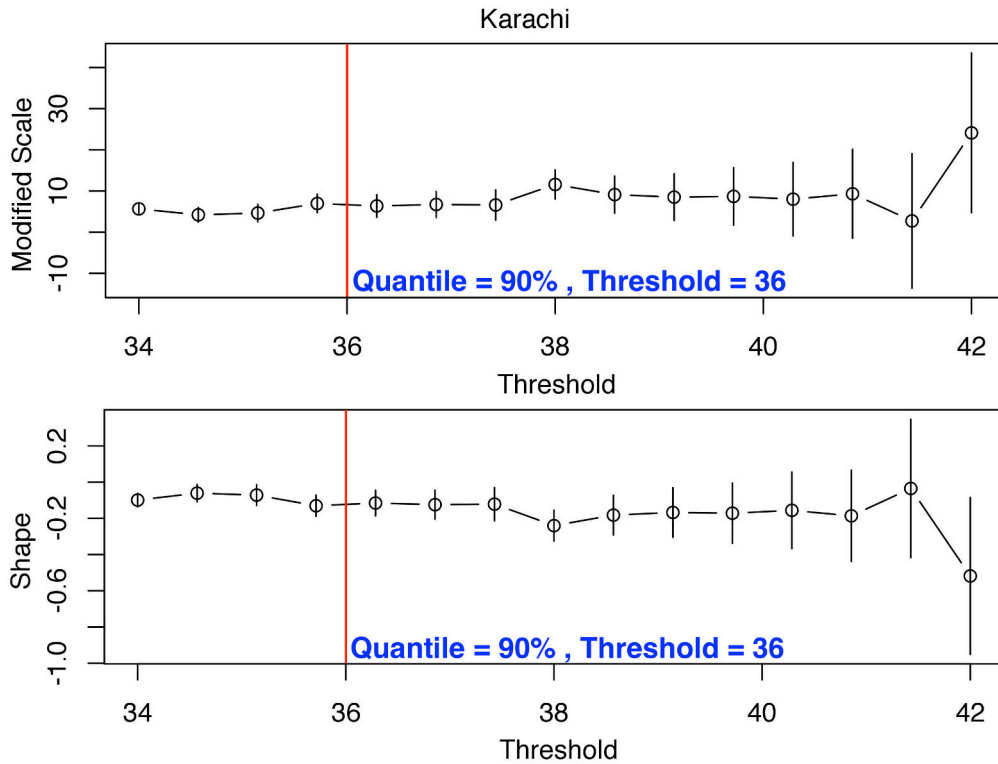
Figure 2.2: Modified scale (σ^*) and shape parameter (ξ) of the observed T_{max} Karachi. The red vertical lines represent the selected threshold according to the station quantiles.

This choice allows for having as many data as possible for performing the statistical inference, thus having lower variance for the estimators of the parameters. Figure 2.2 shows the parameter stability plots of the T_{max} reading for Karachi, as an example to explain the threshold selection procedure.
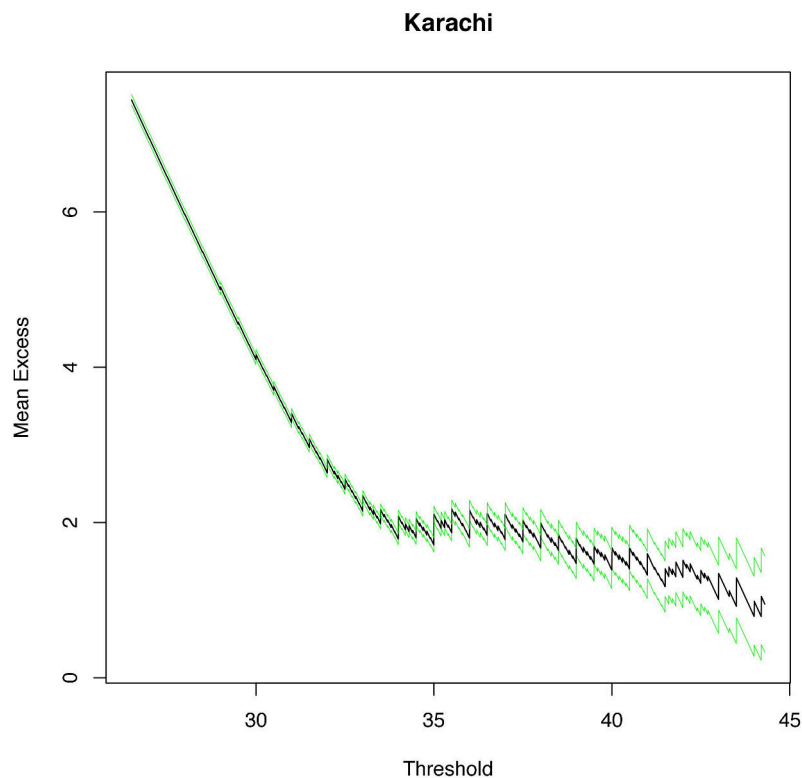
Karachi

Figure 2.3: Mean residual life plot of the station observed T_{max} Karachi.

In addition to diagnostic plots of the modified scale parameter σ^* and the shape parameter ξ, the mean residual life plot is used to select the appropriate threshold for the POT analysis (Davison and Smith, 1990). The idea is to select the lowest value of the threshold when the plot is approximately linear, and the parameters (ξ, σ^*) are stable. In the case of the Karachi, data for T_{max}, the plot appears to be linear and stable for u $= 36°$C, indicating $u = 36$ as the most suitable threshold for the POT analysis (Figure 2.3). We observe that the 90% quantile is an appropriate threshold for all the station data, as well as the ERA Interim datasets, and for both T_{max} and TW_{max}.

2.3.2 GPD Fit

The goodness of fit is evaluated by Quantile-Quantile (Q-Q) plots and hypothesis testing. The Q-Q plot analysis is performed for the stations observed, the ERA Interim, the bias corrected ERA Interim daily T_{max} and TW_{max}. The Q-Q plots of the

observed T_{max} show that the GPD fits well in most stations (Figure 2.4). However, in a few stations like Jacobabad, Mohenjo-daro, Padidan, and Chhor the empirical values show slight deviation from the modeled values. In spite of minor deviations at some stations, still most of the exceedances are well fitted by the model. The Q-Q plots of the observed TW_{max} also fits well to the model in all stations (Figure 2.7).
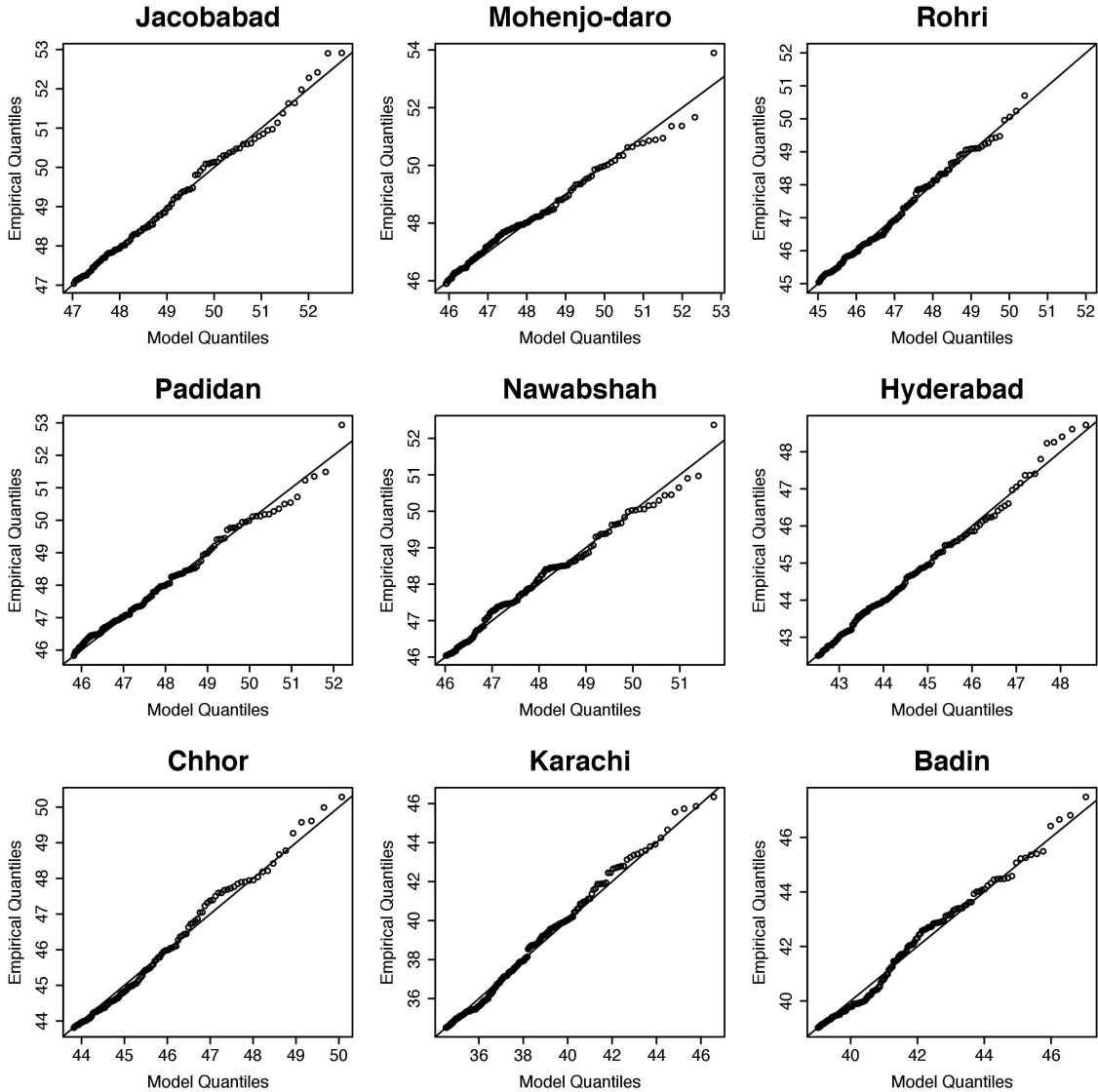

Figure 2.4: Quantile-Quantile plots of station observed T_{max} (°C), u= 90% for 9 stations of southern Pakistan (Sindh).

The Q-Q plots of the empirical ERA Interim T_{max} and TW_{max} data reveals substantial differences corresponding to the GPD (Figure 2.5 and 2.8). The empirical values of the higher quantiles are deviating from the theoretical quantiles in all

stations. However, if the higher quantiles are disregarded, then stations like Jacobabad, Mohenjo-daro, Rohri, Padidan, Nawabshah, Chhor, and Badin fits very well with the model. The Q-Q plots of the bias corrected ERA Interim T_{max}, and TW_{max} show better results than the ERA Interim (Figure 2.6 and 2.9). We notice that the T_{max} of the ERA Interim and bias corrected ERA Interim fits better than the TW_{max} if the higher quantiles are ignored, indicating the bias procedure is, as expected, unable to treat correctly the statistics of the largest events.
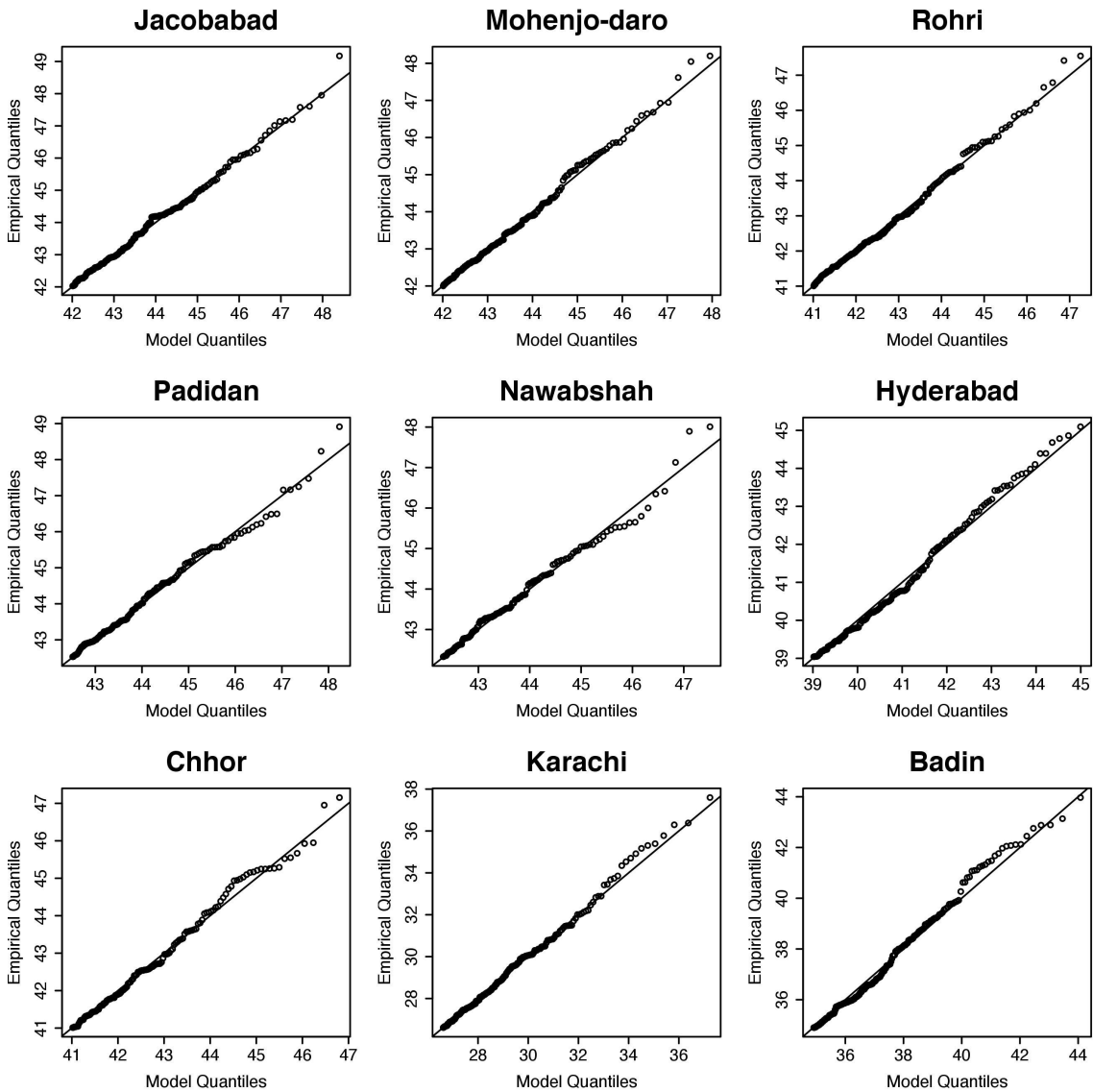
Figure 2.5: Quantile-Quantile plots of station ERA Interim T_{max} (°C), u= 90% for 9 stations of southern Pakistan (Sindh).
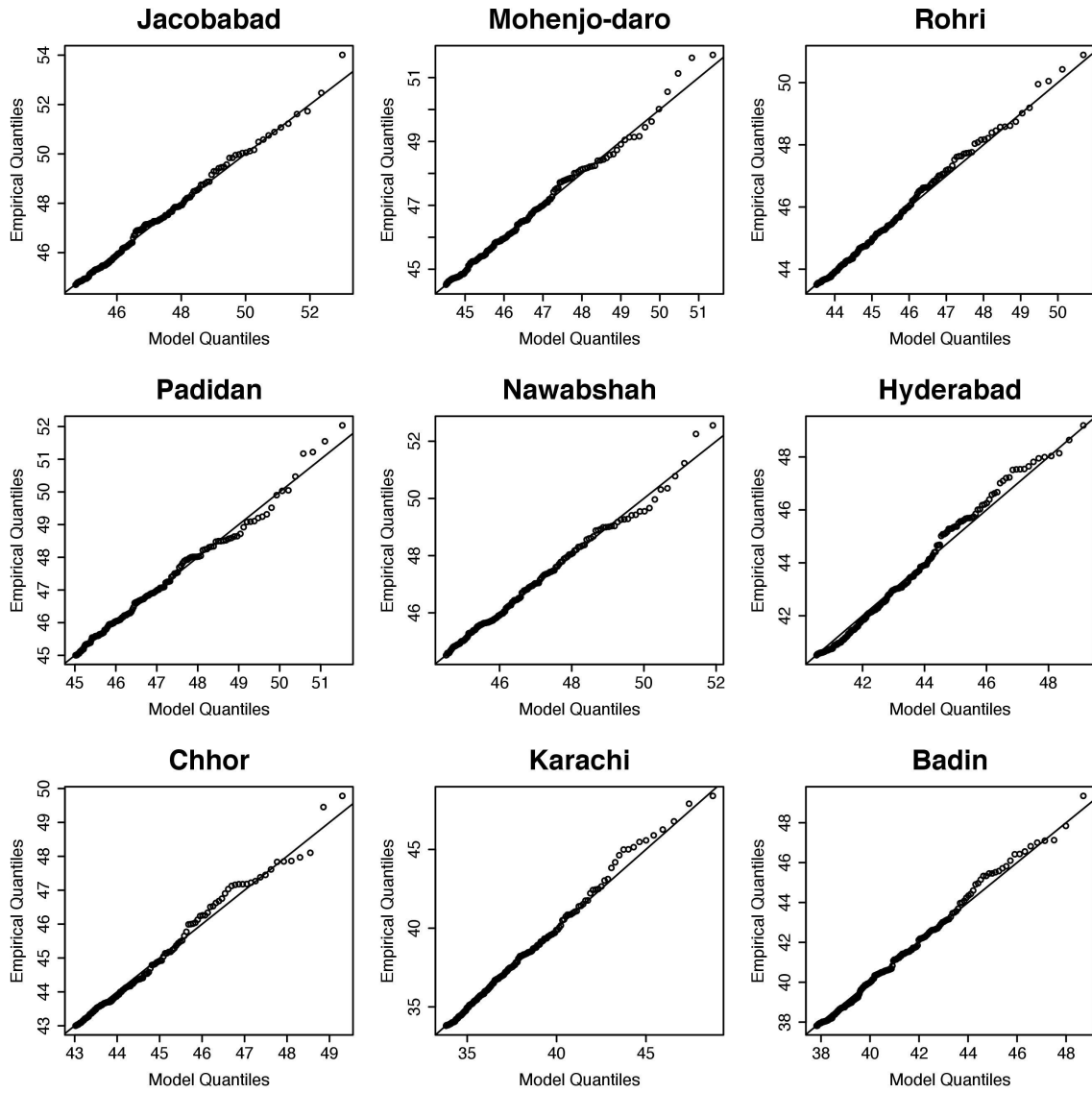
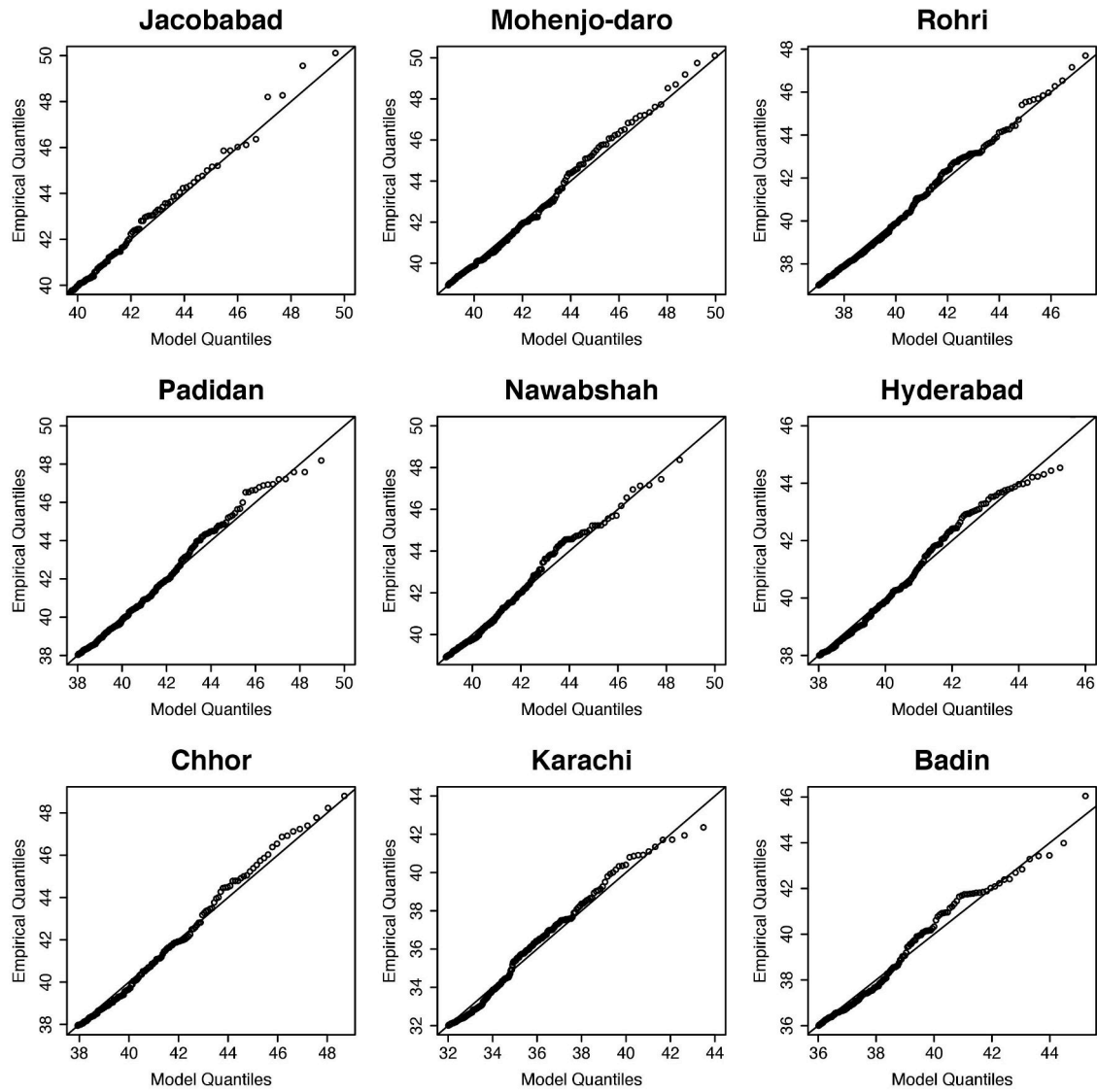Figure 2.6: Quantile-Quantile plots of station bias corrected ERA Interim T_{max} (°C), u= 90% for 9 stations of southern Pakistan (Sindh).

Figure 2.7: Quantile-Quantile plots of station observed TW_{max} (°C), u= 90% for 9 stations of southern Pakistan (Sindh).
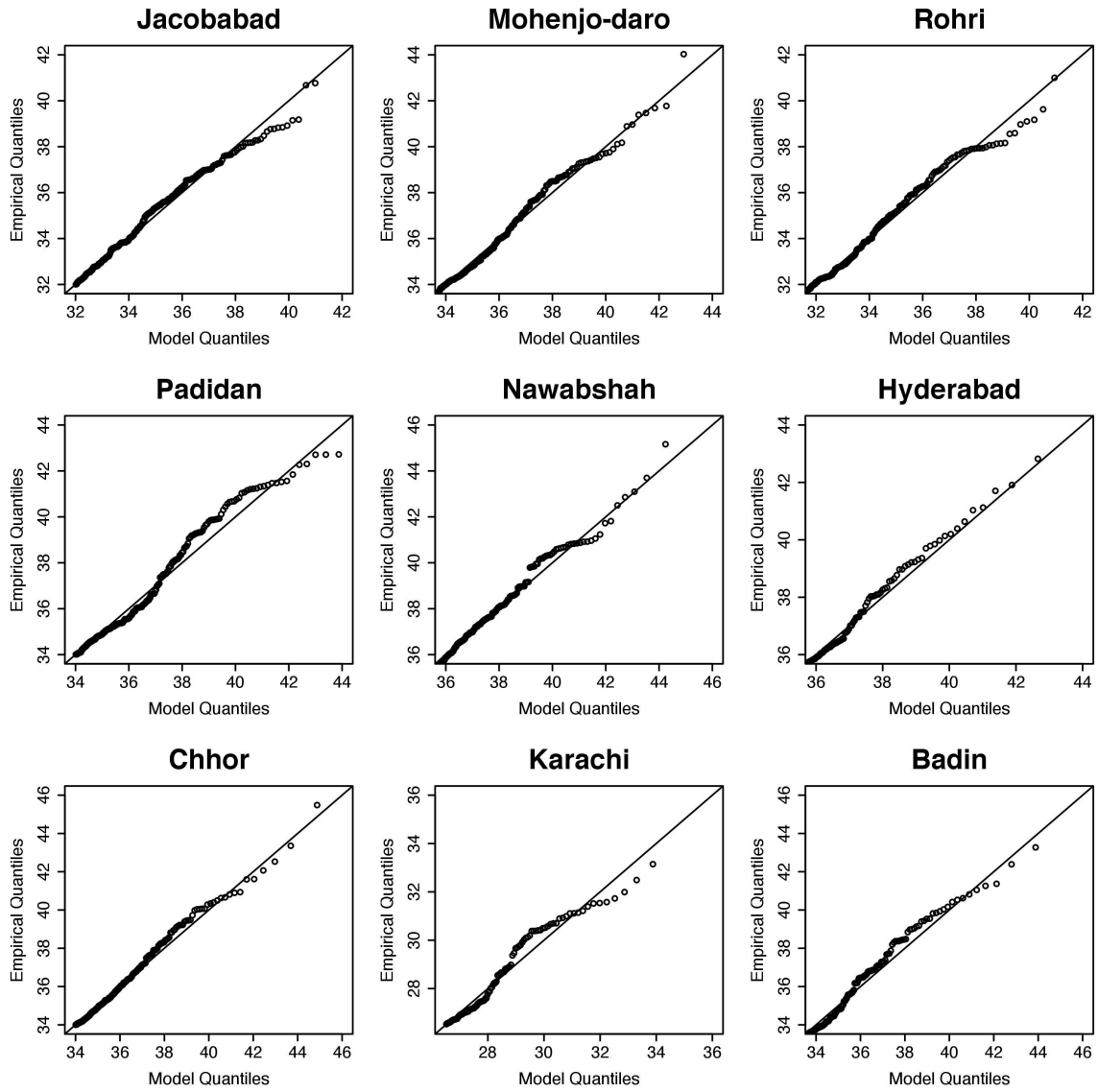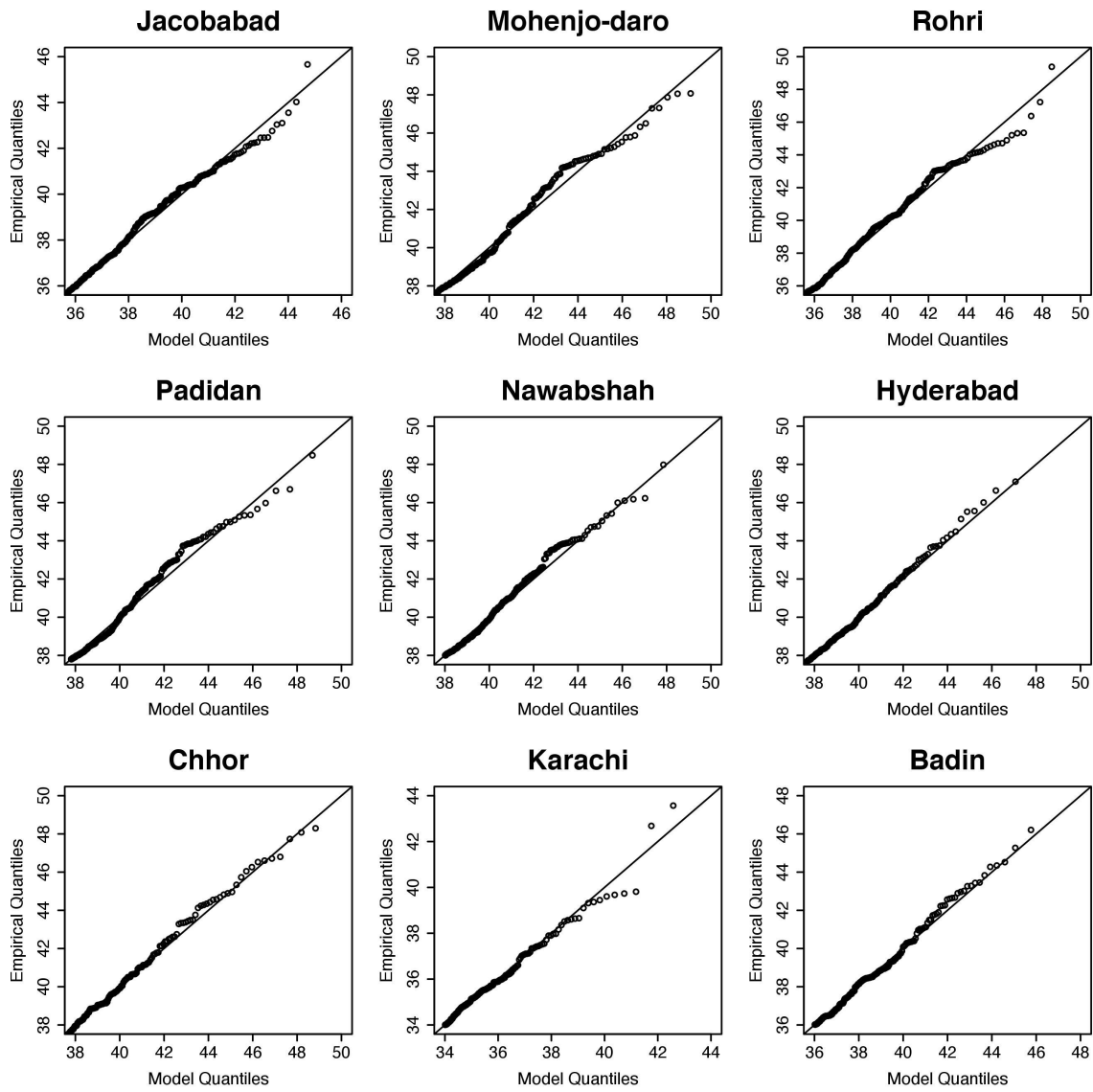
Figure 2.8: Quantile-Quantile plots of station ERA Interim TW_{max} (°C), u= 90% for 9 stations of southern Pakistan (Sindh).

Figure 2.9: Quantile-Quantile plots of station bias corrected ERA Interim TW_{max} (°C), u= 90% for 9 stations of southern Pakistan (Sindh).

In order to assess the goodness-of-fit, we apply the Kolmogorov-Smirnov (K-S) test and Anderson-Darling (A-D) test to the data of meteorological stations, ERA Interim, bias corrected ERA Interim T_{max} and TW_{max}. The p – values indicate a good performance of the fit procedure. Table 2.2 show the results of the K-S and A-D statistics of the T_{max} and TW_{max} in all data sets.

Table 2.2: Results of the Kolmogorov-Smirnov Goodness of fit test and Anderson-Darling test between empirical and GPD fits.

Observed T_{max}										
Test Statistics	Null Hypothesis					p-value				
		JAC	MJD	RH I	PDN	NWB	HYD	CHR	KHI	BDN
Kolmogorov Smirnov	Equality of probability	0.947	0.340	0.996	0.139	0.941	0.385	0.928	0.306	0.666
Anderson Darling	distribution	0.553	0.978	0.654	0.857	0.157	0.649	0.233	0.869	0.145
ERA Interim T_{max}										
Test Statistics	Null Hypothesis					p-value				
		JAC	MJD	RHI	PDN	NWB	HYD	CHR	KHI	BDN
KolmogorovSmirnov	Equality of probability	0.169	0.125	0.553	0.456	0.322	0.187	0.419	0.456	0.332
Anderson Darling	distribution	0.355	0.263	0.165	0.587	0.615	0.398	0.266	0.687	0.425
Bias corrected ERA Interim T_{max}										
Test Statistics	Null Hypothesis					p-value				
		JAC	MJD	RHI	PDN	NWB	HYD	CHR	KHI	BDN
KolmogorovSmirnov	Equality of probability	0.452	0.472	0.197	0.489	0.269	0.137	0.158	0.243	0.312
Anderson Darling	distribution	0.352	0.315	0.235	0.270	0.335	0.289	0.216	0.390	0.227
Observed TW_{max}										
Test Statistics	Null Hypothesis					p-value				
		JAC	MJD	RHI	PDN	NWB	HYD	CHR	KHI	BDN
KolmogorovSmirnov	Equality of probability	0.981	0.111	0.341	0.226	0.457	0.545	0.441	0.385	0.211
Anderson Darling	distribution	0.623	0.745	0.587	0.884	0.199	0.123	0.789	0.669	0.473
ERA Interim TW_{max}										
Test Statistics	Null Hypothesis					p-value				
		JAC	MJD	RHI	PDN	NWB	HYD	CHR	KHI	BDN
KolmogorovSmirnov	Equality of probability	0.712	0.564	0.955	0.425	0.258	0.134	0.856	0.497	0.222
Anderson Darling	distribution	0.236	0.474	0.516	0.219	0.356	0.117	0.537	0.464	0.613
Bias corrected ERA Interim T_{max}										
Test Statistics	Null Hypothesis					p-value				
		JAC	MJD	RHI	PDN	NWB	HYD	CHR	KHI	BDN
KolmogorovSmirnov	Equality of probability	0.268	0.688	0.127	0.372	0.268	0.229	0.591	0.582	0.478
Anderson Darling	distribution	0.373	0.484	0.278	0.432	0.306	0.283	0.365	0.445	0.483

2.3.3   Parameter Estimates

Here, we analyze the shape parameter ξ, the scale parameter σ, and threshold u for all considered datasets. The standard errors of the shape ξ and the scale σ parameters are given in Table 2.3. The spatial distribution of the shape parameter ξ and the scale parameter σ of the GPD in Sindh are shown in Figure 2.10. The shape parameters ξ are negative in all datasets at all stations. This is hardly surprising, as meteorological and physical processes make sure that the temperature cannot grow locally without control. One finds a certain degree of variability across stations in the estimated value of the shape parameter. In the case of the observed T_{max} one obtains for ξ estimates ranging between -0.418 and -0.223, while for TW_{max} the range is between -0.323 and -0.177, so that values slightly closer to zero are found, thus allowing for larger excursions towards very high values with respect to the case of the extremes of the actual temperature. When looking at the bias

corrected ERA Interim data, the range of values for the shape parameter of T_{max} (TW_{max}) is between -0.305 to -0.002 (-0.18 and -0.01). While there is a good match in the spatial patterns of the estimates for the observative vs ERA Interim datasets, the presence of values much closer to zero in the second case suggests the presence of some inadequacies in the representation of extremes in the reanalysis. This is not entirely unexpected, as reanalysis are constructed in such a way that typical conditions are well reproduced. Note that our simple bias correction procedure, while not impacting the estimates of the shape parameters, allows for improving the estimates of the return levels, as discussed below.

The scale parameters σ measures the variability of the GPD distributions. The highest values of the scale parameters σ of T_{max} and TW_{max} are observed at stations such as Jacobabad, Padidan, Karachi, Hyderabad, and Chhor in all datasets. This indicates that the variability of temperature extremes is higher at these stations, and one can expect higher return values of T_{max} and TW_{max} here having similar shape parameter and same threshold according to Equation 4.2. The scale parameters σ of the observed T_{max} range from 2.08 to 2.76, and the TW_{max} are in 1.86 to 2.76. In the ERA Interim analysis, the scale parameter σ of T_{max} is between 1.00 - 1.95, and TW_{max} in 0.74 - 1.75. We observe a difference in the scale parameters of both the observed, ERA Interim T_{max} and TW_{max}. We find that, unsurprisingly, the scale parameters of the bias corrected ERA Interim data are much closer to those estimated for T_{max} and TW_{max} using the station data. In the bias corrected ERA Interim T_{max} the scale parameters σ are in 1.50 - 2.75, while for TW_{max} are in a range 1.40 – 2.40 (Figure 2.10). All the temperature scale parameters are in degree Celsius.

2.3.4   Absolute Maxima

Once the shape parameters ξ, the scale parameters σ, and the thresholds u are determined, it is possible to compute the theoretical absolute maxima using Eq. (2.3) (Section 2.2.4). Theoretical absolute maxima can be compared with the observed ones for each station to better understand whether our fits are in agreement with the observed data. The daily maximum temperature T_{max} and the maximum wet-bulb temperature TW_{max} (station data, the ERA Interim, and the bias corrected ERA Interim) have negative shape parameters ξ at all stations. This means that according to Eq. (4.1) in section 2.2.4, the probability distribution function (pdf) is bounded by the maximum values. These maximum values are the theoretical upper limits predicted by the GPD fit. The analysis shows that the observed absolute maxima T_{max} and TW_{max} at all stations of the three data sets are below the theoretical absolute maximum, as expected (Figure 2.11). This gives us confidence on the quality of our fit. The following piece of information can also be derived: assume that one observes in the future an extreme event larger than the maximum inferred in the present dataset; this may suggest some non-stationarity in the most recent portion of the dataset.
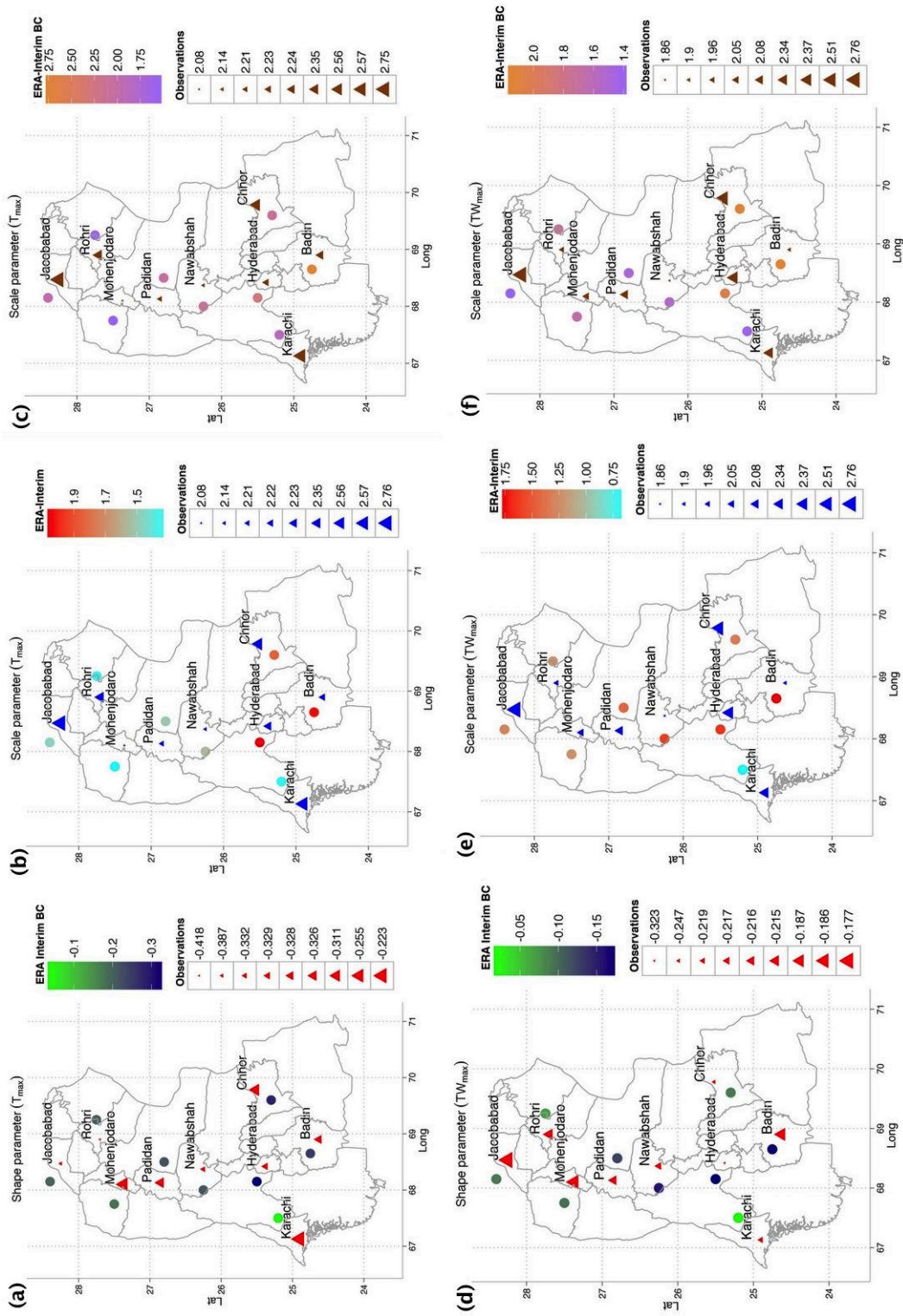
Figure 2.10: . Spatial distribution of the shape parameters ξ and scale parameters σ of the station observed, ERA Interim, and bias corrected ERA Interim T_{max} (upper panel) and TW_{max} (lower panel) in degree Celsius.

Table 2.3: Estimated parameters shape ξ, scale σ and standard error $\Delta\xi$, $\Delta\sigma$ of all data sets.

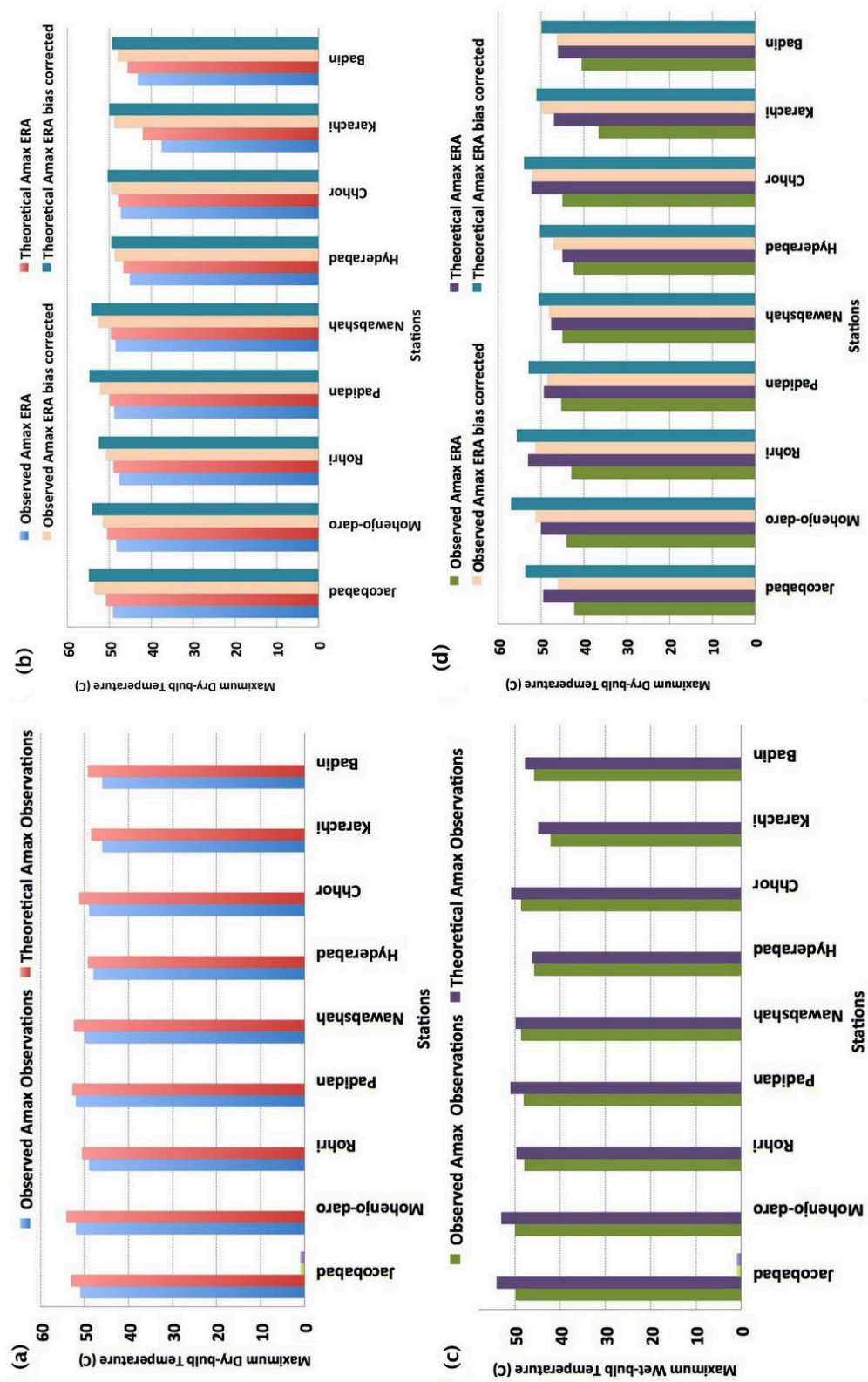| Station observed T_{max}									
Estimates	**JCB**	**MJD**	**RHI**	**PDN**	**NWB**	**HYD**	**CHR**	**KHI**	**BDN**
Shape ξ	-0.3875	-0.2550	-0.4182	-0.3261	-0.3323	-0.3292	-0.3108	-0.2225	-0.3292
Standard Error $\Delta\xi$	0.0317	0.0226	0.0226	0.0218	0.0208	0.0312	0.0371	0.0341	0.0312
Scale σ	2.7540	2.0819	2.3510	2.2144	2.1391	2.2286	2.5629	2.5685	2.2286
Standard Error $\Delta\sigma$	0.1421	0.1040	0.1075	0.1076	0.1031	0.1166	0.1462	0.1444	0.1166
ERA Interim T_{max}									
Estimates	**JCB**	**MJD**	**RHI**	**PDN**	**NWB**	**HYD**	**CHR**	**KHI**	**BDN**
Shape ξ	-0.1959	-0.1788	-0.2076	-0.2185	-0.2135	-0.3380	-0.2850	-0.0376	-0.2514
Standard Error $\Delta\xi$	0.0320	0.0348	0.0343	0.0287	0.0265	0.0316	0.0337	0.0508	0.0371
Scale σ	1.4643	1.3230	1.3440	1.5045	1.5630	2.0656	1.8497	1.3303	2.0410
Standard Error $\Delta\sigma$	0.0798	0.0739	0.0741	0.0788	0.0788	0.1082	0.0949	0.0908	0.1153
Bias Corrected ERA Interim T_{max}									
Estimates	**JCB**	**MJD**	**RHI**	**PDN**	**NWB**	**HYD**	**CHR**	**KHI**	**BDN**
Shape ξ	-0.1959	-0.1788	-0.2076	-0.2185	-0.2135	-0.3380	-0.2850	-0.0376	-0.2514
Standard Error $\Delta\xi$	0.0320	0.0348	0.0343	0.0287	0.0265	0.0316	0.0337	0.0508	0.0371
Scale σ	1.9834	1.7918	1.8205	2.0382	2.1164	2.7980	2.3081	1.8016	2.7636
Standard Error $\Delta\sigma$	0.1081	0.1001	0.1004	0.1068	0.1068	0.1467	0.1233	0.1229	0.1562
Station observed TW_{max}									
Estimates	**JCB**	**MJD**	**RHI**	**PDN**	**NWB**	**HYD**	**CHR**	**KHI**	**BDN**
Shape ξ	-0.1769	-0.1860	-0.2150	-0.2157	-0.2164	-0.3231	-0.2423	-0.2190	-0.1867
Standard Error $\Delta\xi$	0.0383	0.0354	0.0347	0.0442	0.0266	0.0269	0.0347	0.0368	0.0322
Scale σ	2.7590	2.0454	1.9600	2.0780	1.8572	2.3724	2.5126	2.3375	1.9032
Standard Error $\Delta\sigma$	0.1596	0.1146	0.1084	0.1289	0.0938	0.1191	0.1380	0.1328	0.1055
ERA Interim TW_{max}									
Estimates	**JCB**	**MJD**	**RHI**	**PDN**	**NWB**	**HYD**	**CHR**	**KHI**	**BDN**
Shape ξ	-0.0896	-0.0946	-0.0687	-0.1257	-0.1583	-0.1771	-0.0902	-0.0194	-0.1733
Standard Error $\Delta\xi$	0.0379	0.0293	0.0327	0.0342	0.0313	0.0377	0.0357	0.0359	0.0378
Scale σ	1.2879	1.2437	1.2311	1.4408	1.6104	1.6499	1.3423	0.6801	1.7886
Standard Error $\Delta\sigma$	0.0748	0.0660	0.0676	0.0804	0.0875	0.0959	0.0760	0.0398	0.1028
Bias Corrected ERA Interim TW_{max}									
Estimates	**JCB**	**MJD**	**RHI**	**PDN**	**NWB**	**HYD**	**CHR**	**KHI**	**BDN**
Shape ξ	-0.08961	-0.0946	-0.06870	-0.12570	-0.15831	-0.17711	-0.09017	-0.01942	-0.17332
Standard Error $\Delta\xi$	0.03786	0.02931	0.03275	0.03424	0.03134	0.03767	0.03571	0.03593	0.03782
Scale σ	1.35674	1.64650	1.75852	1.49477	1.52013	2.05281	2.14609	1.39943	2.15299
Standard Error $\Delta\sigma$	0.07878	0.08736	0.09651	0.08347	0.08254	0.11924	0.12145	0.08193	0.12370

Figure 2.11: Absolute maxima A_{max} in degree Celsius (a) station observed T_{max} (b) ERA Interim and bias corrected ERA Interim T_{max} (c) station observed TW_{max} (d) ERA Interim and bias corrected ERA Interim TW_{max}.

2.3.5   Return Levels

The return levels (RLs) are computed considering various return periods (2, 5, 10, 20, 50, 100-year). As remarked above, using a statistical approach based on the universality of EVT, we are able to extrapolate the results for time horizons longer than the one for which observations are taken. Clearly, uncertainties grow when longer time horizons are considered. The return level plots of the stations observed, the ERA Interim, the bias corrected ERA Interim daily maximum temperature T_{max} and daily maximum wet–bulb temperature TW_{max} are displayed in Figures 2.12 and 2.13. The values of the RLs follow the north-south gradient of the climatic mean temperatures. The northern part of the Sindh (Jacobabad, Mohenjo-daro, Rohri, Padidan, and Nawabshah) are hotter than the southern part (Hyderabad, Chhor, Karachi, and Badin).

The 2, 5, 10, 20, 50, 100 year RLs estimated in Sindh for station observed Tmax at time reach over 50°C in Jacobabad, Mohenjo-daro, Padidan, Nawabshah, and over 45°C in Rohri, Hyderabad, Chhor, Karachi, Badin. The corresponding ERA Interim T_{max} return levels are at least 3°C to 5°C lower in all stations, while having correct representation of the geographical variability of the field. As example, the RLs of 42°C at Badin has a 3-year return period in the observations T_{max}, but a 30-year return period in ERA Interim (Figure 2.12).

The RLs of TW_{max} are above 35°C in all meteorological stations. As for the ERA Interim, the RLs of TW_{max} are greater than 30°C for all the stations except Karachi, which has RLs less than 30°C. Here, we see again that the RLs of the ERA Interim TW_{max} are lower than the RLs of station TW_{max}. Going again to the Badin stations, the 4-year return period observed for TW_{max} is 38°C, while the ERA Interim dataset show the same RL in a 15-year return period (Figure 2.13).

The bias corrected ERA Interim T_{max} and TW_{max}, show some improvements in the RLs at all stations. When looking at the Nawabshah, Hyderabad, Karachi, and Badin stations, the RLs agree with those obtained from the station data in the range 5-100 years, while disagreements exist in the range 2-5 years. In the rest of the stations, the bias corrected data RLs are closer to those of the station data, yet not statistically compatible with them. When looking at the wet-bulb temperature TW_{max} analysis, the RLs of the bias corrected ERA Interim show some overlap with those derived from station observations in Mohenjo-daro, Hyderabad, Chhor, and while no overlap is found in the other stations. One understands that the proposed simple bias correction methods improves the quality of the representation of extremes by ERA Interim, but many discrepancies remain (Figures 2.12 and 2.13).

We also plot the station and bias corrected ERA Interim T_{max}, and TW_{max} return levels spatially for the 5, 10, 25 and 50 year return periods (Figures 2.14 and 2.15), as a detailed spatial overview of the temperature extremes in Sindh might be of interest to the policy makers. The spatial return levels of the station and
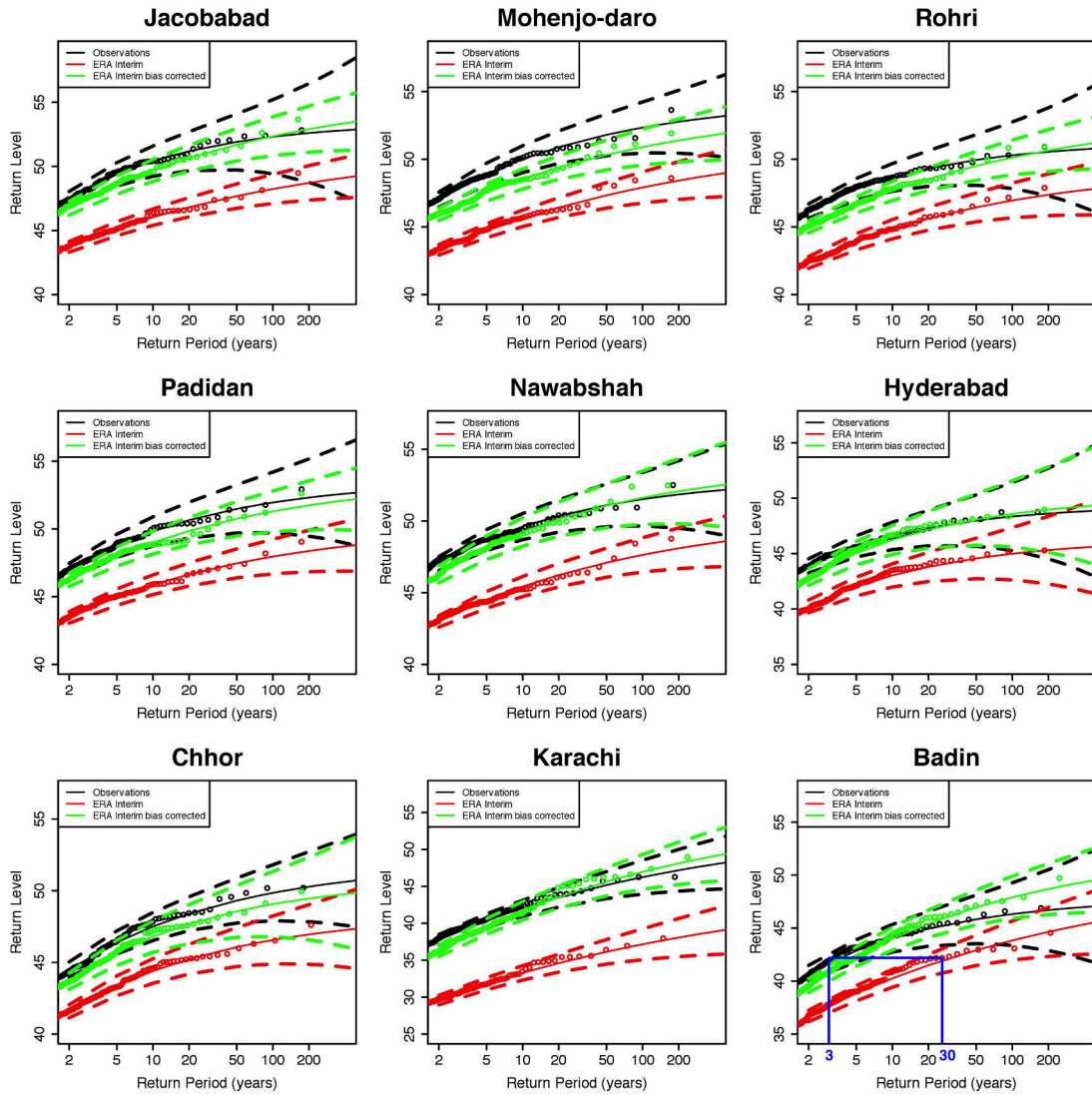
Figure 2.12: Return level plots of the station observed T_{max} (black) , ERA Interim T_{max} (red), and bias corrected ERA Interim T_{max} (green) in degree Celsius. The blue line is to show a difference in the observed and ERA Interim RLs.
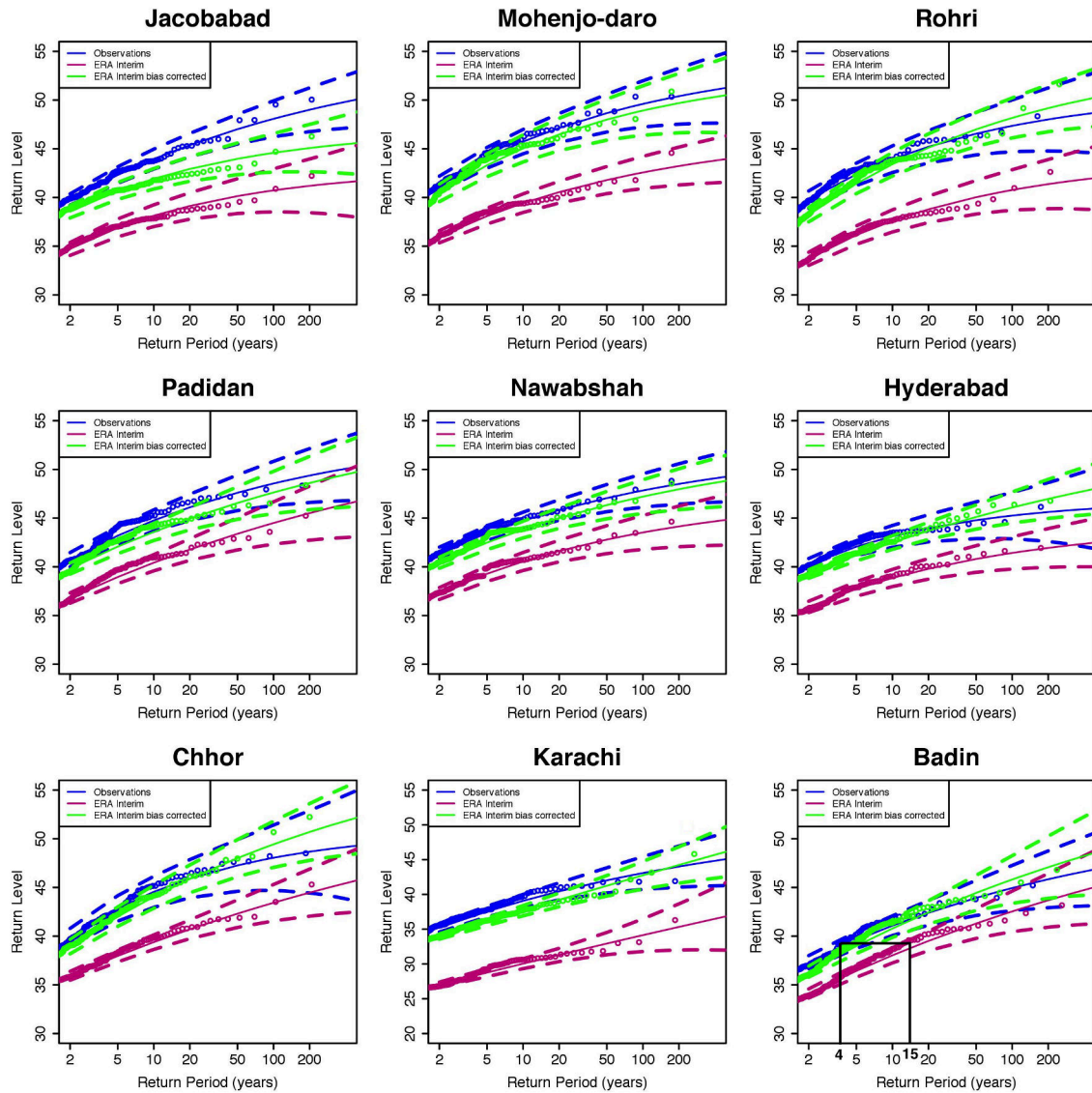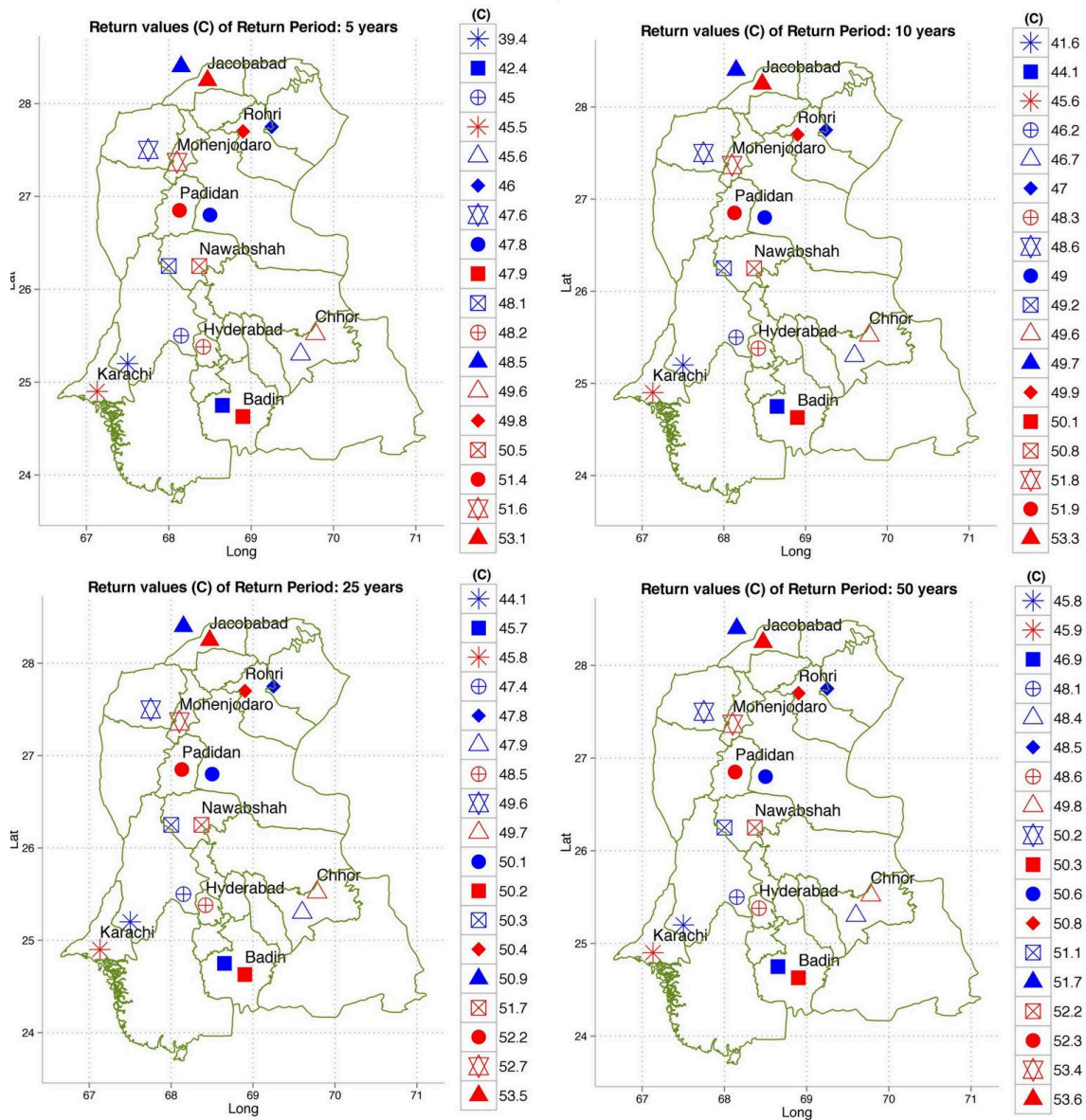
Figure 2.13: Return level plots of the station observed TW_{max} (blue), ERA Interim TW_{max} (pink), and bias corrected ERA Interim TW_{max} (green) in degree Celsius. The black line is to show a difference in the observed and ERA Interim RLs.

Figure 2.14: Spatial distribution of the station observed T_{max} (red) and bias corrected ERA Interim T_{max} (blue) return levels in degree Celsius corresponding to return periods of 5, 10, 25 and 50 years in southern Pakistan.
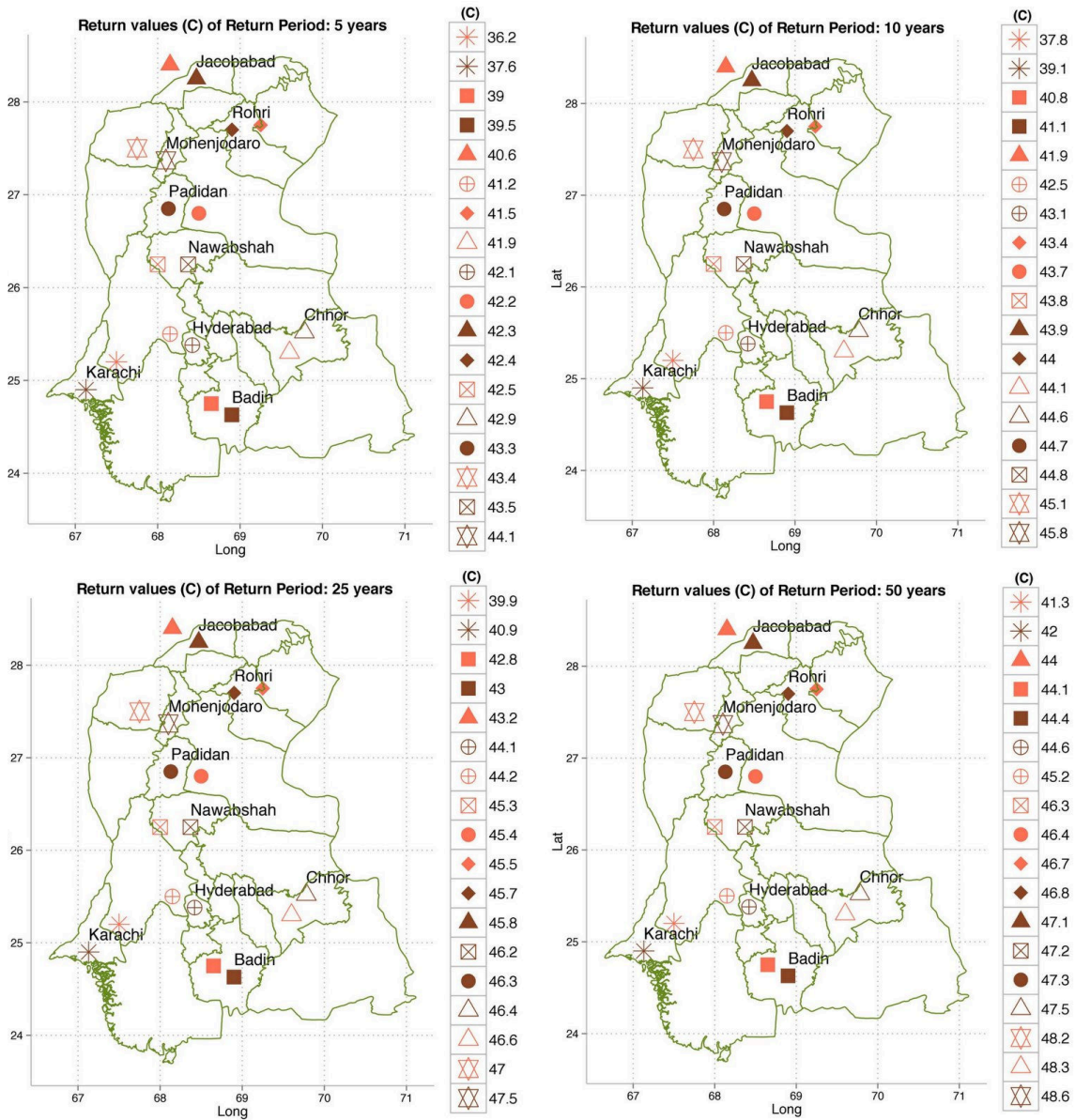
Figure 2.15: Absolute maxima A_{max} in degree Celsius (a) station observed T_{max} (b) ERA Interim and bias corrected ERA Interim T_{max} (c) station observed TW_{max} (d) ERA Interim and bias corrected ERA Interim TW_{max}.

bias corrected ERA Interim T_{max} shows differences in temperature; the hottest stations have the highest return levels. We notice that for Jacobabad, Mohenjo-daro, Padidan, Nawabshah the return levels are between 50°C – 53.6°C and for Rohri, Hyderabad, Chhor, Karachi, and Badin are between 45°C – 50°C in 5 to 50 years return period (Figure 2.14). These extreme temperatures can impact the yields because crops are very sensitive to temperature variations, and even a rise of one degree Celsius can cause detrimental changes in the phenological stages of the crops (Hatfield and Prueger, 2015). Every crop has a certain limit to tolerate the temperature. When temperature exceeds this limit, the crop yield is drastically reduced. Abbas et al. (2017) notices 33% decrease in major crops of Sindh due to warmer and drier weather. Karachi and Badin are expected to decrease rice cultivation, hatching of fisheries, and mangroves forest surrounding these cities. Furthermore, temperature extremes can have serious threat to cotton, wheat, and rice yields in Rohri and Mohenjo-daro areas due to increased crop water requirements.

In summer, the temperature and humidity increase to an extent that there are high chances of a rapid pests spread in the crops. Temperature extremes not just directly impact the quantity and quality of grains, but can also be a reason of urban flooding affecting the agriculture lands. Sindh produces cotton, wheat, rice, mango, banana, and dates, so a correct estimate of temperature extremes is very important. The spatial return levels of station and bias corrected ERA Interim TW_{max} for the 5, 10, 25, and 50 year return periods show highest return level greater than 35°C at all stations (Figure 2.15. This is very serious for the human health due to the working day hours of population in agriculture farms, building construction, and port activities. Karachi and Badin being closet to the coast are at the highest risk of temperature extremes. Thus, an immediate plan for adaptations is needed in Sindh to deal with such a hazard. The high values of TW_{max} also indicate high levels of humidity in the region during summer, which is also proved by Kalim and Shouting (2012); Freychet et al. (2015).

2.4   Summary and Conclusions

The main objective of this chapter is the assessment of the return levels of the extreme daily maximum temperatures T_{max} and wet-bulb temperatures TW_{max} in southern Pakistan (Sindh). In addition, the performance of the ERA Interim TW_{max} is compared to the weather station TW_{max} to assess its ability to estimate temperature extremes in Sindh. Moreover, a simple bias correction is applied to the ERA Interim data to see whether correcting the first two moments of its statistics helps in improving its performance in representing temperature extremes.

The POT method is applied to the daily maximum temperature (T_{max}) and wet-bulb temperature (TW_{max}) data of nine stations and to the corresponding nearest ERA Interim temperature data. After testing the asymptotic statistical properties,

the 90% quantile is found to be appropriate threshold choice for all datasets. The Q-Q plots are used to assess the GPD fit, which results to be acceptable for both T_{max} and TW_{max} station data for all three datasets. However, the bias corrected ERA Interim data shows improved GPD fits than the ERA Interim data. The shape parameters ξ is in general negative at all stations. The scale parameters σ show high values in Jacobabad, Padidan, Karachi, Hyderabad and Chhor indicating higher variability of temperature extremes in these regions. The return levels (RLs) of T_{max} and TW_{max} are estimated for the 2, 5, 10, 25, 50, 100 year return periods in all datasets. The RLs of T_{max} estimated using the meteorological station temperatures are greater than 50°C in Jacobabad, Mohenjo-daro, Padidan, Nawabshah, and greater than 45°C in Rohri, Hyderabad, Chhor, Karachi and Badin. While the RLs of TWmax in station data are larger than 35°C in the entire Sindh, when using ERA Interim temperatures, they are estimated as greater than 45°C in Northern Sindh and greater than 40°C in southern Sindh.

The results predict extremely high values of T_{max} and TW_{max} in the region. The T_{max} extremes contribute to an increase rate of evaporation, which in turn may intensify the hydrological cycle causing precipitation events and flooding (Cheema et al., 2012). Additionally, crops variety needs to be changed under such a hot climate to avoid the risks of temperature extremes. The extremes of daily maximum wet-bulb temperature TW_{max} are estimated as above the human survivability threshold 35°C throughout the region, so the risk of hyperthermia is very high here. The most vulnerable people are those who are involve in the everyday outdoor activities like farming, fishing, building construction, athletes, elderly and infants can have heat strokes, dehydration etc. The human habitability in such a warm region is already at risk and one can expect that these issues will be worse in future climate conditions.

It is found that the RLs of station and ERA interim showed differences are between 3°C and 5°C for both shorter and longer return periods due to the minor variations in the shape and scale parameters. Although the ERA Interim dataset does not capture well the magnitude of the extremes, still it provides a good representation of their spatial fields. The biases between the station and the ERA Interim data are rather relevant when one wishes to address the impact of hot climatic extremes to human life and to active crop production in the region. It would be of primary importance to understand the physical reasons behind such inconsistencies, which makes it hard to use reasonably ERA without bias correction. Clearly, they might result either from a misrepresentation of local processes dominated by near surface processes (namely, heat and water fluxes), or from an inadequacy of the re-analysis in reproducing synoptic and sub-synoptic conditions responsible for extremely hot and humid conditions.

A simple bias correction i.e. adjusting the mean and standard deviation to ERA Interim T_{max} and TW_{max} data is applied to check the improvements in return levels. We noticed that the bias corrected ERA Interim T_{max} and TW_{max} gives the return

levels closer to the meteorological stations observed ones than the original ERA Interim return levels at all stations. Although the bias corrected ERA Interim shows a good correspondence with the meteorological station data, yet statistically differences remain in most cases. Therefore, one must use more advanced bias correction method for analyzing extremes precisely. It is proposed to repeat this analysis in GCMs (CMIP5, CMIP6) and RCMs (CORDEX) to study the properties of extremes. All models use re-analysis as input, and generate information of extremes, which involves biases that if not corrected, can lead to significant errors in prediction of present and future extremes. Therefore, in order to reduce the uncertainties in impact assessment, it is necessary to improve the re-analysis before using it in GCMs and RCMs. The results have practical implications for assessing the risk of extreme temperature events in Sindh. They should be used to prepare the baseline contingency plans for dealing with strong heat waves in Sindh. Such measures are not yet present in the territory and lead to many casualties each year. Besides planning, the resutls are quite useful for the ongoing EU projects (SUCCESS, CSCCC), World Bank project (Sindh Resilience Project) and mega construction projects like China-Pakistan Economic Corridor (CPEC).

Chapter 3

Return levels of sea surface temperature extremes and their link to cyclogenesis

3.1 Introduction

Sea Surface Temperature (SST) is a vital component of the earth's climate system, and a prime indicator of extreme events like cyclones, extreme precipitation, El Nino and sea level rise (Rana et al., 2014; Abram et al., 2008; Hunter, 2010; Levine and Turner, 2012). SST has shown an increasing trend over the past few decades, mainly in regions prone to tropical cyclones (Holland, 1997; Emanuel, 2005; Webster et al., 2005; Gillett et al., 2008; Elsner et al., 2008; Knutson et al., 2010; Sobel et al., 2016). The north Indian Ocean hosts seven percent of the global tropical cyclones (Singh et al., 2001), and showed a warming of approximately 0.5°C between 1970 and 2004 (Christy et al., 2001; Agudelo and Curry, 2004). The north Indian Ocean has two basins, the Bay of Bengal and Arabian Sea, the frequency of tropical cyclones is higher in the Bay of Bengal than in the Arabian Sea. But, recently the Arabian Sea has been warming gradually and experiencing stronger cylonic activity than in the past (Evan and Camargo, 2011). Therefore, here we are focusing on the Arabian Sea SST and cyclonic activity in it.

Geographically, the Arabian Sea is surrounded by Pakistan, Iran, India, and the Arabian Peninsula between latitude 0°N – 30°N and longitude 45°E – 78°E. The SST in the Arabian Sea has a bimodal seasonal cycle, which was identified by Gray (1968). The annual cycle of the Arabian Sea studied by Sayantani et al. (2016) shows the warming of SST in spring (March – April), intensification of SST during pre and post monsoon (May – June and October – November), while cooling in summer and winter monsoon (July – September and December – February). The warming is generally initiated by the high intensity of solar radiation between March and May and continues to increase, until the strong winds and cloud cover arrives in monsoon (June – September). It again increases in October until November because of low wind speed, and decreases from December to February because of low

solar radiation (Muhammad et al., 2016). In a recent past, the trends of Arabian Sea SST are changing and investigated by Mitchell et al. (1990); RupaKumar et al. (2002); Khan et al. (2008); Muhammad et al. (2016). These studies collectively project a rise of SST > 2°C in the Arabian Sea, contributing to the sea level rise. A climate-shift in the Arabian Sea after 1995 accompanied by an increase in the number of cyclones has been identified by Kumar et al. (2009). The spatial and temporal patterns of Arabian Sea warming are discussed more often by investigators, but least attention has been given to the sea surface temperature extremes (Oliver et al., 2014).

Tropical cyclones occur in the Arabian Sea each year but they rarely make a landfall, however some intense tropical cyclones in the past decade have produced severe flooding caused by heavy precipitation and storm surges (Needham et al., 2015). The strongest storm recorded in the history of the Arabian Sea is the super cyclone Gonu (03A), which formed in early June 2007, and badly impacted Oman, Iran, United Arab Emirates and Pakistan. The estimated damage was $4 billion (U.S dollars) with more than 100 casualties collectively (JTWC, 2007). Tropical cyclones normally develop in the Arabian Sea prior or post monsoon season, when the SST exceeds 26°C along with other climatic conditions essential for a cyclone genesis (Gray, 1968). However, to initiate cyclonic activity in the Arabian Sea, SST above 26°C is enough (Gray et al., 1994). The pre-monsoon (May – June) cyclones are associated to an early or late onset of the monsoon, and post-monsoon (October – November) storms are related to high seal level pressure in the Bay of Bengal (Evan and Camargo, 2011).

Evan and Camargo (2011) observed an increase in the frequency and intensity of tropical cyclones in the Arabian Sea since 1998 due to the reduced wind shear. Murakami et al. (2013) reported a substantial increase in the number of tropical cyclones (by 46%) over the Arabian Sea by the end of 21st century. Therefore, there is a strong need to study the probability of cyclongenesis in the Arabian Sea during peak seasons, to avoid the huge socio-economic losses in the vicinity of the Arabian Sea. The cyclones prediction in the Arabian Sea mostly rely either on the empirical genesis indices, or on the new generation of global climate models. Most tropical cyclone genesis indices predict an increase in the frequency of future cyclones, but the models predict decrease in the number of cyclones. It is not clear yet that the problem lies in formulating the indices or models are incorrect (Walsh et al., 2016). The inhomogenity and disagreement on the frequency of cyclones in the Arabian Sea creates a substantial concerns for this basin.

The first part of this chapter estimates the return levels of extreme SST in the Arabian Sea using UK Met office Hadley Center SST data, during pre-monsoon and post-monsoon. The Block Maxima (BM) approach of Extreme value theory (EVT) is applied to estimate the return levels of SST extremes in the Arabian Sea. The BM approach analyzes a series of BM over long blocks, which have theoretical justification for following the Generalized Extreme Value distribution (GEV). The

method is applied extensively in analyzing extremes using the stationary (Papalexiou and Koutsoyiannis, 2013), and non-stationary GEV distribution (Renard, 2013; Gilleland and Katz, 2011) to estimate the risks of the extremes in a static and changing climate (see more details in Section 3.3.1). The stationary GEV distribution indicates no trends in the data, while the non-stationary GEV assesses extremes in presence of trends in the data. Here, we consider both the stationary and non-stationary GEV distribution to model the sea surface temperature extremes. Later, we determine the best-fit GEV model by applying the likelihood-ratio test and Akaike's information criterion. Information on the recurrence of SST extremes is useful for prediction of cyclonic activity, conservation of the marine species such as fish, coral reefs and mangroves and adaptations for the coastal communities in the suburbs of the Arabian Sea.

The second part of the chapter shows the probabilistic prediction of cyclonic activity in the Arabian Sea during pre-monoon and post-monsoon. The Poisson regression model is used to see the correlation among cyclonic activity (predictand), and SST, SOI (predictors). The Poisson regression is preferred here because for linear regression the linearity conditions must be satisfied, which is not possible in case of tropical cyclones due to relatively small number of counts in the large data set. Moreover, a Poisson regression is recommended as a most appropriate approach to predict cyclones by different investigators like Wilks (1995); Elsner and Jagger (2006); Elsner et al. (2008); McDonnell and Holbrook (2004); Kim et al. (2010); Coxe et al. (2017). They have proved that Poisson regression model provides improved predictive skills over the linear statistical models. The data of the tropical depressions (TD), cyclonic storms (CS), and severe cyclonic storms (SCS) is taken for the period 1891 – 2015, from the Indian Meteorological Department. TD, CS, and SCS data is chosen over super cyclone data due to the long-term data availability. Moreover, TD, CS, and SCS have never been explored, although they are more frequent and may also be extremely hazardous for the coastal and marine climate system.

3.2 Data and Domain

We use SST data with resolution $1° \times 1°$ from the UK Met office Hadley Center Sea Ice and Sea Surface Temperature dataset (HadISST) from 1891 to 2015 (Rayner, 2003). Southern Oscillation Index (SOI) data is obtained from the Climate Research Unit (https://climexp.knmi.nl/data/isoi.dat) for the same period as SST. For our analysis, we select the Arabian Sea domain between longitudes $45°E – 78°E$ and latitudes $0°N – 30°N$ as shown in Figure 3.1 because of its highest probability for the formation of the tropical depressions and cyclones (Evan and Camargo, 2011).

The tropical cyclones occurring in the Arabian Sea are classified into different categories on the basis of wind speed Table 3.1. Here, we consider the annual frequency of Arabian Sea TD, CS, and SCS for the duration 1891-2015, taken from the Indian

Figure 3.1: Map of the Arabian Sea domain (45°E – 78°E and 0°N – 30°N)

Meteorological Department (IMD; http://www.rsmcnewdelhi.imd.gov.in/). IMD data shows that the tropical cyclones and depressions occur mainly in pre-monsoon (May – June) or post-monsoon (October – November), so these two periods are preferred in the analysis (for more details see Section 3.4.1).

Table 3.1: Classification of Arabian Sea Tropical Cyclones.

Wind speed (Knots)	Arabian Sea classification
17 - 33	Tropical depression (TD)
34 - 47	Cyclonic storm (CS)
48 - 63	Severe cyclonic storm (SCS)
64 - 119	Very severe cyclonic storm
≥120	Super cyclonic cyclones

The SST time series is constructed for two seasons: pre-monsoon and post-monsoon, by selecting the maximum value of spatially averaged SST over the domain during each season. It is very important to fulfill the stationarity assumption before estimating extreme value statistics by the standard block maxima method. Therefore,

the Augmented Dickey Fuller (ADF) stationarity test is applied on the SST data to check the stationarity in time series (Dickey and Fuller, 1979). In ADF, the null hypothesis, H_0, states non-stationarity and presence of trends while the alternative hypothesis H_1 states stationarity. The ADF shows stationarity in the time series at the 5% significance level. The Mann-Kendall (MK) test is also performed to detect trend in the SST data. If the p - value is less than the significance level α (alpha) = 0.05, H_0 is rejected, which indicates the trend in the data. The MK test detects an upward trend in the SST data over both the seasons. Table 3.2 shows the result of ADF and MK tests, which suggests modeling the SST data under both stationary and non-stationary climate.

Table 3.2: Augmented Dickey Fuller and Mann-Kendall test statistics

Test	Pre-Monsoon	Post-Monsoon
Augmented Dickey Fuller	*p - value (5% CI)*	
	0.024	0.0015
Mann-Kendall	*p - value (upward trend)*	
	0.0197	0.0348

3.3 Research Methodology

Two different methods are applied: (1) Block Maxima (BM), and (2) Poisson regression to perform two different tasks. Firstly, the return levels (RLs) of the SST extremes in the Arabian Sea are estimated during pre-monsoon and post-monsoon by applying BM. Secondly, a Poisson regression is applied to predict the probability of occurence of TD, CS and SCS in Arabian Sea using SST and SOI as predictors. The entire analysis is completed using the R software language (RDevelopment-CoreTeam, 2015). The extRemes package is used for the estimation of the return levels RLs (Gilleland, 2015).

3.3.1 Block Maxima

The BM method utilizes maxima from long blocks (typically annual), which leads to a straightforward interpretation and calculation of return levels. The Generalized Extreme Value distribution (GEV) is obtained as the limiting distribution of the maxima. The GEV is a representation of three types of distributions: Gumbel, Frechet and Weibull. The GEV distribution has three parameters (1) the location, μ, (2) the scale, σ, and the shape, ξ. The shape parameter ξ determines the tail behaviour of the GEV distribution. A positive value, $\xi > 0$, yields the heavy tail (Frechet) distribution while a negative value, $\xi < 0$, results in a bounded upper tail (Weibull) distribution. Defined by continuity, $\xi = 0$ implies a light tail (Gumbel) distribution (Coles, 2001; Cheng et al., 2014; Lucarini et al., 2016). As mentioned earlier in Section 3.1, the block maxima method can be applied using stationary

and non-stationary GEV models, both are discussed below.

3.3.1.1   Stationary GEV model

In a stationary GEV (SGEV) model, the parameters of the distribution (location, scale, and shape) are time invariant (Leadbetter, 1983). Coles (2001) gives the generalized extreme value distribution as

$$
G(z) = \begin{cases} \exp\left\{-\left[1 + \xi\left(\frac{z-\mu}{\sigma}\right)\right]^{-1/\xi}\right\} & \text{for } \xi \neq 0, \\ \exp\left\{-\exp\left[-\left(\frac{z-\mu}{\sigma}\right)\right]\right\} & \text{for } \xi = 0, \end{cases}
\tag{3.1}
$$

where $-\infty < \mu < \infty$, $\sigma > 0$, $1 + \xi(z-\mu)/\sigma > 0$ for $\xi \neq 0$ and $-\infty < z < \infty$ for $\xi = 0$.

The return values are then calculated by solving $G(z_p) = 1/p$, where the return values are z_p, and p is the return period so that z_p is the value that is expected to be exceeded, on average, once every $1/p$ years (Coles, 2001). The equation can be solved analytically, and is given by

$$
z_p = \begin{cases} \mu - \frac{\sigma}{\xi}[1 - \{-\log(1-p)\}^{-\xi}, & \text{for } \xi \neq 0, \\ \mu - \sigma\log\{-\log(1-p)\}, & \text{for } \xi = 0, \end{cases}
\tag{3.2}
$$

3.3.1.2   Non-Stationary GEV model

In the NSGEV model, the parameters of the distribution (location, scale and shape) vary with time (Cheng et al., 2014; Katz, 2010; Cooley, 2009; Felici et al., 2007). The annual maxima reveals a possible trend in SST through time (Figure 3.4), suggesting

$$
\mu(t) = \mu_0 + \mu_1 t
\tag{3.3}
$$

where t represents the year and and μ_0, μ_1 are the coefficients.

Southern Oscillation Index (SOI) extremal behavior is similar to SST so it can also be included as a covariate in the location parameter μ assuming a linear change with time, while keeping the scale and shape parameter constant (Coles, 2001). This can be expressed as;

$$\mu(t) = \mu_0 + \mu_1 SOI(t) \tag{3.4}$$

where SOI(t) denotes the values of SOI in year t, μ is the location parameter, and μ_0, μ_1 are the coefficients.

Combining Equation (3.3) and Equation (3.4) allows for a dependence on time and SOI by letting

$$\mu(t) = \mu_0 + \mu_1 SOI(t) + \mu_2 t \tag{3.5}$$

NSGEV can incorporate different models, such as trends on the scale and shape parameter etc (Renard, 2013). Here, we analyze the non-stationarity with respect to the location parameter μ only, because it is the simplest model to explain the variation in the data (Felici et al., 2007).

3.3.1.3 Model Choice

In order to test whether the non-stationary GEV model provides statistically significant improvement over the stationary one, the likelihood-ratio test (LRT) and Akaike's information criterion (AIC) are applied. The likelihood-ratio test statistics are defined as (Coles, 2001; El Adlouni et al., 2007).

$$\text{LRT} = 2\log(\frac{L_0}{L_1}) \tag{3.6}$$

where L_0 and L_1 are maximum likelihood for the three parameters of stationary GEV and four parameters of non-stationary GEV, which follows a chi-square distribution with degrees of freedom equal to the difference in the number of parameters of L_0 and L_1. L_0 is rejected at the 5% significance level if LRT $> \chi^2 (0.05) = 3.841$, and L_1 is selected. Large values of LRT favor model L_1, suggesting more variation in the data than can be fitted with model L_0. Table 3.3 shows the likelihood ratio test statistics.

Table 3.3: The likelihood-ratio test results

Model$_0$ vs Model$_1$	χ^2	$p-value$
Pre-monsoon	4.136	0.115
Post-monsoon	3.952	0.283

The Akaike information criterion (AIC) is another method of selecting a model from the set of models, the best model is the one with minimum AIC value (Akaike, 1974).

$$\text{AIC} = -2\log[\mathcal{L}\hat{\theta}|y] + 2k \qquad (3.7)$$

Here, $(\mathcal{L}\hat{\theta}|y)$ is the maximized Likelihood and k represents the number of estimated parameters of the model. Akaike differences (AICD) are used to compare the models.

$$\Delta_m = AIC_m - AIC_{min} \qquad (3.8)$$

Here, m (AIC_m) shows the model number. According to AICD, a model with $\Delta_m = 0$ is the best model, but models with $\Delta_m > 2$ are also reasonable candidates (Burnham and Anderson, 2002).

The results of likelihood ratio test and Akaike information criterion (AIC) favors the non-stationary GEV model, suggesting significant improvement over the stationary GEV, and allowing for a dependence in time.

3.3.2   Poisson Regression

Poisson regression is used to similar to regular multiple regression except that the dependent variable is an observed count that follows the Poisson distribution. In Poisson regression, Generalized Linear Model (GLM) use the Ordinary Least Square (OLS) method to model the linear relationships between a response variable and one or more predictor variables. The regression coefficients are estimated using the method of maximum likelihood.

The Poisson distribution is different from normal distribution, and considered ideal for modeling the occurrences of discrete events like droughts, tropical cyclones etc, because it takes on a probability value only for non-negative integers (Elsner and Schmertmann, 1993; Wilks, 1995). One has that expected rate of occurrence $E(Y_i)$ = var$(Y_i) = \mu$, when Y_i obeys a Poisson distribution (Kleinbaum et al., 1988).

The probability mass function for the Poisson distribution (Eq 3.9) models the probability of occurrence of y tropical cyclones and depressions,

$$P(Y_i = y) = \frac{\mu_i^y e^{-\mu_i}}{y!} \qquad y = 0, 1, 2, 3, .., \qquad (3.9)$$

Where μ_i is the mean occurrence rate of cyclone type $i = 1, 2, 3$

In Poisson regression model, for a given β (Poisson regresison coefficient) the μ is calculated for each set of predictors (SST, SOI) and the likelihood of the observed number of cyclones is estimated by Eq (3.9). The Poisson regression model can be depicted as

$$log(\mu_i) = \beta_0 + \sum_{j=1}^{n} \beta_j X_{ij} \qquad j = 1, 2 \tag{3.10}$$

where X_{ij} is the data value for predictor j on observation i and β_j is the corresponding Poisson regression coefficients for predictor j.

The calculations have been done by using the function "glm" in R package "stats", by simply setting the family = "poisson" (Chambers and Hastie, 1992). For "glm" objects, a set of standard methods (including print(), predict(), logLik() etc) are also provided in R. We used method = "predict" to obtain predictions, estimates, and standard error of the fitted generalized linear model (glm). Finally, function "dpois" in the package "stats" is used to estimate the Poisson probabilities.

3.4 Results and Discussion

3.4.1 Seasonal cycle of SST and cyclonic activity in the Arabian Sea

We plot the seasonal cycle of SST from 1891-2015, to identify the peak times of SST in the Arabian Sea. Clearly, SST remains above 26°C in the pre-monsoon (May – June) and post-monsoon (October – Novemeber), and below 26°C in other seasons (Figure 3.2). The seasonal frequency of Arabian Sea TD, CS and SCS shows that the peak activity occurs during May – June and then in October – November. While the monsoon season (July – September) has a very low activity of cyclone development. The months of May and June are generally named as a pre-monsoon period, and the duration from October to November as a post-monsoon period. Figure 3.2 illustrates that 85 TD, 51 CS, and 61 SCS form in pre-monsoon, whereas 96 TD, 55 CS, and 30 SCS occur during post-monsoon in the Arabian Sea over the period of 1891-2015. We observed that the seasonal cycle of SST follows the seasonal cycle of TD, CS and SCS, hence displaying a positive correlation between them.

We also analyze the annual frequency of TDs, CSs and SCS that occur in the Arabian Sea (45°E - 78°E, 0°N - 30°N) from 1891 to 2015. Figure 3.3 shows that the frequency of tropical depressions ranges from 0 to 4, CSs are 0-3, and SCS are
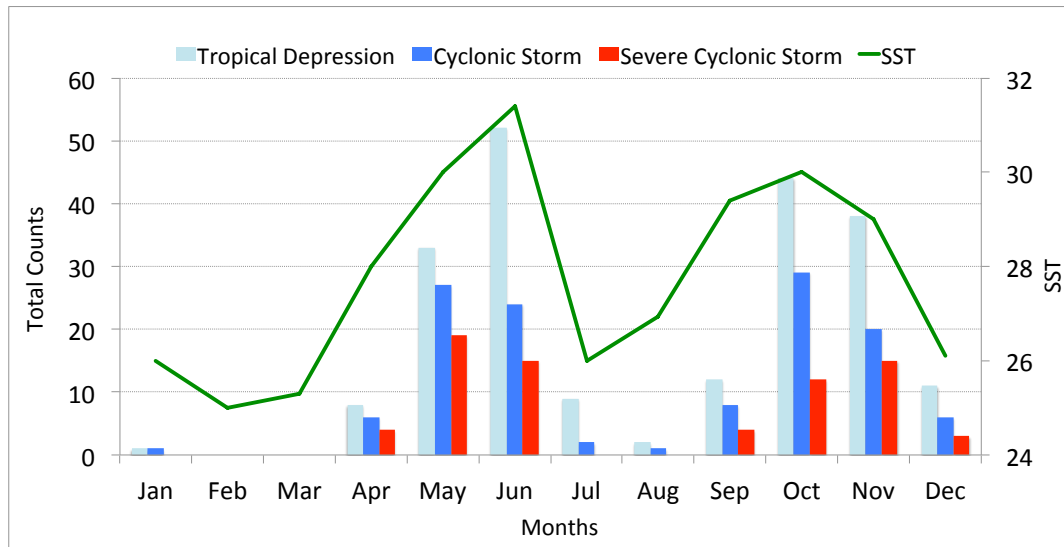
Figure 3.2: Seasonal cycle of SST and annual frequency of TDs, CSs and SCS in the Arabian Sea 1891- 2015)

0-2, from 1950 to 1984, and afterwards only 1-2 tropical depressions are recorded in the Arabian Sea each year until 1991. The rise in the frequency of TD, CS, and SCS started again in 1992, experiencing 5-6 TD, 3-5 CS, and 2-3 SCS events each year. Evan and Camargo (2011) also confirmed that the CS days have increased in the Arabian Sea during 1992-2008 as compared to 1979-91. The range of a lifetime of the TD's and storms are usually 1-9 days. Based on the Indian Meteorological Department (IMD) data for the period 1891-2015, 213 TD's, 124 CS's, and 72 SCS's has been occurred in the Arabian Sea. The increase in cyclonic activity in the Arabian Sea is linked to global warming and rise in SST by few investigators (Hussain, 2011; Haider et al., 2011) but, we could not find the literature on the SST extremes and risks associated to them in the Arabian Sea. Therefore, it is important to assess the probability of occurrence of high SST in Arabian Sea due to the dependence of cyclonic activity on it.
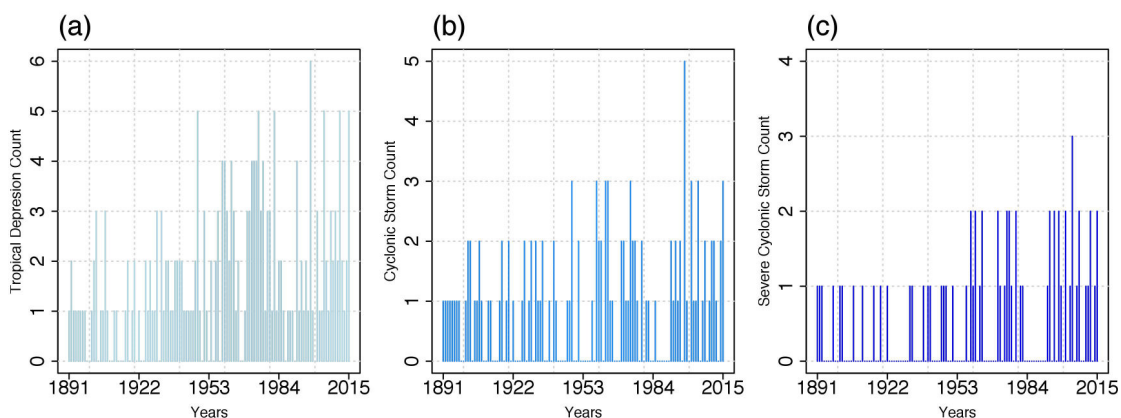
Figure 3.3: Annaual frequency of (a) TDs, (b) CSs, and (c) SCS from 1891 to 2015 in the Arabian Sea.

3.4.2   Extreme value analysis of Arabian Sea SST

In this section, the return levels of the Arabian Sea SST extremes during pre-monsoon and post-monsoon seasons are analyzed using Block Maxima (BM) approach. The first step in applying BM is the division of the SST data into blocks of equal length, and producing a set of block maxima. The GEV is then fit to the block maxima series. The choice of a block size is important in order to have a uniform distribution of the block maxima. A block length of one year is selected, which yields 125 annual maxima. Figure 3.4 shows the annual maxima of sea surface temperatures in the pre-monsoon and post-monsoon seasons from 1891 to 2015.
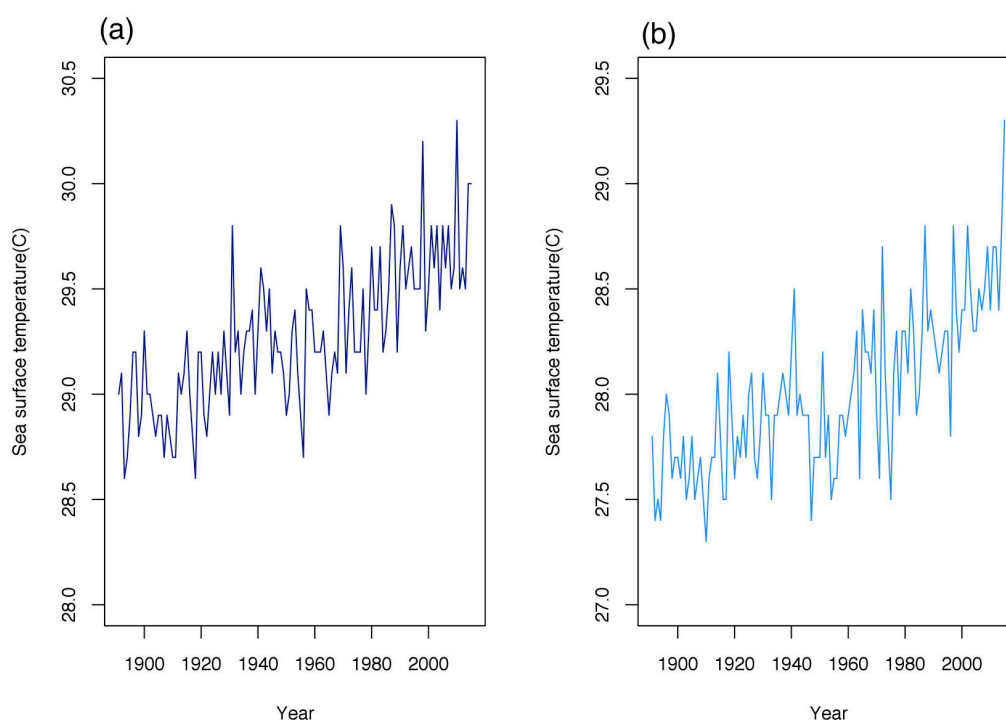
Figure 3.4: Annual maxima of sea surface temperatures (a) pre-monsoon and (b) post-monsoon from 1891 to 2015.

3.4.2.1   GEVfit

Once the annual maxima is achieved, the quantile plots of a stationary GEV (SGEV) and non-stationary GEV (NSGEV) models are constructed to check the goodness-of-fit in a pre-monsoon and post-monsoon. The results show that the qq plots of both the GEV models fits well with the data in both the seasons (Figure 3.5). It must be noted that the qq plots of SGEV model are simple to develop as quantiles does not change with time. But in the NSGEV model the quantiles vary with time and lack homogeneity in the distributional assumption, so modifications are needed before plotting the qq plots. In order to deal with non-stationarity, the sequence of

block maxima first needs to be transformed into the standard Gumbel distribution, $\bar{Z}_t$ using the following equation (Coles, 2001; Felici et al., 2007).

$$\bar{Z}_t = \log\left\{\left[1 + \hat{\xi}\left(\frac{Z_t - \hat{\mu}(SOI)t}{\hat{\sigma}}\right)\right]^{1/\hat{\xi}}\right\}, \qquad t=1,....m \qquad (3.11)$$

If Z_t, is a series of block maxima with distribution $G[\hat{\mu}(SOI)t, \hat{\sigma}, \hat{\xi}]$, then equation (3.11) produces a new standardized block maxima $\bar{Z}_t$ with a standard Gumbel distribution (Coles, 2001).

$$Pr\left\{\bar{Z}_t \leqslant z\right\} = \exp\left\{-e^{-z}\right\} \qquad (3.12)$$

The transformation removes the time dependence from the maxima, and then the quantiles of the transformed maxima can be compared with the empirical quantiles of the standard Gumbel distribution. The Figure 3.5 (b-d) shows the standardized quantiles for the NSGEV model. In addition to quantile plots, the Anderson Darling (AD) and Kolmogorov Smirnov (KS) tests are applied to assess the quality of fits of the GEV models. The null hypothesis of both tests is that the data follows the specified distribution. The p – values of both tests fail to reject the null hypothesis. Table 3.4 shows the result of both the tests.

Table 3.4: Anderson Darling and Kolmogorov Smirnov test statistics (p-values)

Test	Pre-monsoon		Post-monsoon	
	SGEV	NSGEV	SGEV	NSGEV
Anderson darling	0.3456	0.269	0.1263	0.289
Kolmogorov Smirnov	0.1374	0.371	0.225	0.345

3.4.2.2   Parameter estimates

The GEV model fitting provides three parameters (ξ, σ, and μ) for the staionary GEV and four parameters (ξ, σ, μ and μ_1) for non-stationary GEV. The estimated parameters of the stationary and non-stationary GEV in the pre and post monsoon periods are shown in Table 3.5. Maximum likelihood estimation (MLE)is used for the estimation of parameters (shape ξ, scale σ, and location μ). MLE is considered because it is simple to incorporate the non-stationary features in the distribution parameters as covariates (Shang et al., 2011).
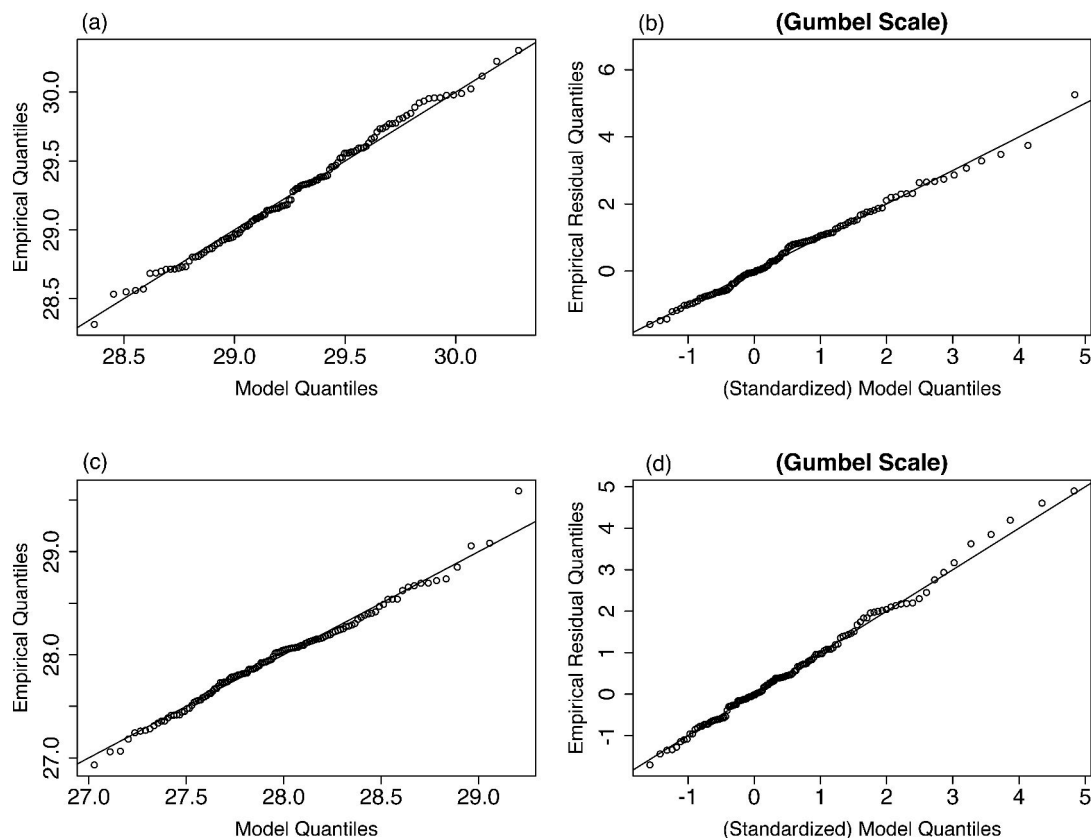
Figure 3.5: Quantile plots of (a-b) Pre-monsoon SGEV and NSGEV model, and (c-d) Post-monsoon SGEV and NSGEV model from 1891 to 2015.

Table 3.5: Parameter estimates and uncertainty of SGEV and NSGEV models

Parameter	SGEV		NSGEV	
	pre-monsoon	post-monsoon	pre-monsoon	post-monsoon
μ	29.08	27.83	28.78	27.49
$\Delta\mu$	0.041	0.045	0.039	0.023
σ	0.427	0.471	0.200	0.228
$\Delta\sigma$	0.028	0.031	0.013	0.014
ξ	-0.154	-0.209	-0.078	-0.245
$\Delta\xi$	0.045	0.044	0.054	0.039
μ_1			0.063	0.101
$\Delta\mu_1$			0.018	0.017
μ_2			0.006	0.007
$\Delta\mu_2$			0.005	0.000

3.4.2.3   Return Levels

The return levels are computed by placing the values of the shape and scale parameters in Eq 3.2, discussed in Section 3.3.1.1. Figure 3.6 displays the return levels versus the corresponding return periods (5, 10, 20, 50, 100, 200 years) of the stationary and non-stationary GEV models in both the seasons. The stationary

GEV model for the pre-monsoon season shows that the return levels of Arabian Sea SST reaches above 29°C, for the return periods of 2, 5, 10 years, and exceeds 30°C for the return periods of 20, 50, 100, and 200 years (Figure 3.6a). Whereas the post-monsoon show the return levels of SST over 27°C for shorter return periods of 2, 5, 10 years and above 28°C for longer return period of 20, 50, 100, 200 years (Figure 3.6c).
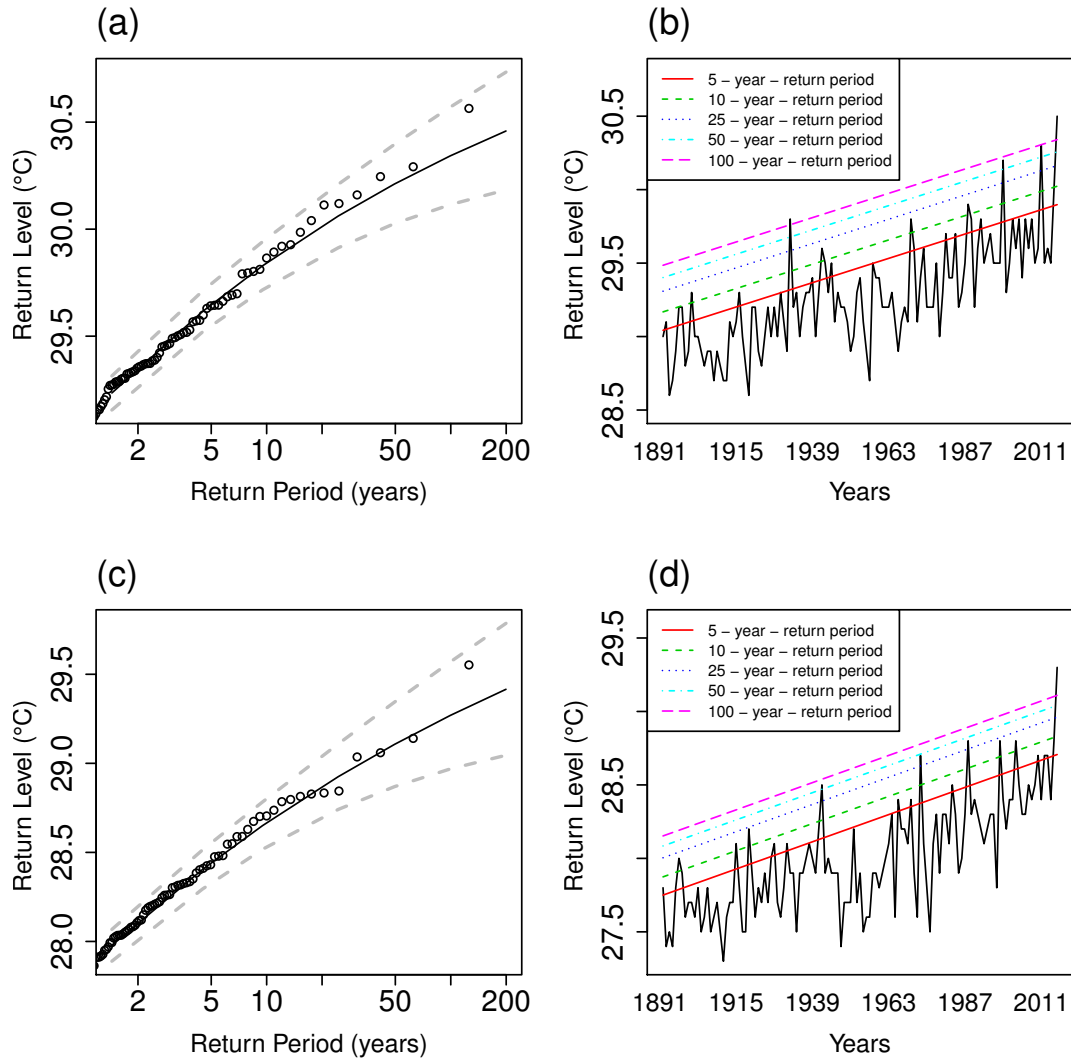
Figure 3.6: Return level plots of (a-b) Pre-monsoon SGEV and NSGEV model, and (c-d) Post-monsoon SGEV and NSGEV model.

The return levels of a non-stationary GEV (termed as effective return levels) is estimated by substituting the values of time-varying location parameter $\mu(t)$ in Eq 3.2. Effective return levels have interpretation similar to the stationary GEV return levels (i.e., the quantile corresponding to a specified return period), except that it varies depending on the time of year, keeping the probability of occurrence of an extreme event constant (Katz et al., 2002; Cheng et al., 2014). We use R-package "extRemes" developed for analysis of extremes to produce effective return levels

(Gilleland and Katz, 2011). Figure 3.6 (b & d) show the return levels versus the time covariate used in the linear regression (Eq 3.4). These plots are used to see the risks of extremes over time. For example, the return level of SST extremes is 29.6 °C corresponding to a 50-year return period (1891 – 1941) in a pre-monsoon, but it changes to 30.3°C over a 125-year (1891–2015) return period (Figure 3.6b). This means that we must expect the return level of SST extremes greater than 30.3°C for another 50-year (2016 –2066) return period. The non-stationary return levels of SST during post-monsoon exhibit the similar results with slight difference in return levels (Figure 3.6d). The return level for a 50-year return period (1891 – 1941) is 28.3 °C, and for a 125-year return period (1891-2015) it is 28.9°C. Thus, the probability of the return levels greater than 28.9°C is very likely in the next 50-years (2016-2066).

The diagnostic plots are not enough to decide that the assumptions are reasonable for both the GEV models (Figure 3.6). Therefore, we compare the models by applying likelihood ratio test and Akaike information criterion (AIC, Coles (2001), Akaike (1974)) discussed in section 3.3.1.3. The likelihood test favors the non-stationary GEV model, due to its significant improvement over the stationary GEV (Table 3.3. The Akaike criterion also supports the non-stationary model, as it acquires the minimum values of AIC in both the seasons.

3.4.3   Prediction of cyclogenesis using Poisson regression model

The tropical cyclones mostly develop in the Arabian Sea during inter-monsoon seasons, depending upon the intensity of sea surface temperature (SST). Higher SST ($> 26°C$) increase the chances of a cyclone to develop in the Arabian Sea, but lower SST ($< 26°C$) reduces this probability (Evan and Camargo, 2011). Along with a high SST, thermodynamically unstable atmosphere, and weak tropospheric wind shear is required to have a favorable environment for the cyclone development during these seasons (McPhaden et al., 2009). But all these favorable conditions can be influenced by the Southern Oscillation Index (SOI) which measures the strength of El Niño and La Niña events,that is indicated by its negative (El Niño) and positive (La Niña) phases (Ho et al., 2006; Trenberth, 2013).

The relationship of tropical cyclogenesis with El Niño (SOI -ve) and La Niña (SOI +ve) has been studied by several researchers (Camargo et al., 2007; Girishkumar and Ravichandran, 2012; Sumesh and Ramesh, 2013; Mahala et al., 2015). They observed severe cyclonic activity during La Niña conditions, and low cyclonic activity during El Niño conditions in the north Indian Ocean. Most of these studies have either included the entire north Indian Ocean or only focused on the Bay of Bengal, but the cyclonic activity occurring in the Arabian Sea and factors influencing it has not been investigated separately. Here, we have used a Poisson regression model to analyze a correlation of cyclonic activity with different variables (SST, SOI).

We develop a Poisson regression model (Eq 3.10) with cyclonic activity (TD, CS, and SCS) in the Arabian Sea as a predictand, and SST (favorable, $> 26°C$ and unfavorable conditions, $< 26°C$) and SOI phases (+ve, -ve) as predictors. We selected SST and SOI as predictors due to their strong influence on tropical cyclones (Gray et al., 1992, 1994; Elsner and Schmertmann, 1993; Kim et al., 2010). Moreover, we concentrated mainly on two predictors in our regression model because more predictors may encounter a problem of over fitting and become no longer independent, making the model biased. The results of Poisson regression clearly shows a strong dependence of the cyclonic activity on the SST and SOI (Table 3.6), which gives us the confidence to use them in our model, to predict the frequency of TD, CS, and SCS in the Arabian Sea. The estimates and uncertainties of the regression parameter is shown in Table 3.6. It must be noted that the Poisson regression model we study here is the first one for the Arabian Sea basin.

For our analysis, we set three different ranges for the SST favorable conditions, i– $SST_{fav1} = 26°C - 28°C$, ii– $SST_{fav2} = 28° - 30°C$, and iii– $SST_{fav3} = 30°C - 32°C$, but for the SST unfavorable conditions a range is $SST_{unfav} = 23°C - 25°C$. We set different ranges because the extreme value analysis of SST shows that the Arabian Sea may experience high return values of SST during the cyclogenesis seasons, particularly in the pre-monsoon (Section 3.4.2.3). Furthermore, it will be interesting to see that out of three ranges which one is responsible for the highest probability of occurrence of TD, CS, and SCS in the Arabian Sea. In case of SOI, we consider the highest value of SOI during a negative (El Niño) and a positive (La Niña) phase over the last 125 years (1891–2015).

Table 3.6: Summary of a Poisson regression for the pre-monsoon and post-monsoon

Pre-Monsoon						
Parameter	**SST~ TDs**	**SST ~ CSs**	**SST ~ SCS**	**SOI~ TDs**	**SOI ~ CSs**	**SOI ~ SCS**
Estimate	0.49	0.35	0.58	0.11	0.25	0.27
Standard error	0.10	0.12	0.09	0.10	0.14	0.12
p–value	0.02	0.007	0.01	0.008	0.005	0.03
Post-Monsoon						
Estimate	0.43	0.57	0.61	0.23	0.29	0.24
Standard error	0.22	0.15	0.30	0.11	0.16	0.15
p–value	0.01	0.02	0.006	0.04	0.02	0.007

Firstly, we apply the Poisson regression taking the maximum value of SOI positive phase (La Niña) under all the ranges of SST. Later, we repeat the procedure taking maximum value of SOI negative phase (El Niño) with all sets of SST. The results of a Poisson regression model combining SST and SOI (+ve,-ve) during pre-monsoon and post-monsoon are shown in the Figures 3.7 and 3.8. In figures, the Arabian Sea shows no cyclonic activity occur under unfavorable conditions (SST $< 26°C$ and SOI +ve,-ve) in both the seasons.

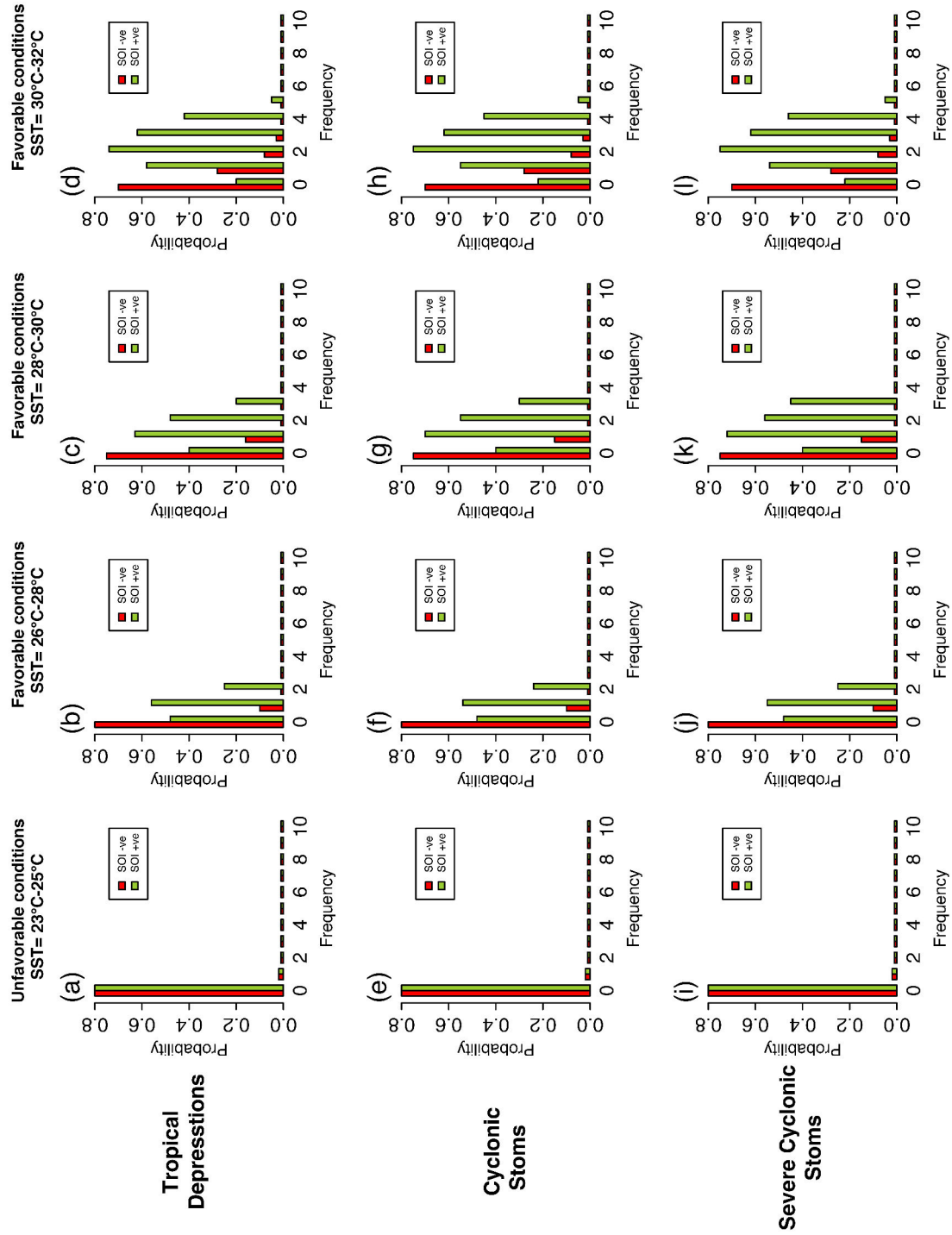We observe that the Arabian Sea experiences more TD, CS, and SCS under favor-
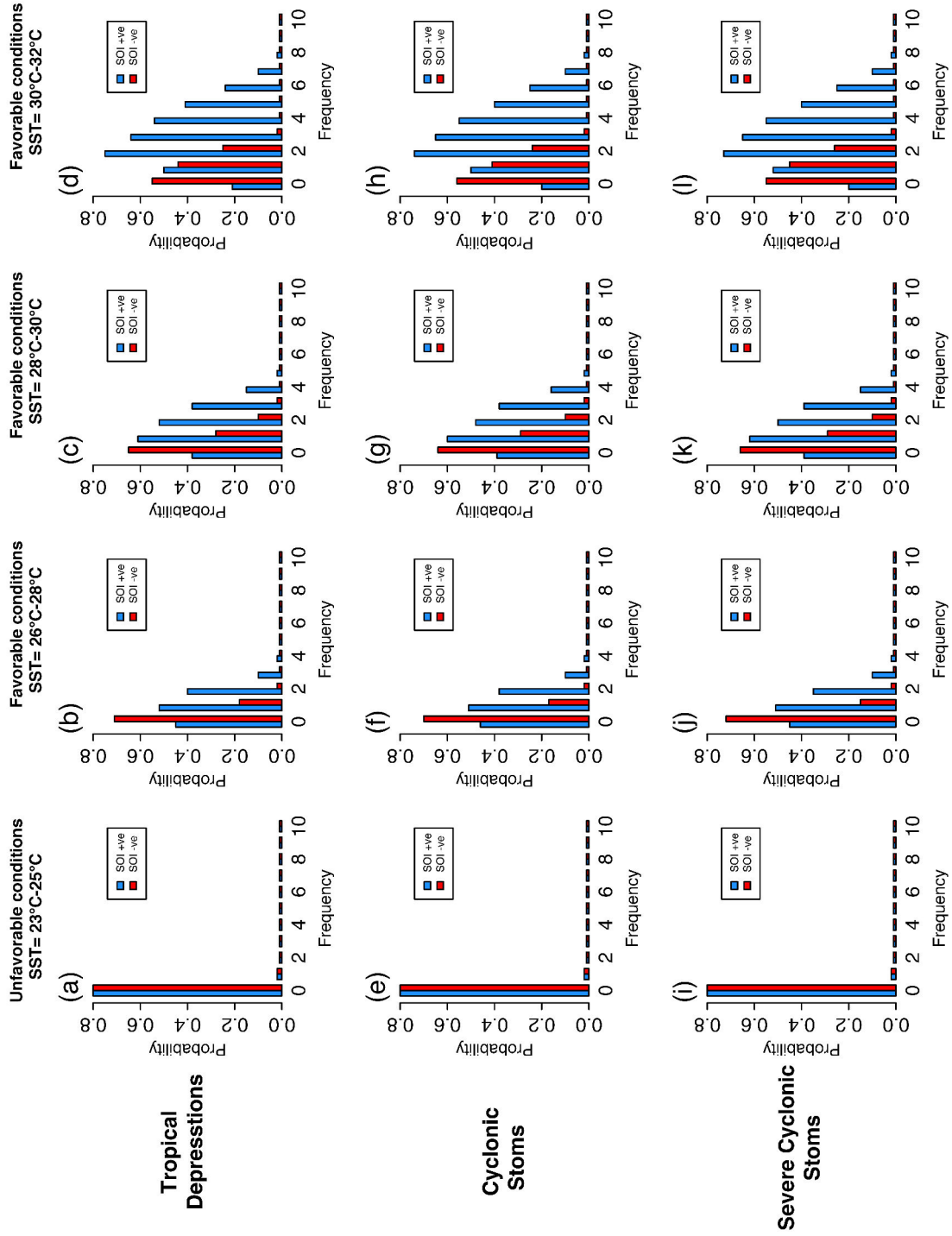
Figure 3.7: Probabilistic prediction of TD, CS and SCS during pre-monsoon in the Arabian Sea under unfavorable conditions SST $< 26°$C (a, e i), and favorable conditions i– $SST_{fav1} = 26°$C $- 28°$C, (b, f ,j), ii– $SST_{fav2} = 28° - 30°$C,(c, g, k), iii– $SST_{fav3} = 30°$C $- 32°$C (d, h, l).

Figure 3.8: Probabilistic prediction of TD, CS and SCS during post-monsoon in the Arabian Sea under unfavorable conditions SST < 26°C (a, e i), and favorable conditions i– SST$_{fav1}$ = 26°C − 28°C, (b, f ,j), ii– SST$_{fav2}$ = 28° − 30°C, (c, g, k), iii– SST$_{fav3}$ = 30°C − 32°C (d, h, l).

able conditions (SST > 26°C and SOI +ve) but, low frequency of TD, CS, and SCS under favorable conditions (SST > 26°C and SOI -ve) in the pre-monsoon and post-monsoon. The pre-monsoon (May – June) probabilistic prediction of TD, CS, and SCS occurring in the Arabian Sea shows that with every 2 degree rise in SST, particularly in a SOI +ve phase there is an increase in the frequency of TD, CS, and SCS . A threshold range SST_{fav1} predicts 1–2, SST_{fav2} indicates the likelihood of 3–4, and SST_{fav3} projects 5–7 TD, CS, SCS in the Arabian Sea during +ve SOI. While an obvious reduction in the frequency of TD, CS, and SCS has been observed under similar sets of SST favorable conditions during -ve SOI in the Arabian Sea. For instance, a low probability of 1, 2, 3 TD, CS, and SCS is predicted by the SST_{fav1}, SST_{fav2} and SST_{fav3} (Figure 3.7).

The post-monsoon (October – November) probabilistic prediction of TD, CS and SCS frequency in the Arabian Sea exhibits similar pattern like pre-monsoon, but with minor differences in the number of TD, CS, and SCS. The changes in the frequency of TD, CS, and SCS are apparent with the changes in the set threshold ranges of the SST and SOI phases (+ve, -ve). During SOI +ve phase the range SST_{fav1} shows 1–2 TD, SST_{fav2} predicts 2–3 CS, and SST_{fav3} indicates probability of 3–4 SCS in the Arabian Sea. On the contrary, during SOI -ve phase all the ranges of SST (SST_{fav1}, SST_{fav2}, SST_{fav3}) a very low probability of cyclonic activity (TD, CS, and SCS) is observed in the Arabian Sea. The probability of cyclonic activity in a post-monsoon is comparatively less than a pre-monsoon. One possible reason could be the change in the state of the ocean, as it started getting cooler during the post-monsoon period, resulting in less favorable conditions for the occurrence of SCS.

3.5   Summary and Conclusions

In this chapter, we have estimated the return levels of the SST extremes in the Arabian Sea during the pre-monsoon (May – June) and the post-monsoon (October –November) from 1891 – 2015, in a stationary and non-stationary climate.It is important to study the SST extremes in a changing climate because of the potential impacts it could have on the marine climate system and coastal communities. The changes in SST influence large-scale phenomena, such as tropical cyclones, El Nino, and south Asian monsoon systems, which impedes activities, such as fishing, trade etc. in the coastal communities. We have focused on the Arabian Sea SST extremes because they have never been extensively investigated. Furthermore, we have attempted to understand the connection of SST extreme values and SOI with the frequency of cyclogenesis in the Arabian Sea. We analyzed the probability of occurrence of cyclonic activity like TD, CS and SCS in the Arabian Sea using SST and SOI as an indicator for the selected seasons.

The Block Maxima (BM) method is applied to the UK Met office SST data for a duration 1891 – 2015, in order to estimate the return levels of SST in the Arabian

Sea over different return periods (2, 5, 10, 20, 50, 100, 200) during pre-monsoon and post-monsoon. The stationarity and trends in the SST data are handled by performing statistical tests like Augmented Dickey Fuller (ADF),and the Mann-Kendall (MK) tests. The block maxima are fitted to both the stationary and non-stationary Generalized Extreme Value distribution (GEV). The quality of the fits are tested with the Anderson-Darling and Kolmogorov-Smirnov tests. Both the GEV models fits well with the data. Therefore, likelihood ratio test and and Akaike Criterion is applied to choose the best model. Both tests favors a non-stationary GEV model(NSGEV) over the stationary GEV (SGEV).

The pre-monsoon SST extremes are assessed by the both GEV models. The 2, 5, 10, 20, 50,100, 200 year return periods shows return levels $> 29°C$ in the Arabian Sea. While in post-monsoon the return levels show SST $> 28°C$ from 5 to 200 year return time. It is well known that the cyclonic activity starts when the underlying SST is above a threshold $26°C$ (Gray, 1968). The SST extremes in both seasons show probability of a cyclogenesis in the Arabian Sea. But the return levels of SST extremes during pre-monsoon show slightly higher values than the post-monsoon. Hence, indicating more chances of a cyclonic activity in the Arabian Sea during a pre-monsoon than a post-monsoon under the changing climate.

The SST above $26°C$ is considered as one of the triggering factors in cyclone formation in the Arabian Sea (Dare and Mcbride, 2011). So, we plot a seasonal cycle of SST and frequency of TD, CS, and SCS in the Arabian Sea from 1891 to 2015, to observe a relation between them. It is found that the peak activity of TD, CS and SCS in the Arabian Sea occurs either during May – June or October– November, when SST are $>26°C$. Southern oscillation index (SOI) also palys a vital role in an active or passive cyclonegensis (Mahala et al., 2015). Since, SST and SOI are two important indicators of cyclogenesis, we applied Poisson regression to investigate the dependence of TD, CS, SCS on the SST and SOI. The results show positive correlation and dependence of cyclogenesis on SST and SOI. This correlation can be used to predict the cyclones in the Arabian Sea using a predictive power of the Poisson regression model.

We developed a Poisson regression model to predict TD, CS and SCS in the Arabian Sea using predictors; SST and SOI. Two types of SST conditions are set in the Arabian Sea (1) favorable ($SST_{fav1}= 26 - 28°C$, $SST_{fav2}= 28 - 30°C$, and $SST_{fav2}= 30 - 32°C$), and (2) unfavorable ($SST_{unfav}= 23 - 25°C$). SOI is considered for both positive phase (La Niña) and negative phase (El Niño). The results show that under unfavorable conditions of SST and SOI +ve,-ve phases no cyclonic activity occurs in the Arabian Sea. The favorable conditions reveal more cyclonic activity (TD, CS, and SCS) in Arabian Sea when the SOI is positive rather than negative during both inter-monsoon seasons. Our model predicts likelihood of $1 - 2$ TD, $3 - 4$ CS and 5–7 SCS in a pre-monsoon, and $1 - 2$ TD, $2 - 3$ CS and $3 - 4$ SCS in a post-monsoon, under favorable conditions of SST and SOI +ve phase. A very low probability of TD, CS and SCS is predicted by the model during SOI -ve phase.

The coastal communities in Pakistan are vulnerable to hazards both from land (e.g river flooding) and the Arabian Sea (cyclones, storm surge and sea level rise). The TD, CS, and SCS are more more frequent than super cyclones in the Arabian Sea specifically in a pre-monsoon and a post monsoon. Our findings reveal that with an each degree rise in SST, there is a high probability of TD, CS and SCS genesis in a pre-monsoon than a post-monsoon in the Arabian Sea. This increase in the cyclonic activity can affect the port activities, fishing, and may harm the marine species like coral reef and mangroves. Moreover, strong winds, sea water intrusion, and rainfall creates problems for the nearby coastal communities (Pelling and Blackburn, 2014). Therefore, an effort has been made here to provide an information regrading cyclonic activity in Arabian Sea to the local coastal administrations for planning against the upcoming challenges and minimizing the risks for the coastal communities.

Chapter 4

Return levels of precipitation extremes in southern Pakistan

4.1 Introduction

Extreme precipitation events have gained considerable attention worldwide due to the hazardous consequences and significant economic damages (Easterling et al., 2000). An extreme precipitation event can be referred to as a very intense precipitation in a short duration or persistent precipitation over a long period of time in a region (Beguería et al., 2011). The extreme precipitation events and their impacts are now more pronounced in many regions around the world. (Mueller and Pfister, 2011; Zahid and Rasul, 2011; Dourte et al., 2013; Yilmaz et al., 2014). For instance, Sindh province of southern Pakistan has become an extremely vulnerable region due to changing precipitation patterns, extreme precipitation events, and floods associated to them.

Sindh has an arid climate and requires a supplementary irrigation for agriculture activities (Chaudhry and Rasul, 2004). It is mostly prone to prolong droughts with an occasional extreme precipitation events that leads to flooding. Historically, Sindh has experienced the worst prolong droughts extending over a couple of years (1968–69, 1971–74, 1985–87, and 1999–2002). The major source of precipitation is summer monsoon (June – September) in Sindh. Several studies have analyzed precipitation variability in this region, and found no trends in summer monsoon precipitation over the last 50 years (Chaudhry et al., 2009; Afzal et al., 2012; Salma et al., 2012; Hanif et al., 2013). However, extreme precipitation and flood events are more apparent recently (Zahid and Rasul, 2011; Tariq and Van de Giesen, 2012; Hussain and Lee, 2014; Kazi, 2014).

Extreme precipitation events have complex and non-uniform spatial patterns during monsoon in Sindh. Therefore, diagnostic studies have been carried out to understand the link between the occurrence of intense precipitation and changes in monsoon by the regional researchers (Rasul et al., 2005; Hasan and Rasul, 2008).

The orientation and titling of the Tibetan High is held responsible for a heavy precipitation in 2011, as it blocks the monsoon currents to enter the northern parts and persists over Sindh (Cheema et al., 2012). A link between the changes in extreme precipitation and monsoon dynamics have also been investigated with the CMIP5 future scenarios by Freychet et al. (2015). They observed an increase in the atmospheric moisture content during monsoon which is a key factor in explaining the changes in precipitation extremes. Kalim and Shouting (2012) also reported an enhancement in moisture flux over Arabian Sea that can contribute in more intense precipitation in southern Pakistan.

The southern Pakistan has a warm climate and it is becoming even warmer (Zahid and Rasul, 2012). Scoccimarro et al. (2013) examined the heavy precipitation events in a warm climate and predicted more frequent precipitation extremes by the end of the twenty-first century. Ikram et al. (2016) also found that the extreme precipitation are more likely in coastal areas like Karachi and Badin of southern Pakistan. Hence, we need more reliable estimates of the probability of the precipitation extremes in Sindh for coastal-land planning and management.

In this chapter, we estimate the return levels of precipitation extremes in 5, 10, 25, 50, 100, and 200 year return periods. We apply Peaks Over Threshold (POT) method on the daily precipitation data of nine weather stations of Pakistan Meteorological Department. The study period comprises summer monsoon (June-September) for a period 1980 – 2013 (33 years). The POT provides more efficient use of data since it takes into account more than one extreme value per year, and has better properties of convergence when finite datasets are considered (Lucarini et al., 2016).

4.2   Data

The data analyzed in this study is the daily precipitation data from 1980 – 2013, provided by Pakistan Meteorological Department. The data is obtained from nine weather stations; Jacobabad, Mohenjo-daro, Rohri, Padidan, Nawabshah, Hyderabad, Chhor, Karachi, and Badin. We have selected nine stations, which contain precipitation records with minimum missing values after 1980, and are suitable for the extreme precipitation analysis. An additional criterion is that only those stations are chosen where no changes occurred in measuring instruments during the last 33 years (Brunetti et al., 2006). We restrict our analysis to summer monsoon season, June-July-August-September (JJAS), as it is a peak period for extreme precipitation spells and floods.

4.2.1   Extreme precipitation data preparation and threshold selection

The preparation of extreme precipitation data for all the nine stations is the most important step in the extreme value analysis. There are two popular ways to do it, 1) Block Maxima (BM) and 2) Peaks Over Threshold (POT) (Thompson et al., 2009). Here, we preferred POT approach due to the short duration of data (33 years), as in BM the smaller sample size affects the accuracy of the parameter estimates (Frei and Schär, 2001). Moreover, the POT method can investigate the frequency as well as magnitude of the extremes, and is recommended for the estimation of frequency and intensity of extreme events (Re and Barros, 2009; Tramblay et al., 2013). However, the single limitation of POT is that it produces dependent data (in clusters), so we need to remove the dependency of data prior to its use. The independence of data is very important in extreme value analysis, therefore we use extremal index θ to remove the data dependencies (Loynes, 1965; O'Brien, 1974; Davison and Smith, 1990). Extremal Index θ measures the degree of clustering of extremes. It ranges between 0 and 1, ($\theta = 0$ means strong clustering and dependence, $\theta = 1$ absence of clusters and independence). Leadbetter (1983) interprets $\frac{1}{\theta}$ as the mean number of exceedances in a cluster. The short-term correlations (daily time scale) lead to the clusters in the time series, are investigated by computing the extremal index θ in all time series, and are treated using the standard declustering technique by Ferro and Segers (2003).

The selection of an appropriate threshold is another critical step of the POT analysis. It is essential to choose a threshold that is high enough to be in the asymptotic limit of the distribution of exceedances, but low enough to have ample data for the fit.Several procedures of threshold selection are suggested by the researchers (Coles, 2001; Katz et al., 2005). One of them is the use of mean residual plot, recommended by Beguería et al. (2011); Coles (2001). The mean residual plots show the relationship between different thresholds and mean excesses (i.e. peaks above the threshold). Basically, mean excess is a linear function of threshold in Generalized Pareto Distribution (GPD) (Coles, 2001). So, the threshold is selected where the mean residual plot shows linearity (Hu, 2013). In this study, we use the mean residual plots to select the threshold for all nine time series.

4.3   Methodology

Precipitaiton extremes are analyzed by the Peaks Over Threshold (POT) approach (Coles, 2001; Lucarini et al., 2016) for all nine stations. In this analysis, extremes are defined as exceedances over threshold distributed according to the Generalized Pareto Distribution (GPD), which is characterized by two parameters, the shape ξ and the scale σ. The shape parameter ξ determines the tail behaviour while the scale parameter σ measures the spread of the distribution (Sugahara et al., 2009).

The cumulative distribution function of GPD isgiven by (Coles, 2001).

$$H(y) = \begin{cases} 1 - \left(1 + \frac{\xi y}{\tilde{\sigma}}\right)^{-1/\xi} & \text{for } \xi \neq 0, \\ 1 - \exp\left(-\frac{y}{\tilde{\sigma}}\right) & \text{for } \xi = 0, \end{cases} \tag{4.1}$$

where $1 + \xi y/\tilde{\sigma} > 0$ for $\xi \neq 0$, $y > 0$ and $\tilde{\sigma} > 0$.

For a negative shape parameter, $\xi < 0$, the distribution is bounded (beta distribution), for vanishing shape parameter, $\xi = 0$, the distribution is exponential, and for a positive shape parameter, $\xi > 0$, the distribution has no upper bound (Pareto distribution). The shape parameter ξ and the scale parameter σ for all the time series are calculated by the maximum likelihood estimation method (MLE). On the basis of the shape and scale parameters ξ , σ, the return levels (RLs) of the precipitation extremes (frequency and intensity) are estimated for various return periods (2,5,10,20,50,100, and 200) by using Equation (4.2) for all stations (Coles, 2001).

$$y_N = u + \frac{\sigma}{\xi}[(Nn_y\zeta_u)^\xi - 1] \tag{4.2}$$

where N represents the return period, n_y is the number of observations per year, ζ_u is the probability of an individual observation exceeding the threshold u, the shape parameter is ξ and the scale parameter is σ. Further details of GPD can be studied in Lucarini et al. (2016); Sugahara et al. (2009); Coles (2001).

This study is performed in three steps:

1. The data is prepared for the POT analysis as discussed in Section 4.2.1 and passed through trend and stationary tests to check the trends and stationarity in all time series.

2. Thresholds are selected using the mean residual plots of all stations.

3. GPD model is used to estimate the return levels of the extreme precipitation events for different return periods (2, 5, 10, 20, 50, 100, and 200) considering the time interval from 1980 to 2013.

4.4 Results and Discussion

4.4.1 Trend and Stationarity tests

Trend tests are mostly grouped in to two types: parametric and non-parametric tests. Bouza-Deaño et al. (2008) suggests that the non-parametric tests are more

appropriate for precipitation data. Mann-Kendall (MK) test is a widely used non-parametric test to detect the trends and long term correlations in the precipitation data (Yue et al., 2002). The details of MK test can be seen in Kundzewicz and Robson (2000). The MK test is applied to the daily precipitation data of all nine stations, over a period of 1980 – 2013 in southern Pakistan. MK test can detect a trend in the data, but can not assure the non-stationary of the time series, even if the trends are statistically significant. Therefore, we use Augmented Dickey Fuller (ADF) test to check the stationarity in the data (Dickey and Fuller, 1979; Sen and Niedzielski, 2010). The ADF test is proved to have a good capability to see stationarity in hydrometeorological data (Wang et al., 2006; Yoo, 2007). The null hypothesis of the ADF test is non-stationarity of the data. We apply ADF to the data at 0.05 significance level. Therefore, if the p–value is higher than the significance level, the null hypothesis is rejected. The trend analysis (MK test) has indicated no significant trends of extreme precipitation in any of the stations. Similar findings about summer monsoon precipitation in Sindh are reported by Chaudhry et al. (2009); Afzal et al. (2012). Furthermore, the stationarity analysis (ADF test) has shown no significant trends in any of the nine stations. Table 4.1 show the results of trends and stationarity tests.

Table 4.1: Trend and Stationarity test resutls

Stations	Test Statistics (p–values)	
	Mann-Kendall	Augmented Dickey Fuller
Jacobabad	0.76844	0.040
Mohenjo-daro	0.2641	0.016
Rohri	0.4384	0.031
Padidan	0.1734	0.027
Nawabshah	0.3083	0.019
Hyderabad	0.3483	0.012
Chhor	0.4583	0.045
Karachi	0.1145	0.038
Badin	0.1714	0.005

4.4.2   Threshold selection

The mean residual plots are used to determine the appropriate threshold for all nine stations as mentioned earlier in Section 4.2.1. The mean residual plots, involves plotting u against the 'mean excess' (the mean of the exceedances of u, minus u), for a range of values of u. The plot should be linear above the threshold at which the GPD model becomes valid (Bramati et al., 2014).

For instance, in case of Jacobabad the graph curve is approximately linear and stable from $u = 0$ to $u = 40$, and after that it decays. It means that we should choose the threshold $u = 40$ because after that there is no stability. But if we take $u = 40$, we will have too few exceedances above a threshold to make meaningful inferences. Moreover, the information in the plot for large values of u is unreliable due to the limited amount of data on which the estimate and confidence interval
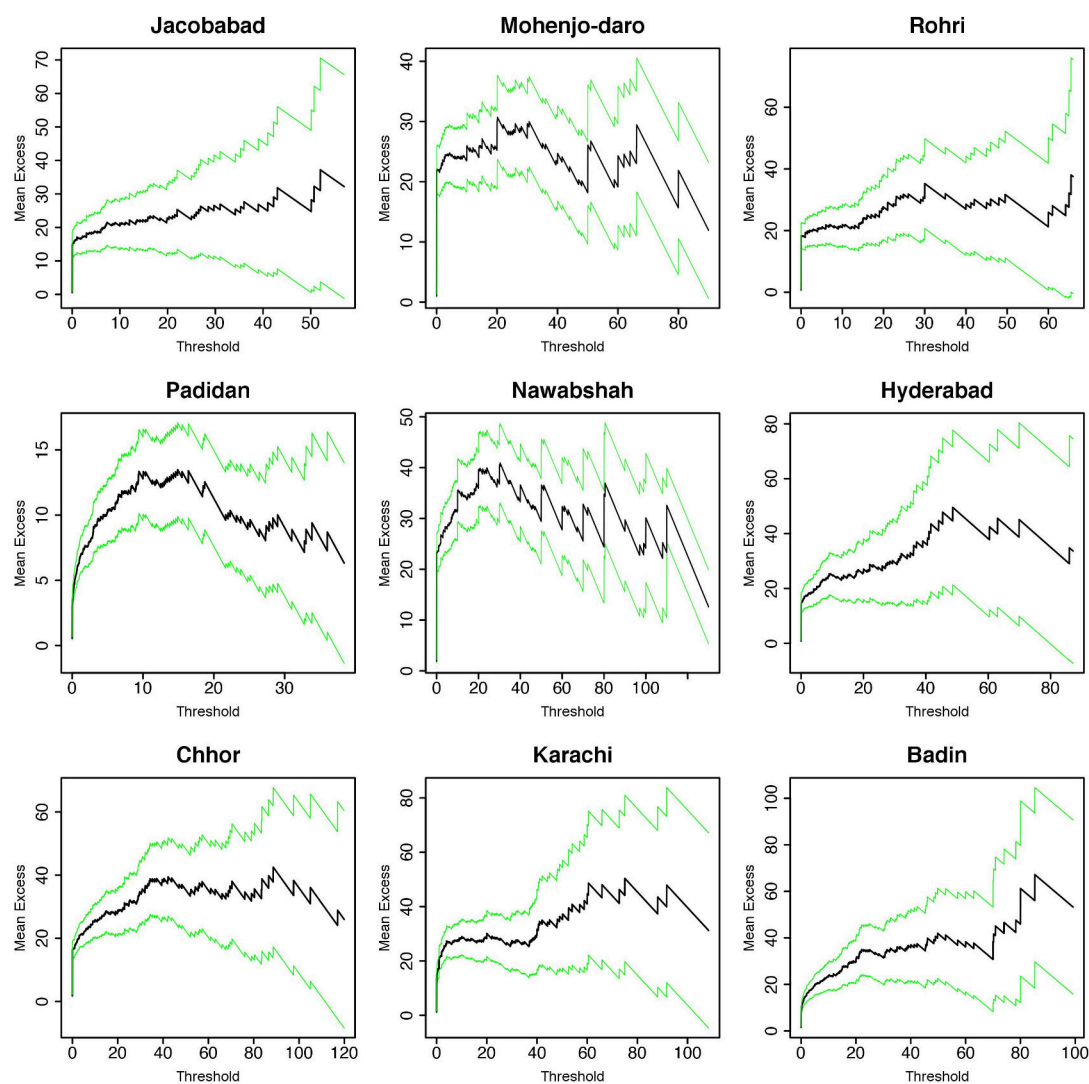
Figure 4.1: Mean residual life plots of daily precipitation (mm/day) in all nine-stations of Sindh.

are based (Coles, 2001). Therefore, it is probably better to set the threshold low enough to be in the asymptotic regime and high enough to have ample data above it, like for Jacobabad $u = 15$ is good enough to perform the POT analysis. The threshold values differ from station to station in a range $10 - 25$ mm according to the mean residual plots of that station. The extreme precipitation events in Sindh, Pakistan are investigated by following a threshold of individual station (Figure 4.1).

4.4.2.1   Goodness of Fit

The next step after the threshold selection is to determine the goodness-of-fit using the quantile plots usually known as qq plots. The qq plots are the most common diagnostic plots to check that how well data fits to the GPD model.

In qq plots, the observed data is displayed on the y-axis and model quantiles are
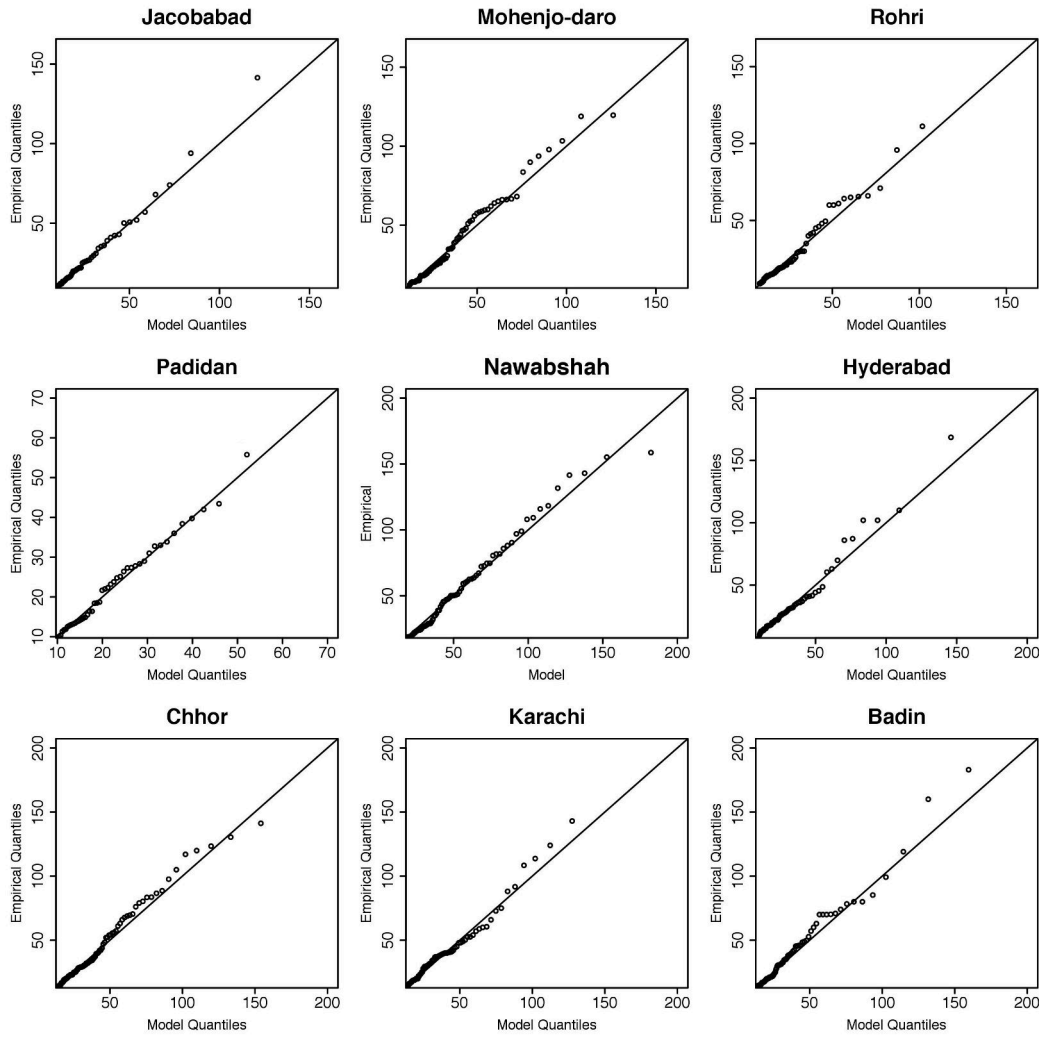
Figure 4.2: QQ plots of extreme precipitation (mm/day) data in all nine-stations of Sindh.

shown on x-axis (Figure 4.2). The results show that the extreme rainfall data fits well with the GPD in almost all stations with some deviations at the higher quantiles in Hyderabad and Badin. The statistical tests like Kolmogorov- Smirnov (KS) test and Anderson darling (AD) test are applied on all the stations to check the quality of the fits (Di Baldassarre et al., 2009). The p – values given in Table 4.2 shows that the two distributions are homogeneous.

Table 4.2: Results of the Kolmogorov Smirnov (KS) and Anderson Darling (AD) tests.

	GPD model								
	$p-$ **value**								
Test Statistics	**JAC**	**MJD**	**RHI**	**PDN**	**NWS**	**HYD**	**CHR**	**KHI**	**BDN**
Kolmogorov Smirnov	0.2993	0.2682	0.8334	0.4342	0.6591	0.8437	0.4881	0.4335	0.2732
Anderson Darling	0.2339	0.1374	0.7873	0.1348	0.6367	0.8835	0.3665	0.4077	0.1425

4.4.2.2   Parameter Estimates

The shape ξ and the scale σ parameters of GPD are estimated using maximum likelihood estimation (MLE) method Shang et al. (2011). The shape parameter ξ determines the tail behavior of the distribution. The results show that the shape parameter ξ is larger than zero at all stations and lie within a range 0.01 – 0.82 (Table 4.3. The positive value of the shape parameter indicates a heavy-tailed distribution, with no upper bound and decays polynomially. The highest values of shape parameter ξ are found in Nawabshah, Hyderabad, Chhor, Karachi, and Badin, which means that the extreme precipitation events are more likely in these regions.

Table 4.3: Parameter estimates and standard errors for the summer monsoon precipitation.

Stations	Shape ξ	Standard Error $\Delta\xi$	Scale σ	Standard Error $\Delta\sigma$
Jacobabad	0.03	0.05	4.1	0.34
Mohenjo-daro	0.20	0.13	3.69	1.73
Rohri	0.01	0.19	3.41	0.43
Padidan	0.04	0.14	4.21	0.67
Nawabshah	0.82	0.13	8.00	1.13
Hyderabad	0.58	0.17	6.51	1.31
Chhor	0.56	0.09	8.30	0.85
Karachi	0.53	0.12	8.40	0.21
Badin	0.52	0.11	9.55	1.25

The scale parameter σ measures the width and variability of the GPD distribution. The scale parameter σ range from 3.41 to 9.55 showing high variability in all stations (Table 4.3). The highest values of the scale parameter σ is observed in Nawabshah, Hyderabad, Chhor, Karachi, and Badin (Table 4.3). This indicates that the variability of precipitation extremes is higher at these stations, and one can expect higher return values of precipitation here than one might have expected.

4.4.2.3   Return Levels

The return levels (RLs) derived from the GPD model are shown in Figure 4.3. Here, the RLs indicates the probability of the precipitation intensity over 2, 5, 10, 20, 50, 100 and 200 years return period. The results show a RL of 50 mm/day for a 10 year return period, and between 50 mm/day - 100 mm/day for a 25 year return period in all stations.

The urban flash floods are produced when the precipitation intensity exceeds 100 mm/day, and due to the poor drainage capacity of that station, for example floods 2010 and 2011 in Karachi (Rasul et al., 2005; Kazi, 2014). Our results demonstrate the precipitation events > 100 mm/day, and > 150 mm/day against a 50 year return period, and 100 year return period in Jacobabad, Mohenjo-daro, Rohri, Nawabshah, Hyderabad, Chhor, Karachi, and Badin. (Ali and Iqbal, 2013). In
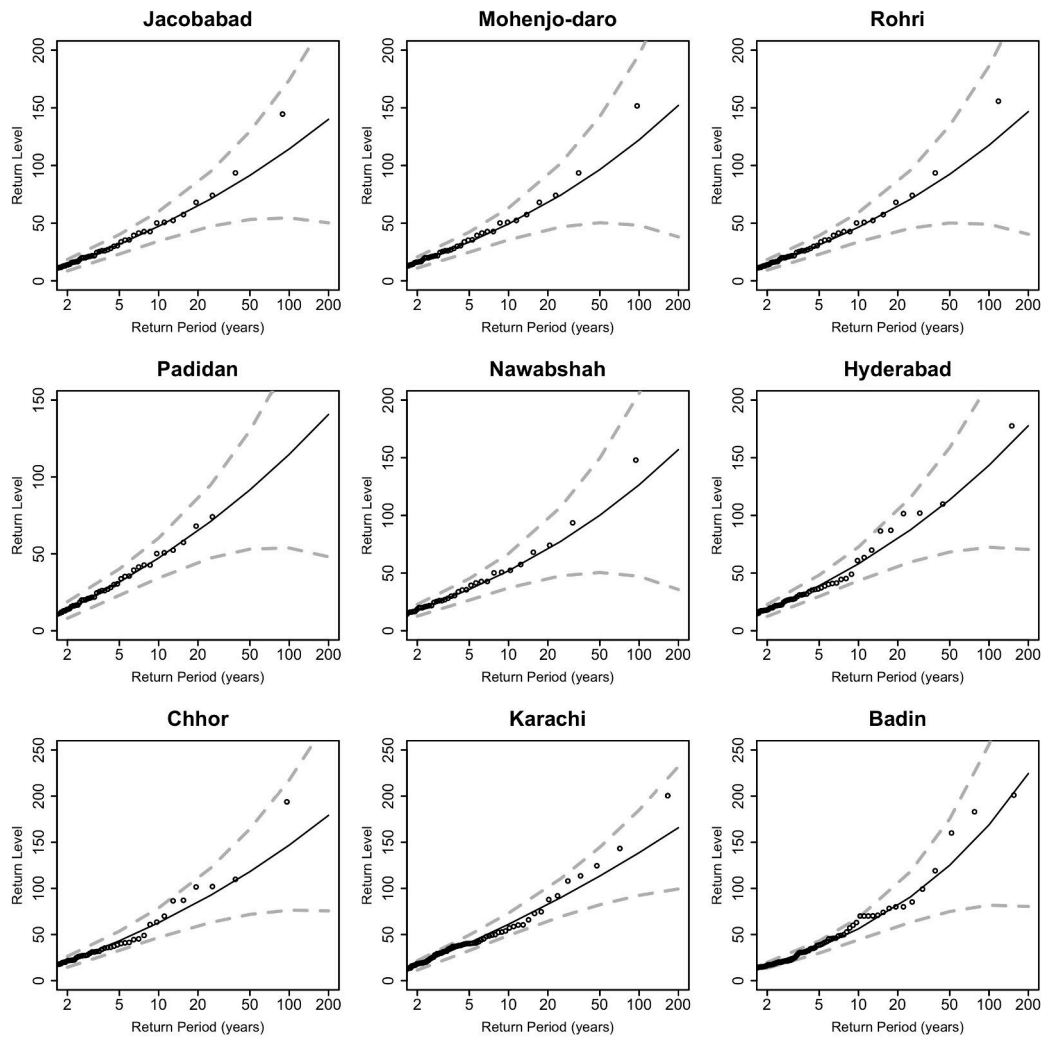
Figure 4.3: Return levels of extreme precipitation (mm/day) derived from GPD model in all nine-stations of Sindh.

this analysis, Padidan is the only station where the precipitation intensity (RLs) exceeds 50 mm in a 50 year return period.

The spatial maps of the precipitation return levels are also prepared to give a detailed overview of precipitation extremes in Sindh (Figure 4.4). The maps are restricted to 5, 10, 25, and 50 years return period due to short duration of a base period (1980 – 2013). The results show a probability of precipitation events greater than 100 mm/day in 25 and 50 years return period throughout Sindh except Padidan. While the RL above 150 mm/day are more evident in southern regions like Nawabshah, Hyderabad, Chhor, Karachi and Badin. Padidan is the only station which differs form others in the region, but it seems to have RL greater than 50 mm/day in 50 years, which is above its existing rainfall capacity. It is obvious from the maps that the higher return levels of precipitation are expected in regions like Nawabshah, Hyderabad, Chhor, Karachi, and Badin. Therefore, there is a strong need for planing an adaptation strategies for these regions to avoid the
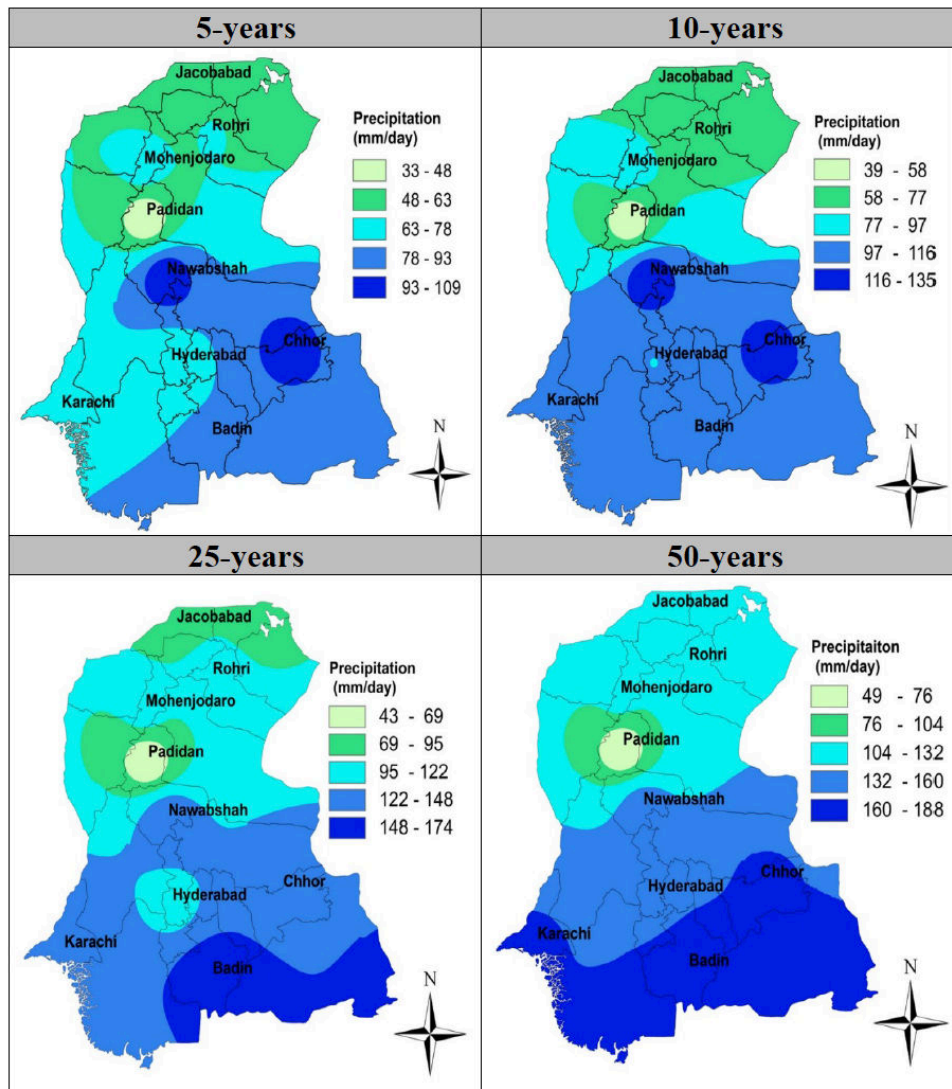
Figure 4.4: Spatial maps of extreme precipitation return levels (mm/day) in Sindh.

socio-economic losses in future.

4.5   Summary and Conclusions

The primary theme of this chapter is the assessment of the return levels for the extreme daily precipitation in the southern Pakistan (Sindh). We analyze daily rainfall data from 9 weather stations in Sindh over a period of 33 years (1980 – 2013). The largest frequencies of the extreme precipitation events concentrated during summer monsoon (JJAS), therefore it is selected for the study. Peaks over Threshold (POT) is implemented on all nine stations by constructing an extreme rainfall data (declustered POT data), checking trends and non-stationarity in the

data, and selecting a suitable threshold before applying a Generalized Pareto Distribution (GPD) on the POT data to estimate the return levels. POT method used in this study is not only suitable for the current research work, but it is applicable to several other case studies in different regions. It is good for finite data sets but the duration, quality and availability of data are the main limitations in this method.

Extreme precipitation events are considered as a natural hazard because of their association with the urban flooding. They severely impact the crops yield, livestocks, infrastructure, and port activities etc. The main findings of this study can be summarized as follows.

1. No linear trends are found in extreme precipitation data during summer monsoon in Sindh, because the extreme precipitation events are quite recent here. The rareness of events and short duration (33 years) of data in Sindh are not enough to detect a climate change signal in Sindh (Frei and Schär, 2001).

2. We used Generalized Pareto Distribution (GPD) to investigate the extreme precipitation events in Sindh. We found that GPD model fitted well to the precipitation data of all stations, according to the graphical qq plots and statistical tests.

3. We conclude that there are substantial differences in the return levels of extreme precipitation at all stations in Sindh with respect to a 50 year and 100 year return periods. The highest return levels at 2, 5, 10, 25, 50, and 100 years time is greater than 150 mm/day recorded in areas like Rohri, Nawabshah, Hyderabad, Chhor, Karachi, Badin, and exceeds 100 mm/day in areas such as Jacobabad and Mohenjo-daro. The lowest return levels are observed in Padidan station with precipitation intensity above 50 mm/day in a 50 to 100 year return period. This is due to the higher shape and scale parameters estimated for the southern stations. Our findings are in agreement with Ali and Iqbal (2013), who used GEV distribution and found similar results for the regions in Sindh.

The possible explanation of high return levels of precipitation in Nawabshah, Hyderabad, Chhor, Karachi, and Badin can be due to the intense warming of land (Zahid and Rasul, 2012, 2011), which increases the rate of evaporation in the atmosphere, creating instability in the hydrological cycle resulting into more extreme precipitation. Additionally, another important factor is the enhanced rate of moisture flux over the Arabian Sea that strengthened during summer monsoon. Kalim and Shouting (2012) investigated the link between moisture flux over Arabian Sea and extreme precipitation, and found that the moisture flux from Arabian Sea can contribute to intense precipitation events during monsoon in southern Pakistan.

Chapter 5

Introduction to web tool SindheX

5.1 Introduction

SindheX is a new online web-based tool (www.sindhex.org), which provides information on the return levels and return periods of major climate extremes occurring in Sindh, Pakistan. It focuses on extremes like temperature, wet-bulb temperature, precipitation, and sea surface temperature/cyclones of Arabian Sea) affecting Sindh. This web tool is an end product of the Climate-KIC project title "Extreme Events in Pakistan: Physical processes and impacts of changing climate", which belongs to the adaptation services platform (Decision Metrics & Finance theme) of the Climate-KIC. The results are shared for both the public and private stakeholders, who are interested in the frequency and intensity of extremes in Sindh. This tool is especially designed to guide the local administrations to prioritize the regions in terms of adaptations.

5.2 Graphical User Interface

The Graphical User Interface (GUI) of SindheX shows two types of maps 1) Google map and 2) Sindh map (Figure 5.1). A Google map is provided to describe the geography of the study domain, and a map of Sindh is used to show the results of different parameters at the nine stations considered in the study. GUI consists of four parameters; maximum temperature T_{max}, wet-bulb temperature TW_{max}, precipitation, and sea surface temperature, which are hold responsible for the extreme events in Sindh almost every year. The information regarding the SindheX, data, method, and visualization of the results is given in the left panel.
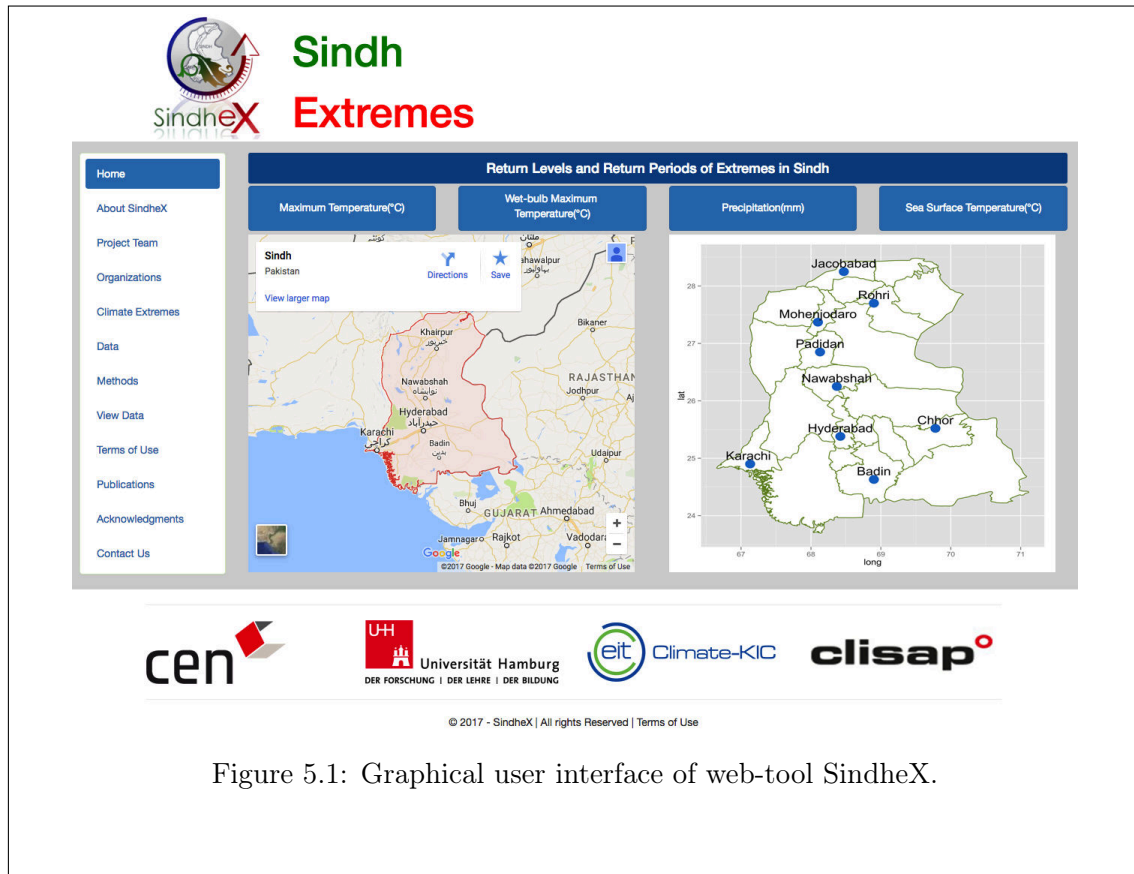
Figure 5.1: Graphical user interface of web-tool SindheX.

5.3   View results

Go to a website www.sindhex.org. To view results, users are required to register and login to visualize maps. Click "Register" to proceed to registration and "Login" to proceed to log in. Once you log in, please do the following;

1. Choose one of the variables for example "Wet-bulb Maximum Temperature" (Figure 5.2). You will see two categories.

   a. Temporal Maps

   b. Spatial Maps

2. Select "Temporal Maps Tab" it will activate all the stations geographically in the map of Sindh (Figure 5.3). Now click on the name of the city to view the data.

3. Click "Spatial Maps Tab", select the return period e.g. 5 years from the drop-down menu to view the maps (Figure 5.4).

4. Repeat the above-mentioned steps to view the results of other variables.
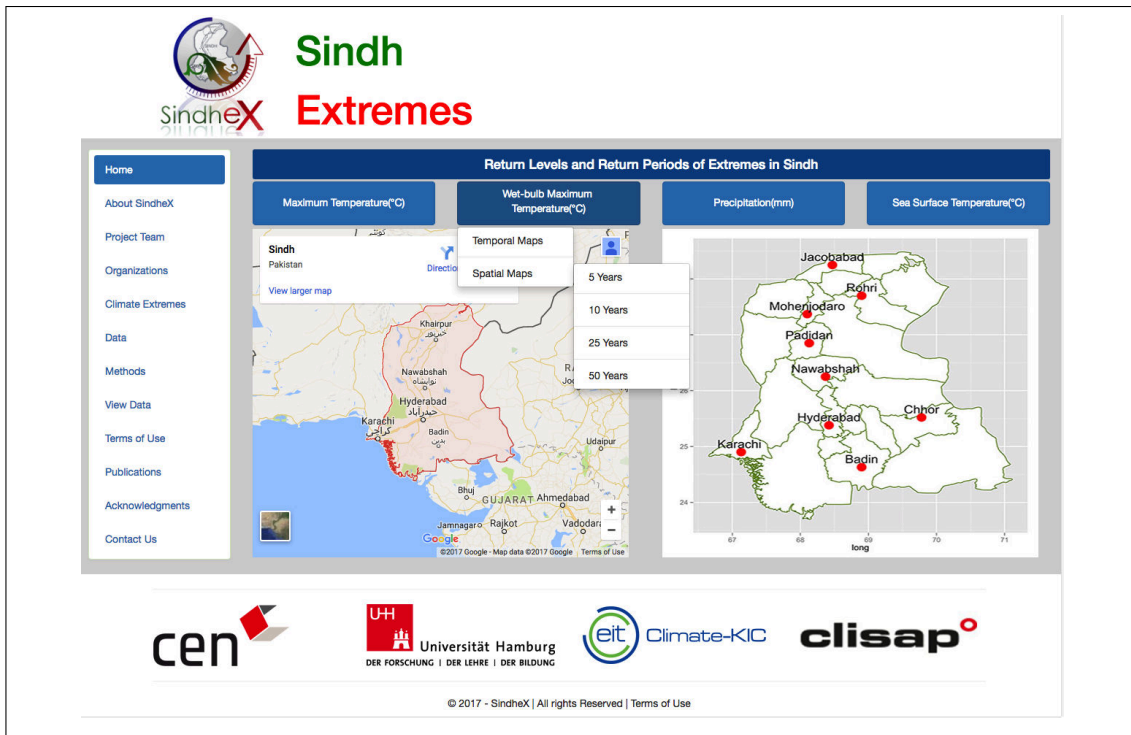
Figure 5.2: Visualization of the return levels of extremes in the graphical user interface.
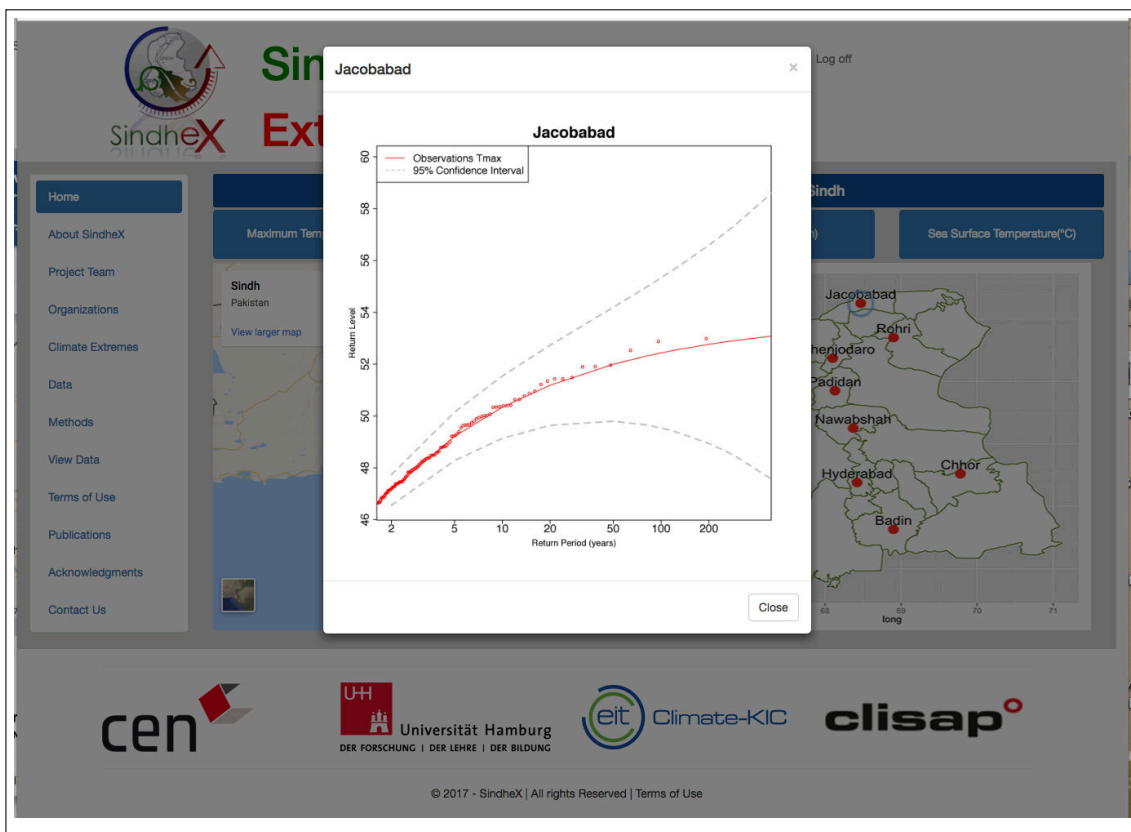
Figure 5.3: A temporal map showing max temperature (°C) return levels in Jacobabad.
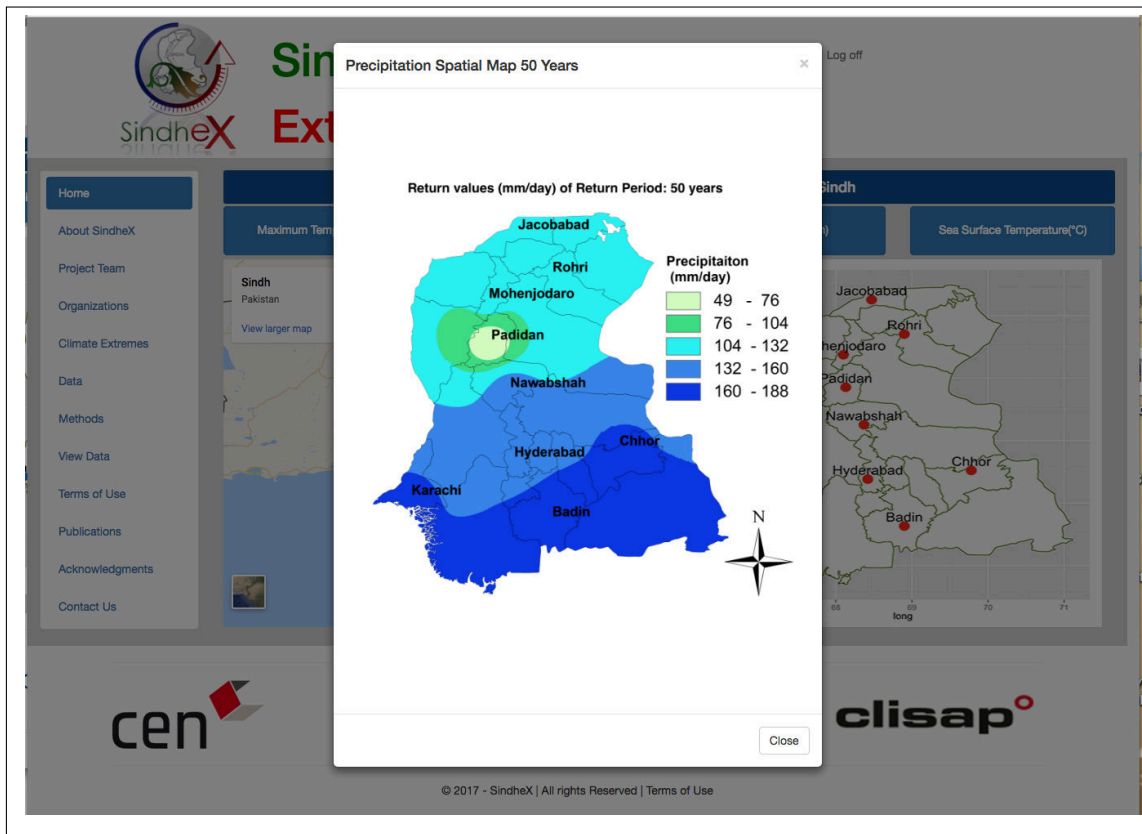
Figure 5.4: A spatial map showing precipitation (mm/day) return levels in 50 years.

Chapter 6

Conclusion and Outlook

This thesis analyzes the probability of occurrence of major extreme events in Sindh province of southern Pakistan. The statistical methods such as Block Maxima (BM) and Peaks over threshold (POT) based on a classical Extreme Value Theory (EVT) are applied to estimate the return periods and return levels of extreme events in Sindh. The main motivation of using EVT is that it provides a robust theoretical framework to estimate the probability of occurrence of extreme events larger than observed. Whereas, other statistical inference based on empirical models lack this predictive power. Additionally, EVT is quite a relevant approach in assessing the risks of extremes, but unfortunately it is vaguely mentioned and basically no results based on it are reported in the IPCC special report on managing the risks of extreme events to climate change adaptations in 2012 (IPCC, 2012). In this thesis, the analysis of extremes using EVT in Pakistan has been done for the first time, with a goal to convey this approach to the potential readers who might not familiar with this method. Moreover, all the results of thesis are shared with the local administrations and policy makers via web based tool "SindheX", so that they can make some concrete plans and implement adaptations region-wise.

Sindh province in southern Pakistan is the focal point in this work due to its susceptibility to recent frequent and intense climate extremes. Sindh is among one of the most vulnerable regions in Pakistan. Although, it is adversely affected by three types of extreme events i.e. temperature, precipitation and sea surface temperature/cyclones repeatedly almost each year, but least attention has been given to plan any type of adaptation strategies due to no information on recurrence of extremes. The region is unaware of the fact that these extremes are a single event or to which extent the event might occur in future. To address these concerns, all three extreme events are investigated separately in different parts of Sindh to identify the regions at high risks and in need of an immediate attention.

Sindh becomes very hot and humid during summer and many people become a victim of these extremely high temperatures (Zahid and Rasul, 2012; Imtiaz and Rehman, 2015). Two types of temperature extremes: (i) maximum air temperature extremes, T_{max} and (ii) maximum wet-bulb temperature extremes, TW_{max} are

considered in this thesis. The results show that the return levels reach above 50°C in Jacobabad, Mohenjo-daro, Padidan, Nawabshah, and exceeds 45°C in Rohri, Hyderabad, Chhor, Karachi, and Badin. The RLs of TW_{max} are analyzed above the human survivability threshold 35°C throughout the region. It is clear from the results that the human habitability in Sindh is already at high risks of hyperthermia, heat strokes, nausea, headaches, dehydration etc during summer (May –September) season. More than half of the population works in open fields to earn their livelihoods and becomes a victim of these extreme events. Besides population, the agriculture sector is also badly affected by the temperature extremes. The crops have certain threshold to tolerate heat and even a rise of one degree Celsius can cause detrimental changes in the phenological stages of the crops (Hatfield and Prueger, 2015). Moreover, a hot and humid weather are favorable for the production of pests and rapid spread in the crops. Sindh produces cotton, wheat, rice, mango, banana, and dates, so it is very important to know the correct frequency and intensity of temperature extremes. It is highly recommended that a contingency plan must be prepared and early warning system should be implemented for dealing with temperature extremes in Sindh.

The sparse network of weather stations and lack of long-term data are the main limitations in analyzing extremes. This is why the return levels of temperature extremes are also estimated by using ERA Interim reanalysis to look at how well ERA Interim data performs in Sindh against observations. The main objective is that if the ERA Interim dataset characterizes well the extremes, it could be an option for the regions within Sindh where no observational data is available. The findings show a clear difference of 3°C and 5°C in RLs between the weather station and ERA Interim datasets. Therefore, a simple bias correction is applied to the ERA Interim data to see the improvements in its performance in representing RLs of temperature extremes. The bias corrected ERA Interim T_{max} and TW_{max} show good correspondence with the meteorological station data, but statistically differences remains in most cases. Therefore, a more advanced bias correction method is recommended for analyzing extremes in any region before using the reanalysis precisely. All models (CMIP5, CMIP6, RCMs, CORDEX) use re-analysis as input, and generate information of extremes, that can lead to significant errors in prediction of present and future extremes. Therefore, in order to reduce the uncertainties in impact assessment, it is necessary to improve the re-analysis before using it in GCMs and RCMs. Furthermore, it is strongly proposed to use EVT approaches in all models to the study the properties of extremes, for meaningful predictions.

Sindh is vulnerable to extremes both from land (e.g river flooding) and the Arabian Sea (cyclones, storm surge, and sea level rise). The warming of Sea Surface Temperature (SST) and enhanced cyclonic activity in the Arabian Sea is obvious lately (Khan et al., 2008; Evan and Camargo, 2011; Muhammad et al., 2016). The cyclones develop in Arabian Sea every year but rarely make a landfall, yet they can impact the coastal communities with a heavy precipitation, storm surge, strong winds and flooding (Needham et al., 2015). In this thesis, the return levels (RLs) of Arabian Sea SST extremes are assessed in pre-monsoon (May – June) and post-

monsoon (October –November) seasons due to an extreme cyclonic activity within these seasons. The results show the RLs of pre-monsoon SST extremes > 29°C and the post-monsoon SST extremes > 28°C in the Arabian Sea. This concludes that the likelihood of cyclonic activity is equal in both the seasons, as SST above 26°C is known as one of the triggering factors for a cyclone formation in the Arabian Sea (Gray, 1968; Dare and Mcbride, 2011). But one must understand that with a changing climate and rise in SST more cyclones can appear in pre-monsoon rather than a post-monsoon. The tropical depressions (TD), cyclonic storm (CS), and severe cyclonic storms (SCS) are more frequent in the Arabian Sea than the super cyclones. In order to predict the probability of TD, CS, and SCS, a poission regression model is developed using SST and Southern Oscillation Index (SOI) as predictors. The results predict likelihood of 1–2 TD, 3–4 CS and 5–7 SCS in a pre-monsoon, and 1–2 TD, 2–3 CS and 3–4 SCS in a post-monsoon, under favorable conditions of SST and SOI +ve phase. A very low probability of TD, CS and SCS is predicted by the model during SOI -ve phase.

The precipitation extreme analysis in Sindh concludes no linear trends in the precipitation data during summer monsoon (June – September). However, the extreme precipitation events (> 100 mm/day) are more apparent and new in Sindh (Zahid and Rasul, 2011). These extreme precipitation events have been linked to the extremely high land temperatures, changes in monsoon dynamics and an enhancement in moisture flux over the Arabian Sea during summer monsoon (Kalim and Shouting, 2012; Freychet et al., 2015). The main reasons of the sudden extreme precipitation events in Sindh is not yet completely clarified by researchers. In this thesis, the return levels of the precipitation extremes in Sindh are analyzed by applying the Peaks over Threshold (POT) method on daily precipitation data during summer monsoon (June – September) from 1980 to 2013. The results predict the return levels of precipitation greater than 100 mm/day in Jacobabad, Mohenjo-daro, and greater than 150 mm/day of precipitation events in Rohri,Nawabshah, Hyderabad, Chhor, Karachi, and Badin of Sindh, in 50 and 100 year return periods. Padidan is the only station with return levels of precipitation exceeding 50 mm/-day in 50 - 100 years. The precipitation extremes > 100 mm/day and 150 mm/day are predicted in Sindh, which can cause urban flash flooding, for instance 2010 and 2011 floods in Karachi (Rasul et al., 2005; Kazi, 2014). Therefore, there is a strong need to plan the adaptation measures like rain water harvesting, small dams, building levees near the river to avoid floods, improved drainage capacity and establishment of flash flood forecasting system to minimize the risks from such an events.

The results of this thesis clearly show that the recurrences of extreme temperature, extreme sea surface temperature leading to cyclogenesis, and extreme precipitation is very likely in Sindh province of southern Pakistan in 50 year return period. The northern parts (Jacobabad, Mohenjo-daro, Rohri, Padidan) of Sindh are mostly affected by the temperature extremes, central parts (Nawabshah, Hyderabad) are impacted by both the temperature and precipitation extremes. While the southern parts (Chor, Karachi, and Badin) or the coastal communities are the most vulnerable to all three types of extreme events analyzed in this work. Therefore, it

is crucial that the administrations and policy makers take some serious actions to adapt to the future extreme temperatures, extreme sea surface temperature, frequent cyclonic activity, and extreme precipitation. All three types of extremes are currently affecting the region and will make situation worse if the accurate planning and adaptations are not implemented timely in the region.

Clearly, the probability of the extreme events is higher in Sindh, so an action plan must be prepared to implement adaptations in the vulnerable regions without further delays. It was important to convey and share the results of this thesis via proper platform to the all the stakeholders such as local administrators, energy sector, food and agriculture organizations (FAO), port authorities, water management authorities, governmental and non-governmental organizations, national disaster management authorities (NDMA), trade sector etc. in Sindh. Therefore, a web-tool "SindheX" is developed as a prototype for other regions in Pakistan and neighboring countries (India, Nepal, Iran, Afghanistan and Bangladesh). South Asian region share similar climatic characteristics, hence extreme events occurring in one region can easily influence the adjoining areas. For instance, any people died both in India and Pakistan due tot heatwave in 2015. Similarly, million of people were affected across India, Bangladesh and Nepal as a result of flooding in August 2017. Moreover, Cyclone Nilofar in Arabian Sea in 2014 affected the countries surrounding Arabian Sea. Therefore, a strong networking through research is required among these countries and different departments to reduce the risks of these disasters. This thesis can serve as a blue print for all South Asian countries. They can also analyze extreme events more robustly using the extreme value theory approaches and plan adaptations accordingly.

The results of this thesis will not only contributes to the regional planning, but can also be useful for the ongoing EU projects like Sindh Union Council and Community Economic Strengthening Support (SUCCESS), Civil Society Coalition on Climate Change (CSCCC), World Bank project like Sindh Resilience Project (SRP) and mega construction projects like China-Pakistan Economic Corridor (CPEC). As I repeatedly stated in this thesis, that the information on the returns of extremes are generated solely for the adaptation purposes. This is the first step to see the extent of extremes independently in Sindh. In future studies, the same analysis will be repeated for all the other regions of Pakistan and neighboring country like India to see the spatial extent of extreme events. It will also be interesting to link all these extremes with physical meteorological phenomenon and with each other. Apparently, no relation is found among the temperature, SST, and precipitation extremes, as they occur in different times. But a more detail study with long-term datasets might unfold some important information on their relationship.

References

Abbas, F., Rehman, I., Adrees, M., Ibrahim, M., Saleem, F., Ali, S., Rizwan, M., and Salik, M. R. (2017). Prevailing trends of climatic extremes across Indus-Delta of Sindh-Pakistan. *Theoretical and Applied Climatology*.

Abram, N. J., Gagan, M. K., Cole, J. E., Hantoro, W. S., and Mudelsee, M. (2008). Recent intensification of tropical climate variability in the Indian Ocean. *Nature Geoscience*, 1(12):849–853.

Acero, F. J., García, J. A., Gallego, M. C., Parey, S., and Dacunha-Castelle, D. (2014). Trends in summer extreme temperatures over the Iberian Peninsula using nonurban station data. *Journal of Geophysical Research Atmospheres*, 119(1):39–53.

Acharya, N., Chattopadhyay, S., Mohantay, U., Dasha, S. K., and Sahoo, L. N. (2013). On the bias correction of general circulation model output for Indian summer monsoon. *Meteorological Applications*, (20):349–356.

Afzal, M., Rasul, G., Zahid, M., and Bukhari, S. A. A. (2012). Climate Change in Pakistan: Focused on Sindh Province. Technical Report 1214, Paksitan Meteorological Department.

Agudelo, P. A. and Curry, J. A. (2004). Analysis of spatial distribution in tropospheric temperature trends. *Geophysical Research Letters*, 31(22):1–5.

Ahmad, F. (2011). Human response to hydro-meteorological disasters: A case study of the 2010 flash floods in Pakistan. *Journal of Geography and . . .*, 4(9):518–524.

Akaike, H. (1974). A new look at the statistical model identification. *IEEE Trans*, 19:716–723.

Ali, M. and Iqbal, M. J. (2013). Extreme rainfall incidents over Sindh province, against different return periods. *Proceedings of the Pakistan Academy of Sciences*, 50(2):159–166.

Beguería, S., Angulo-Martínez, M., Vicente-Serrano, S. M., López-Moreno, J. I., and El-Kenawy, A. (2011). Assessing trends in extreme precipitation events intensity and magnitude using non-stationary peaks-over-threshold analysis: A case study in northeast Spain from 1930 to 2006. *International Journal of Climatology*, 31(14):2102–2114.

Bouza-Deaño, R., Ternero-Rodríguez, M., and Fernández-Espinosa, A. J. (2008). Trend study and assessment of surface water quality in the Ebro River (Spain). *Journal of Hydrology*, 361(3-4):227–239.

Bramati, M. C., Tarragoni, C., Davoli, L., and Raffi, R. (2014). Extreme rainfall in coastal metropolitan areas of Central Italy: Rome and Pescara case studies. *Geografia Fisica e Dinamica Quaternaria*, 37(1):3–13.

Brown, S. J., Caesar, J., and Ferro, C. A. T. (2008). Global changes in extreme daily temperature since 1950. *Journal of Geophysical Research Atmospheres*, 113(5).

Brunetti, M., Maugeri, M., Monti, F., and Nanni, T. (2006). Temperature and precipitation variability in Italy in the last two centuries from homogenised instrumental time series. *International Journal of Climatology*, 26(3):345–381.

Burgueño, A., Lana, X., and Serra, C. (2002). Significant hot and cold events at the Fabra Observatory, Barcelona (NE Spain). *Theoretical and Applied Climatology*, 71(3-4):141–156.

Burnham, K. P. and Anderson, D. R. (2002). Model Selection and Multimodel Inference: A Practical Information-Theoretical Approach. page 496.

Camargo, S., Emanuel, K., and Sobel, A. (2007). Use of a genesis potential index to diagnose ENSO effects on tropical cyclone genesis. *J Clim*, 20:4819âĂŞ–4834.

Chambers, J. and Hastie, T. e. (1992). Statistical Models in S. Chapman & Hall, London. pages 317 – 321.

Chaudhry, Q. and Rasul, G. (2004). Agro-Climatic Classification of Pakistan. *Quarterly Science Vision*, 9(1974):59–66.

Chaudhry, Q., Rasul, G., Kamal, A., Mangrio, M., and Mahmood, S. (2015). Government of Pakistan Ministry of Climate Change Technical Report on Karachi Heat wave June 2015. Technical Report July, Pakistan Meteorological Department.

Chaudhry, Q. Z., Mahmood, A., Rasul, G., and Afzaal, M. (2009). Report on Climate Change Indicators of Pakistan by Pakistan Meteorological Department. Technical report, Paksitan Meteorological Department.

Cheema, S., Chaudhry, Q., and Rasul, G. (2012). Persistent Heavy Downpour in Desert Areas of Pakistan in South Asian Monsoon 2011. *Pakistan Journal of Meteorology*, 9(17):71–84.

Cheng, L., AghaKouchak, A., Gilleland, E., and Katz, R. W. (2014). Non-stationary extreme value analysis in a changing climate. *Climatic Change*, 127(2):353–369.

Christidis, N., Stott, P. A., Brown, S., Hegerl, Gabriele, C., and Caesar, J. (2005). Detection of changes in temperature extremes during the second half of the 20th century. *Geophysical Research Letters*, 32(20):1–4.

Christidis, N., Stott, P. A., Zwiers, F. W., Shiogama, H., and Nozawa, T. (2010). Probabilistic estimates of recent changes in temperature: A multi-scale attribution analysis. *Climate Dynamics*, 34(7):1139–1156.

Christy, J., Parker, D., Brown, S., Macadam, I., and Norris, B. (2001). Differential trends in tropical sea surface and atmospheric temperatures since 1979. *Geophysical research letters*, 28(1):183–186.

Coelho, C. A. S., Ferro, C. A. T., Stephenson, D. B., and Steinskog, D. J. (2007). Methods for Exploring Spatial and Temporal Variability of Extreme Events in Climate Data. *Journal of Climate*.

Coles, S. G. (2001). An introduction to Statistical Modeling of Extreme Values. *Springer Series in Statistics*, page 221.

Compo, G. P., Whitaker, J. S., Sardeshmukh, P. D., Matsui, N., Allan, R. J., Yin, X., Gleason, E., Vose, R. S., Rutledge, G., Bessemoulin, P., Br, S., Marshall, G. J., Maugeri, M., Mok, H. Y., Nordli, Ø., Ross, T. F., Trigo, R. M., Wang, X. L., Woodruff, S. D., Worley, S. J., Weather, A., and Africa, S. (2011). The Twentieth Century Reanalysis Project. (January):1–28.

Cooley, D. (2009). Extreme value analysis and the study of climate change. *Climatic Change*, 97:77–83.

Cornes, R. C. and Jones, P. D. (2013). How well does the ERA-Interim reanalysis replicate trends in extremes of surface temperature across Europe ? 118(August):262–276.

Coxe, S., West, S. G., Aiken, L. S., Coxe, S., West, S. G., Aiken, L. S., and Analysis, T. (2017). The Analysis of Count Data : A Gentle Introduction to Poisson Regression and Its Alternatives The Analysis of Count Data : A Gentle Introduction to Poisson. 3891(July).

Dare, R. A. and Mcbride, J. L. (2011). The threshold sea surface temperature condition for tropical cyclogenesis. *Journal of Climate*, 24(17):4570–4576.

Davison, A. C. and Smith, R. L. (1990). Models for Exceedances over High Thresholds. *Journal of the Royal Statistical Society. Series B (Methodological)*, 52(3):393–442.

Dee, D. P., Uppala, S. M., Simmons, A. J., Berrisford, P., Poli, P., Kobayashi, S., Andrae, U., Balmaseda, M. A., Balsamo, G., Bauer, P., Bechtold, P., Beljaars, A. C. M., van de Berg, L., Bidlot, J., Bormann, N., Delsol, C., Dragani, R., Fuentes, M., Geer, A. J., Haimberger, L., Healy, S. B., Hersbach, H., H??lm, E. V., Isaksen, L., K??llberg, P., K??hler, M., Matricardi, M., Mcnally, A. P., Monge-Sanz, B. M., Morcrette, J. J., Park, B. K., Peubey, C., de Rosnay, P., Tavolato, C., Th??paut, J. N., and Vitart, F. (2011). The ERA-Interim reanalysis: Configuration and performance of the data assimilation system. *Quarterly Journal of the Royal Meteorological Society*, 137(656):553–597.

Deidda, R. and Puliga, M. (2006). Sensitivity of goodness-of-fit statistics to rainfall data rounding off. *Physics and Chemistry of the Earth*, 31(18):1240–1251.

Di Baldassarre, G., Laio, F., and Montanari, A. (2009). Design flood estimation using model selection criteria. *Physics and Chemistry of the Earth, Parts A/B/C*, 34(10-12):606–611.

Dickey, D. A. and Fuller, W. A. (1979). Distribution of the Estimators for Autoregressive Time Series With a Unit Root, 48. *Journal of Geophysical Research*, 74(336):427.

Dourte, D., Shukla, S., Singh, P., and Haman, D. (2013). Rainfall Intensity-Duration-Frequency Relationships for Andhra Pradesh, India: Changing Rainfall Patterns and Implications for Runoff and Groundwater Recharge. *Journal of Hydrologic Engineering*, 18(3):324–330.

Easterling, D. R., Meehl, G., Parmesan, C., Changnon, S., Karl, T. R., and Mearns, L. O. (2000). Climate extremes: observations, modeling, and impacts. *Science*, 289(5487):2068–2074.

El Adlouni, S., Ouarda, T. B., Zhang, X., Roy, R., and Bobée, B. (2007). Generalized maximum likelihood estimators for the nonstationary generalized extreme value model. *Water Resources Research*, 43(3):1–13.

Elsner, J. B., Kossin, J. P., and Jagger, T. H. (2008). The increasing intensity of the strongest tropical cyclones. *Nature*, 455(7209):92–95.

Elsner, J. B. and Schmertmann, C. P. (1993). Improving Extended-Range Seasonal Predictions of Intense Atlantic Hurricane Activity.

Elsner, T. and Jagger, J. (2006). Prediction models for annual U.S. 552 hurricane counts. *Journal of Climate*, 19:2935–2952.

Emanuel, K. (2005). Increasing destructiveness of tropical cyclones over the past 30âĂĽyears. *Nature*, 436(7051):686–688.

Evan, A. T. and Camargo, S. J. (2011). A climatology of Arabian Sea cyclonic storms. *Journal of Climate*, 24(1):140–158.

Faranda, D., Lucarini, V., Turchetti, G., and Vaienti, S. (2011). Numerical Convergence of the Block-Maxima Approach to the Generalized Extreme Value Distribution. *Journal of Statistical Physics*, 145(5):1156–1180.

Felici, M., Lucarini, V., Speranza, A., and Vitolo, R. (2007). Extreme Value Statistics of the Total Energy in an Intermediate Complexity Model of the Mid-latitude Atmospheric Jet . Part II : trend detection and assessment. *Journal of the Atmospheric Science*, 64(Mc):2159–2175.

Ferro, C. A. T. and Segers, J. (2003). Statistical Methods for Clusters of Extreme Values. *Journal of Royal Statistics Society B*, 65(2):545–556.

Fisher, R. A. and Tippett, L. H. C. (1928). Limiting forms of the frequency distribution of the largest or smallest member of a sample. *Mathematical Proceedings of the Cambridge Philosophical Society*, 24(02):180.

Frei, C. and Schär, C. (2001). Detection Probability of Trends in Rare Events : Theory and Application to Heavy Precipitation in the Alpine Region. *Journal of Climate*, 14:1568–1584.

Freychet, N., Hsu, H.-H., Chia, C., and Wu, C.-H. (2015). Asian Summer Monsoon in CMIP5 Projections : A Link between the Change in Extreme Precipitation and Monsoon Dynamics. *Journal of Climate*, pages 1477–1493.

Furrer, E. M., Katz, R. W., Walter, M. D., and Furrer, R. (2010). Statistical modeling of hot spells and heat waves. *Climate Research*, 43(3):191–205.

Ghil, M., Yiou, P., Hallegatte, S., Malamud, B. D., Naveau, P., Soloviev, A., Friederichs, P., Keilis-Borok, V., Kondrashov, D., Kossobokov, V., Mestre, O., Nicolis, C., Rust, H. W., Shebalin, P., Vrac, M., Witt, A., and Zaliapin, I. (2011). Extreme events: Dynamics, statistics and prediction. *Nonlinear Processes in Geophysics*, 18(3):295–350.

Gilleland, E. (2015). R Package ExtRemes. *Available: http://www.assessment.ucar.edu/toolkit/ (Accessed 2016 Jan 2)*.

Gilleland, E. and Katz, R. (2011). New software to analyze how extremes change over time. *Eos*, 92(2):13–14.

Gillett, N. P., Stott, P. A., and Santer, B. D. (2008). Attribution of cyclogenesis region sea surface temperature change to anthropogenic influence. *Geophysical Research Letters*, 35(9):1–5.

Girishkumar, M. S. and Ravichandran, M. (2012). The influences of ENSO on tropical cyclone activity in the Bay of Bengal during October-December. *Journal of Geophysical Research: Oceans*, 117(2):1–13.

Gnedenko, B. (1943). "Sur la distribution limite du terme maximum dâĂŹune sÂťerie alÂťeatoire". *Annals of Mathematics*, 44:423–453.

Gray, W. M. (1968). Global View of the Origin of Tropical Disturbances and Storms.

Gray, W. M., Landsea, C. W., Mielke Jr., P. W., and Berry, K. J. (1992). Predicting Atlantic seasonal hurricane activity 6âĂŞ11 months in advance.

Gray, W. M., Landsea, C. W., Paul, W., Berry, K. J., and Mielke, J. (1994). Predicting Atlantic basin seasonal tropical cyclone activity by 1 June.

Haider, K., Rasul, G., and Afzaal, M. (2011). A study on tropical cyclones of the Arabian sea in June 2007 and their connection with sea surface temperature. *Pakistan Journal of Meteorology*, 4(8):37–48.

Hanif, M., Hayyat, A., and Adnan, S. (2013). Latitudinal precipitation characteristics and trends in Pakistan. *Journal of Hydrology*, 492:266–272.

Hasan, A. B. M. and Rasul, G. (2008). DIAGNOSIS OF THE IMPACT OF DEEP DEPRESSIONAL ACTIVITY IN NORTHERN ARABIAN SEA OVER KARACHI DURING MONSOON Abstract : Introduction :. *Pakistan Journal of Meteorology*, 5(5):77–96.

Hatfield, J. L. and Prueger, J. H. (2015). Temperature extremes: Effect on plant growth and development. *Weather and Climate Extremes*, 10:4–10.

Ho, C.-H., Kim, J.-H., Jeong, J.-H., Kim, H.-S., and Chen, D. (2006). Variation of tropical cyclone activity in the South Indian Ocean: El NiñoâĂŞSouthern Oscillation and Madden-Julian Oscillation effects. *Journal of Geophysical Research*, 111(D22):D22101.

Holland, G. J. (1997). Estimating the maximum potential intensity of tropical cyclones. *Russian Meteorology and Hydrology*, 35(6):371–377.

Hu, Y. (2013). Extreme Value Mixture Modelling with Simulation Study and Applications in Finance and Insurance. *New Zealand*, page 115.

Hunter, J. (2010). Estimating sea-level extremes under conditions of uncertain sea-level rise. *Climatic Change*, 99(3):331–350.

Hussain, A. (2011). Persistency Analysis of Cyclone History in Arabian Sea. *The Nucleus*, 48(4):273 – 277.

Hussain, M. S. and Lee, S. (2014). The Regional and the Seasonal Variability of Extreme Precipitation Trends in Pakistan. *Asia-pacific Journal Atmospheric Sciences*, 49(4):1–21.

Ikram, F., Afzaal, M., Bukhari, S., and Ahmed, B. (2016). Past and Future Trends in Frequency of Heavy Rainfall Events over Pakistan. *Pakistan Journal of Meteorology*, 12(24):57–78.

Imtiaz, S. and Rehman, Z. (2015). Death Toll From Heat Wave in Karachi, Pakistan, Hits 1,000, June 25,The New York Times.

IPCC (2012). Managing the risks of extreme events and disasters to advance climate change adaptation. *Ipcc*, page 594.

IPCC (2014). Summary for Policymakers. Technical report, IPCC.

Islam, S. U., Rehman, N., and Sheikh, M. M. (2009). Future change in the frequency of warm and cold spells over Pakistan simulated by the PRECIS regional climate model. *Climatic Change*, 94(1-2):35–45.

Izumo, T., Montegut, C. d. B., Luo, J. J., Behera, S. K., Masson, S., and Yamagata, T. (2008). The role of the Western Arabian Sea upwelling in Indian monsoon rainfall variability. *Journal of Climate*, 21(21):5603–5623.

Jonkman, S. N. (2005). Global perspectives on loss of human life caused by floods. *Natural Hazards*, 34(2):151–175.

JTWC (2007). Section 3: Detailed cyclone reviews: TC 02A (Gonu). -2007 annual tropical cyclone report. *JTWC Rep*, pages 62–64.

Kalim, U. and Shouting, G. A. O. (2012). Moisture Transport over the Arabian Sea Associated with Summer Rainfall over Pakistan in 1994 and 2002. *Advances in Atmospheric Sciences*, 29(3):501–508.

Katz, R. (2010). Statistics of extremes in climate change. *Clim Chang.*, 100(1):71–76.

Katz, R., Ichard, W. K., Rush, G., and Race, S. B. (2005). Statistics of Extremes : Modeling Ecological Disturbances. *Ecology*, 86(5):1124–1134.

Katz, R. W., Parlange, M. B., and Naveau, P. (2002). Statistics of extremes in hydrology. *Advances in Water Resources*, 25:1287âĂŞ1304.

Kazi, A. (2014). A review of the assessment and mitigation of floods in Sindh, Pakistan. *Natural Hazards*, 70(1):839–864.

Khan, T., Khan, F., and Jilani, R. (2008). Sea surface temperature variability along Pakistan coast and its relation to El Nino-Southern Oscillation. *Journal of Basic and Applied*, 4(2):67–72.

Kharin, V., Zwiers, F., Zhang, X., and Hegerl, G. C. (2007). Changes in temperature and precipitation extremes in the IPCC ensemble of global coupled model simulations. *Journal of Climate*, 20:1419âĂŞ1444.

Kim, H. S., Ho, C. H., Chu, P. S., and Kim, J. H. (2010). Seasonal prediction of summertime tropical cyclone activity over the east China sea using the least absolute deviation regression and the poisson regression. *International Journal of Climatology*, 30(2):210–219.

Kleinbaum, D. G., Kupper, L., and KE, M. (1988). *Applied Regression Analysis and Other Multivariate Methods 2nd ed.* PWS-Kent, Boston, Mass.

Knutson, T. R., McBride, J. L., Chan, J., Emanuel, K. A., Holland, G., Landsea, C., Held, I., Kossin, J. P., Srivastava, A., and Sugi, M. (2010). Tropical cyclones and climate change. *Nature Geoscience*, 3(3):157–163.

Kumar, S. P., Roshin, R. P., Narvekar, J., Kumar, P. K. D., and Vivekanandan, E. (2009). Response of the Arabian Sea to global warming and associated regional climate shift. *Marine Environmental Research*, 68(5):217–222.

Kundzewicz, Z. W. and Robson, A. (2000). Detecting Trend and Other Changes in Hydrological Data. *World Climate Programme-Water, World Climate Programme Data and Monitoring*, page 158.

Leadbetter, M. R. (1983). Extremes and local dependence in stationary sequences. *Zeitschrift f??r Wahrscheinlichkeitstheorie und Verwandte Gebiete*, 65(2):291–306.

Levine, R. C. and Turner, A. G. (2012). Dependence of Indian monsoon rainfall on moisture fluxes across the Arabian Sea and the impact of coupled model sea surface temperature biases. *Climate Dynamics*, 38(11-12):2167–2190.

Loynes, R. M. (1965). Extreme Values in Uniformly Mixing Stationary Stochastic Processes. *The Annals of Mathematical Statistics*, 36(3):993–999.

Lucarini, V., Faranda, D., Freitas, A. C. M., Freitas, J. M., Kuna, T., Holland, M., Nicol, M., Todd, M., and Vaienti, S. (2016). *Extremes and Recurrence in Dynamical Systems*, volume 14. Wiley.

Lucarini, V., Faranda, D., J, W., and Kuna, T. (2014). Towards a General Theory of Extremes for Observables of Chaotic Dynamical Systems. *Journal of statistical physics*, 154:723–750.

Mahala, B. K., Nayak, B. K., and Mohanty, P. K. (2015). Impacts of ENSO and IOD on tropical cyclone activity in the Bay of Bengal. *Natural Hazards*, 75(2):1105–1125.

McDonnell, K. A. and Holbrook, N. J. (2004). A Poisson regression model approach to predicting tropical cyclogenesis in the Australian/southwest Pacific Ocean region using the SOI and saturated equivalent potential temperature gradient as predictors. *Geophysical Research Letters*, 31(20):1–5.

McPhaden, M. J., Foltz, G. R., Lee, T., Murty, V. S. N., Ravichandran, M., Vecchi, G. A., Vialard, J., Wiggert, J. D., and Yu, L. (2009). Ocean-atmosphere interactions during cyclone nargis. *Eos*, 90(7):53–54.

Mitchell, J., Manabe, S., and et al (1990). *Equilibrium Climate Change and its Implications for the Future.* Cambridge University Press, Cambridge, United Kingdom and New York, NY, USA.

Morak, S., Hegerl, G. C., and Christidis, N. (2013). Detectable changes in the frequency of temperature extremes. *Journal of Climate*, 26(5):1561–1574.

Morak, S., Hegerl, G. C., and Kenyon, J. (2011). Detectable regional changes in the number of warm nights. *Geophysical Research Letters*, 38(17).

Mueller, E. N. and Pfister, A. (2011). Increasing occurrence of high-intensity rainstorm events relevant for the generation of soil erosion in a temperate lowland region in Central Europe. *Journal of Hydrology*, 411(3-4):266–278.

Muhammad, S., Memon, A. A., Muneeb, M., and Ghauri, B. (2016). Seasonal and spatial patterns of {SST} in the northern Arabian Sea during 2001âĂŞ2012. *The Egyptian Journal of Remote Sensing and Space Science*, 19(1):17–22.

Murakami, H., Sugi, M., and Kitoh, A. (2013). Future changes in tropical cyclone activity in the North Indian Ocean projected by high-resolution MRI-AGCMs. *Climate Dynamics*, 40(7-8):1949–1968.

Naveau, P., Guillou, A., Cooley, D., and Diebolt, J. (2009). Modelling pairwise dependence of maxima in space. *Biometrika*, 96:1âĂŞ17.

Needham, H. F., Keim, B. D., and Sathiaraj, D. (2015). A review of tropical cyclone-generated storm surges: Global data sources, observations, and impacts. *Reviews of Geophysics*, 53(2):545–591.

Nogaj, M., Yiou, P., Parey, S., Malek, F., and Naveau, P. (2006). Amplitude and frequency of temperature extremes over the North Atlantic region. *Geophysical Research Letters*, 33(10).

O'Brien, G. L. (1974). The maximum term of uniformly mixing stationary processes. *Zeitschrift für Wahrscheinlichkeitstheorie und Verwandte Gebiete*, 30(1):57–63.

Oliver, E. C. J., Wotherspoon, S. J., Chamberlain, M. A., and Holbrook, N. J. (2014). Projected Tasman Sea extremes in sea surface temperature through the twenty-first century. *Journal of Climate*, 27(5):1980–1998.

Pal, J. S. and Eltahir, E. A. B. (2015). Future temperature in southwest Asia projected to exceed a threshold for human adaptability. *Nature Climate Change*, 18203(October):1–4.

Papalexiou, S. M. and Koutsoyiannis, D. (2013). Battle of extreme value distributions : A global survey on extreme daily rainfall. *Water Resources Research*, 49(1):187–201.

Paulikas, M. J. and Rahman, M. K. (2015). A temporal assessment of flooding fatalities in Pakistan (1950-2012). *Journal of Flood Risk Management*, 8(1):62–70.

Pelling, M. and Blackburn, S. (2014). *Megacities and the coast: risk, resilience and transformation*. Routledge.

Pickands, I. J. (1975). Statistical inference using extreme order statistics. *The Annals of Statistics*, page 119âĂŞ131.

Provincial Disaster Management Authority - Sindh (2013). PDMA Mulit Hazard Contingency Plan 2013. Technical report, Rehabilitation Department, Karachi.

Rana, A. S., Zaman, Q., Afzal, M., and Haroon, M. A. (2014). Characteristics of Sea Surface Temperature of the Arabian Sea Coast of Pakistan and Impact of Tropical Cyclones on SST. *Pakistan Journal of Meteorology*, 11(21):61–70.

Rasul, G., Chaudhry, Q.-u.-z., and Sixiong, Z. (2005). A Diagnostic Study of Heavy Rainfall in Karachi Due to Merging of a Mesoscale Low and a Diffused Tropical Depression during South Asian Summer Monsoon. *Advances in Atmospheric Sciences*, 22(3):375–391.

Rasul, G., Mahmood, a., Sadiq, a., and Khan, S. I. (2012). Vulnerability of the Indus Delta to Climate Change in Pakistan. *Pakistan Journal of Meteorology*, 8(16):89–107.

Rayner, N. A. (2003). Global analyses of sea surface temperature, sea ice, and night marine air temperature since the late nineteenth century. *Journal of Geophysical Research*, 108(D14):4407.

RDevelopmentCoreTeam (2015). R, a language and environment for statistical computing. *R Foundation for Statistical Computing, Vienn, Austria, 2015.*

Re, M. and Barros, V. R. (2009). Extreme rainfalls in SE South America. *Climatic Change*, 96(1):119–136.

Renard, B., e. a. (2013). *Bayesian methods for non-stationary extreme value analysis.* Springer.

RupaKumar, R., KrishnaKumar, K., Ashrit, RG Patwardhan, S., and Pant, G. (2002). *Climate change in India: observations and model projections.In: Shukla, P.R., Sharma, S.K., Venkata Ramana, P. (Eds.), Climate Change and India: Issues, Concerns and Opportunities.* Tata McGraw-Hill Publishing Company Limited, New Delhi.

Salma, S., Rehman, S., and Shah, M. A. (2012). Rainfall Trends in Different Climate Zones of Pakistan. *Pakistan Journal of Meteorology*, 9(17):37–47.

Sayantani, O., Gnanaseelan, C., Chowdary, J. S., Parekh, A., and Rahul, S. (2016). Arabian Sea SST evolution during spring to summer transition period and the associated processes in coupled climate models. *International Journal of Climatology*, 36(6):2541–2554.

Scarrott, C. and Macdonald, A. (2012). a Review of Extreme Value Threshold Estimation and Uncertainty Quantification. *REVSTAT âĂŞ Statistical Journal*, 10(1):33–60.

Schott, F., Xie, S.-P., Julian, P., and McCreary, J. (2009). Indian Ocean Circulation and Climate Variability. *Reviews of Geophysics*, 47:1–46.

Scoccimarro, E., Gualdi, S., Bellucci, A., Zampieri, M., and Navarra, A. (2013). Heavy Precipitation Events in a Warmer Climate : Results from CMIP5 Models. *Journal of Climate*, 26:7902–7911.

Sen, A. K. and Niedzielski, T. (2010). Statistical characteristics of riverflow variability in the Odra River basin, southwestern Poland. *Polish Journal of Environmental Studies*, 19(2):387–396.

Shang, H., Yan, J., and Zhang, X. (2011). El Ni??o-Southern Oscillation influence on winter maximum daily precipitation in California in a spatial model. *Water Resources Research*, 47(11):1–9.

Sheridan, S. C. and Allen, M. J. (2015). Changes in the Frequency and Intensity of Extreme Temperature Events and Human Health Concerns. *Current Climate Change Reports*, 1(3):155–162.

Sherwood, S. C. and Huber, M. (2010). An adaptability limit to climate change due to heat stress. *Pnas*, 107(21):9552–9555.

Shukla, J. (1975). Effect of Arabin Sea Surface Temperature Anomaly on Indian Summer Monsoon Numerical Experiment with GFDL Model. *Journal of the Atmospheric Sciences*, 32(3):503–511.

Singh, O. P., Ali Khan, T. M., and Rahman, M. S. (2001). Has the frequency of intense tropical cyclones increased in the north Indian Ocean? *Current Science*, 80(4):575–580.

Sobel, A. H., Camargo, S. J., Hall, T. M., Lee, C.-y., Tippett, M. K., and Wing, A. a. (2016). Cyclone Intensity. *Natural Hazards*, 353(6296).

Stull, R. (2011). Wet-bulb temperature from relative humidity and air temperature. *Journal of Applied Meteorology and Climatology*, 50(11):2267–2269.

Sugahara, S., Rosmeri, P., and Reinaldo, S. (2009). Non-stationary frequency analysis of extreme daily rainfall in Sao Paulo, Brazil. *International journal of Climatology*, 29:1339–1349.

Sumesh, K. G. and Ramesh, K. M. R. (2013). Tropical cyclones over north Indian Ocean during El-Ni??o Modoki years. *Natural Hazards*, 68(2):1057–1074.

Tariq, M. A. U. R. and Van de Giesen, N. (2012). Floods and flood management in Pakistan. *Physics and Chemistry of the Earth*, 47-48(December):11–20.

Tebaldi, C., Hayhoe, K., Arblaster, J. M., and Meehl, G. A. (2006). Going to the extremes: An intercomparison of model-simulated historical and future changes in extreme events.

Thompson, P., Cai, Y., Reeve, D., and Stander, J. (2009). Automated threshold selection methods for extreme wave analysis. *Coastal Engineering*, 56(10):1013–1021.

Tramblay, Y., Neppel, L., Carreau, J., and Najib, K. (2013). Non-stationary frequency analysis of heavy rainfall events in southern France. *Hydrological Sciences Journal*, 58(2):280–294.

Trenberth, K. (2013). El Niño Southern Oscillation (ENSO). *Reference Module in Earth Systems and Environmental Sciences*.

Walsh, K. J. E., Mcbride, J. L., Klotzbach, P. J., Balachandran, S., Camargo, S. J., Holland, G., Knutson, T. R., Kossin, J. P., cheung Lee, T., Sobel, A., and Sugi, M. (2016). Tropical cyclones and climate change. *Wiley Interdisciplinary Reviews: Climate Change*, 7(1):65–89.

Wang, W., Vrijling, J. K., Van Gelder, P. H., and Ma, J. (2006). Testing for nonlinearity of streamflow processes at different timescales. *Journal of Hydrology*, 322(1-4):247–268.

Webster, P. J., Holland, G. J., Curry, J. A., and Chang, H.-R. (2005). Changes in tropical cyclone number, duration, and intensity in a warming environment. *Science (New York, N.Y.)*, 309(5742):1844–6.

Wilks, D. S. (1995). Statistical Methods in the Atmospheric Sciences. *Academic, San Diego, Calif.*, page 47.

Yilmaz, A. G., Hossain, I., and Perera, B. J. C. (2014). Effect of climate change and variability on extreme rainfall intensity-frequency-duration relationships: A case study of Melbourne. *Hydrology and Earth System Sciences*, 18(10):4065–4076.

Yoo, S.-H. (2007). Urban Water Consumption and Regional Economic Growth: The Case of Taejeon, Korea. *Water Resources Management*, 21(8):1353–1361.

Yue, S., Pilon, P., and Cavadias, G. (2002). Power of the Mann-Kendall and Spearman's rho tests for detecting monotonic trends in hydrological series. *Journal of Hydrology*, 259(1-4):254–271.

Zahid, M. and Rasul, G. (2010). Rise in Summer Heat Index over Pakistan. *Pakistan Journal of Meteorology*, 6(12):85–96.

Zahid, M. and Rasul, G. (2011). Frequency of extreme temperature& precipitation events in Pakistan 1965-2009. *Science International*, 23(4):313–319.

Zahid, M. and Rasul, G. (2012). Changing trends of thermal extremes in Pakistan. *Climatic Change*, 113(3-4):883–896.

Zhang, X., Zwiers, F. W., and Li, G. (2004). Monte Carlo experiments on the detection of trends in extreme values. *Journal of Climate*, 17(10):1945–1952.

Symbols

ξ	Shape parameter
σ	Scale parameter
μ	Location parameter
μ_1	Location parameter of the non-stationary GEV model
u	Threshold
σ^*	Modified scale parameter
$\Delta\xi$	Standard error in the shape parameter
$\Delta\sigma$	Standard error in the scale parameter
$\Delta\mu$	Standard error in the location parameter
$\Delta\mu_1$	Standard error in the location parameter of the non-stationary GEV model
θ	Extremal Index
x_N	Return level
N	Return period
ζ_u	Probability of an individual observation exceeding the threshold u
n_y	number of observations per year
$\bar{z}$	Mean of meteorological station temperature data
σ_z	Standard deviation of meteorological station temperature data
y_{ERA}	ERA Interim time series
$\bar{y}$	Mean of the ERA Interim time series
σ_y	Standard deviation of the ERA Interim time series
z_p	Return values
λ_i^y	Mean occurrence rate
P_r	Poisson regression
β	Poisson regression coefficient
$\bar{z}_t$	Block maxima with standard Gumbel distribution
$\hat{\mu}$	Location parameter of the standard Gumbel distribution
$\hat{\xi}$	Shape parameter of the standard Gumbel distribution
$\hat{\sigma}$	Scale parameter of the standard Gumbel distribution
χ^2	Chi square

Acronyms

EVT	Extreme Value Theory
GPD	Generalized Pareto Distribution
GEV	Generalized Extreme Value Distribution
POT	Peaks Over Threshold
BM	Block Maxima
MLE	Maximum Likelihood Estimation
RL	Return Levels
SST	Sea Surface Temperature
TD	Tropical Depression
CS	Cyclonic Storm
SCS	Severe Cyclonic Storm
LRT	Likelihood Ratio Test
AIC	Akaike's Information Criterion
MK	Mann-Kendall
ADF	Augmented Dickey Fuller
KS	Kolmogorov- Smirnov
AD	Anderson Darling
SOI	Southern Oscillation Index
NSGEV	Non-stationary GEV
SGEV	Stationary GEV

Subscripts, Superscripts and Annotations

T_{max}	Maximum Temperature
TW_{max}	Maximum Wet-bulb Temperature
RH_{max}	Maximum Relative Humidity
A_{max}	Absolute Maxima
SST_{fav1}	Sea surface temperature with first set of favorable conditions
SST_{fav2}	Sea surface temperature with second set of favorable conditions
SST_{fav3}	Sea surface temperature with third set of favorable conditions
SST_{unfav}	Sea surface temperature with unfavorable conditions

List of Figures

List of Tables

Aus dieser Dissertation hervorgegangene Vorveröffentlichungen und Einsendungen
List of Publications and Submissions

Zahid, M., Blender, R., Lucarini, V., and Bramati, M. C.: Return Levels of Temperature Extremes in Southern Pakistan, Earth Syst. Dynam. Discuss., https://doi.org/10.5194/esd-2016-72, in review, 2017 (see Appendix A).

Own Contribution: Formulation of idea and designing of the paper, literature review, data collection, development of scripts, plotting figures, and write-up.

Co-authors: VL contributed in formulating the study. VL, RB, and MCB contributed to the text.

.1 Appendix A

1 **Return Levels of Temperature Extremes in Southern Pakistan**
2
3 Maida Zahid[1], Richard Blender[1], Valerio Lucarini[1,2] and Maria Caterina Bramati[3]

4 1. Meteorological Institute, University of Hamburg, Hamburg Germany
5 2. Department of Mathematics and Statistics, University of Reading, Reading, UK
6 3. Department of Statistical Science, Cornell University, New York, United States
7
8 *Correspondence to:* Maida Zahid (maida.zahid@uni-hamburg.de)
9
10 **Abstract.** Southern Pakistan (Sindh) is one of the hottest regions in the world and is highly vulnerable to

11 temperature extremes. In order to improve rural and urban planning, information about the recurrence of

12 temperature extremes is required. In this work, return levels of the daily maximum temperature T_{max} are

13 estimated, as well as the daily maximum wet-bulb temperature TW_{max} extremes. The method used is the Peak

14 Over Threshold (POT) and it represents a novelty among the approaches previously used for similar studies in

15 this region. Two main datasets are analyzed: temperatures observed in nine meteorological stations in southern

16 Pakistan from 1980 to 2013, and the ERA Interim data for the nearest corresponding locations. The analysis

17 provides the 2, 5, 10, 25, 50 and 100-year Return Levels (RLs) of temperature extremes. The 90% quantile is

18 found to be a suitable threshold for all stations. We find that the RLs of the observed T_{max} are above 50°C in

19 northern stations, and above 45°C in the southern stations. The RLs of the observed TW_{max} exceed 35°C in the

20 region, which is considered as a limit of survivability. The RLs estimated from the ERA Interim data are lower

21 by 3°C to 5°C than the RLs assessed for the nine meteorological stations. A simple bias correction applied to

22 ERA Interim data improves the RLs remarkably, yet discrepancies are still present. The results have potential

23 implications for the risk assessment of extreme temperatures in Sindh.
24
25 **Key words**
26
27 Extreme temperature, return levels, peak over threshold, Generalized Pareto Distribution, declustering.

28 **1 Introduction**
29
30 Extreme maximum temperature events have received much attention in recent years, because of the associated

31 risk of mortality and their likely increase in intensity and frequency in climate change scenarios (Sheridan and

32 Allen, 2015). An example of the potential impact of raising maximum temperatures is the recent heat wave in

33 Southern Pakistan (Sindh), which occurred between June 17th and June 24th 2015 and broke all the records with a

34 death toll of 1400 people, and over 14000 people hospitalized. The temperatures in different cities of the Sindh

35 region were in the range of 45°C - 49°C during the event (Imtiaz and Rehman, 2015). Karachi had the highest

36 number of fatalities (1200 people approximately). The Pakistan Meteorological department issued a technical

37 report stating a very high heat index (measuring the heat stress on humans due to high temperature and relative

38 humidity) during this heat wave (Chaudhry et al., 2015).
39
40 In summer, Sindh becomes very hot and with the arrival of a monsoon the humidity increase in the region

41 (Chaudhry and Rasul, 2004). This lethal combination of high temperature and relative humidity is known as wet-

42 bulb temperature, which increases the death rates, and severely impacts the human habitability (Pal and Eltahir

43 2015). The human body generally maintains the temperature around 37°C. However, the human skin regulates at

Earth System
Dynamics
Discussions

1   or below 35°C to release heat (Sherwood and Huber, 2010). Under high levels of the moisture content in the
2   atmosphere, the human body cannot maintain the skin temperature below 35°C and can develop ailments like
3   hyperthermia, heat strokes and cardiovascular problems. Hyperthermia can occur even in the fittest human
4   beings, if they are exposed to an environment where wet-bulb temperature is greater than 35°C for at least six
5   hours. Hyperthermia is a condition where extremely high body temperature is reached, resulting from the
6   inability of the body to get rid of the excess heat. It occurs mostly when temperature and relative humidity levels
7   are extremely high at the same time.
8
9   This study devotes special attention to Sindh because of its exposure to the frequent and intense temperature
10 extremes in the past (Zahid and Rasul, 2012). This region is considered as one of the most vulnerable regions in
11 Pakistan. Sindh stretches from 23.5° N – 28.5° N and 66.5°E - 71.1°E, and is bounded on the west by the Kirthar
12 Mountains, to the north by the Punjab plains, to the east by the Thar desert and to the south by the Arabian Sea
13 (Indian Ocean) and in the center fertile land around Indus river. The Indus river is the source of water for the
14 agriculture lands. Cotton, wheat and sugar cane are grown on the left bank of the Indus and rice, wheat and gram
15 on the right bank (Chaudhry and Rasul, 2004). Cotton is the cash crop of the country.
16
17 The climate in Sindh is arid and subtropical with less than 250 mm annual rainfall. The temperature frequently
18 exceeds 45°C in summer (May-September) and the minimum average temperature recorded during winter
19 (December- January) is 2°C. Table 2 shows the mean monthly climatic characteristics of the region from 1980-
20 2010. Figure 1 shows the spatial distribution of all nine weather stations of Pakistan meteorological department,
21 and the ERA Interim grid points close to the corresponding locations. High population density, limited resources,
22 poor infrastructure and high dependence of the local agriculture on climatic factors, mark this region as highly
23 vulnerable to the impacts of climate change.
24
25 The Intergovernmental Panel on Climate Change (IPCC) scenarios estimates for this region an increase in the
26 surface temperature of the order of 4°C in this region by the end of 2100. This may significantly reduce crop
27 yields, and cause huge economic losses to the country (Islam et al., 2009; Rasul et al., 2012; IPCC, 2012;
28 Pachauri et al., 2014). Furthermore, it might increase the risks of heat strokes, cardiac arrest, high fever, diarrhea,
29 cholera and vector borne diseases. Heat waves became more frequent and intense during 90's in Southern
30 Pakistan. Zahid and Rasul (2010) reports the significant rise in heat index and heat waves events longer than ten
31 days in Sindh. The enhanced mortality rate related to the heat waves is a serious problem, and two obvious
32 examples are the 1991 and the previously mentioned 2015 heat waves (Imtiaz and Rehman, 2015).
33
34 The analysis of extreme climatic events is a very active area of research in geosciences (Christidis et al., 2005,
35 2010; Tebaldi et al., 2006; Zwiers et al., 2011; Morak et al., 2011, 2013). In order to facilitate and standardize the
36 analysis of extremes, the World Meteorological Organization (WMO) has suggested 27 specific climate indices,
37 like the number of hot days, cold days, wet days, dry days, etc. (Tank et al., 2006; 2009, Frisch et al., 2002; Choi
38 et al., 2009; Lustenberger et al., 2014). The investigation and analysis of such climate indices has now reached a
39 high level of popularity.
40

1 Extreme value theory (EVT) represents an increasingly widespread approach in climate studies (Coles, 2001,
2 Zhang et al., 2004; Brown et al., 2008; Faranda et al., 2011; Acero et al., 2014) to estimate the occurrence of the
3 extreme events. The peak over threshold (POT) approach determines the distribution of the exceedances above a
4 threshold. The exceedances are asymptotically distributed according to the Generalized Pareto Distribution
5 (GPD). GPD has remarkable properties of universality when the asymptotic behavior is considered (Lucarini et
6 al., 2016), while one can expect that the threshold level above which the asymptotic behavior is achieved depends
7 on the specifics of the analyzed time series. In particular, when looking at spatial fields, it will depend on the
8 geographical location.

9
10 In this study, we have chosen to use the POT method to assess the temperature extremes in the Sindh region,
11 because it is the most practical approach in modeling the risks of extremes. It is applied for studying temperature
12 extremes in different regions of the world (Burgueño et al., 2002; Nogaj et al., 2006; Coelho et al., 2008; Ghill et
13 al., 2011). However, to our knowledge, the POT method has never been used to analyze the risk of temperature
14 extremes in Sindh. The POT approach allows in principle for estimating the return periods and the return levels
15 (RLs) also for time ranges longer than what has been currently observed. This information and this predictive
16 power can be beneficial for policy makers and other stakeholders. Note that this is exactly the kind of information
17 planners need when, e.g., designing infrastructures that are deemed to last a very long time.

18
19 It is useful to consider two indicators of extreme temperatures: (1) temperature extremes T_{max}, and (2) Wet-bulb
20 temperature extremes TW_{max}, and are interlinked, but rarely studied together. The southern Pakistan (Sindh)
21 lacks the information about both the temperature extremes and faces the consequences of heat waves almost
22 every year. Thus, considering the need and relevance of the information such a study is necessary and timely.

23
24 Therefore, we estimate the return levels of extreme daily maximum temperatures T_{max} and daily maximum wet-
25 bulb temperatures TW_{max} over the different return periods in Sindh. We apply the peak over threshold (POT)
26 method on the observational data of the nine weather stations provided by Pakistan meteorological department,
27 and the ERA Interim data of European center for medium range weather forecast (ECMWF) model for the
28 corresponding grid points from 1980 to 2013. If the ERA Interim dataset characterizes well the extremes, it could
29 be an option for the regions inside Sindh where no observational data is available. Furthermore, a standard bias
30 correction is applied on the ERA Interim data to improve the results.

31
32 The paper is organized as follows. In Section 2, the statistical modeling of extremes using peak over threshold
33 method is briefly illustrated along with a description of the data used. The estimation of daily maximum wet-bulb
34 temperature is discussed in detail in this Section. Section 3 presents the main results of the POT analysis on the
35 meteorological station observations, ERA Interim, and bias corrected ERA Interim daily maximum temperature
36 T_{max} and wet-bulb temperature TW_{max} data at nine locations, viz. Jacobabad, Mohenjo-daro, Rohri, Padidan,
37 Nawabshah, Hyderabad, Chhor, Karachi, and Badin. The performance of the ERA Interim and bias corrected
38 ERA Interim in comparison to observations is also described in Section 3. All computations and graphics in this
39 work are done using the R free open source statistical software, using the packages ismev and extRemes (see
40 www.R-project.org and R Development core team 2015). Section 4 summarizes the major findings of the study
41 and concludes our work.

Earth System
Dynamics

Discussions

2. Data and Methodology

2.1 Meteorological Station Data

The daily maximum temperature and relative humidity data recorded at nine meteorological stations in Sindh from 1980 to 2013 are provided by the Pakistan Meteorological Department (see Table 1). We select nine stations, which contain a negligible amount of missing values after 1980, and are suitable for the POT analysis. An additional criterion is that only those stations are chosen where no changes occurred in measuring instruments during the last 33 years (Brunetti et al., 2006). None of the station data shows gaps with a duration longer than two days, which are treated by replacing the missing values with the average of the two previous values.

The temperature data are discretized unevenly with intervals up to 1 degree Celsius. Deidda and Puliga (2006) uses a Monte Carlo study for simulating various resolutions to show that the discretization in precipitation data affects the convergence of parameter estimation in the extreme value analysis. For this reason, we produce high resolution data to compensate the effect of discretization and thus to improve the convergence of the estimator. To convert station data to higher resolution, we add them to a uniform noise with the magnitude corresponding to the discretization steps (1 degree C). The noise r is a uniform random variable in the interval [-0.5, 0.5]. The main property of this noise is to round $(T+r) = T$, where T is the temperature with 1-degree resolution and 'round' is the numerical function, which maps the interval [T-0.5, T+0.5] to T. Thus, adding the noise does not perturb the information content of the observations. This procedure is applied to all temperature data, irrespective of the actual resolution, and replicated 100 times using a Monte Carlo approach. Results are then averaged. We check the influence of this noise parameterization and find no significant bias in the return level estimates.

2.2 ERA Interim Reanalysis Data

The gridded daily maximum temperature and relative humidity data of ERA Interim reanalysis is downloaded from the website ECMWF Public Datasets web interface (http://apps.ecmwf.int/datasets/). The ERA Interim is produced from the European center for medium range weather forecast (ECMWF) model with resolution 0.75° × 0.75° (Dee et al., 2011). The gridded data is then extracted at the closest grid point of all stations, for the period 1980-2013. The latitude and longitude of the ERA Interim stations are displayed in Table 1.

One of the main requirements to perform the POT analysis is a stationary time series. Therefore, similar to Bramati et al. (2014), the ADF test of stationarity (Dickey and Fuller, 1979) is performed on all the time series. The test results show no sign of long-term correlations in the data. High short-term correlations (daily time scale) typically lead to clusters of extreme values and require the use of a declustering method (see more detail in Section 2.4).

2.3 Wet-bulb Temperature Calculations

The wet-bulb temperature measures the heat stress better than other existing heat indices, because it establishes the clear thermodynamic limit on heat transfer that cannot be overcome by adaptations like clothing, activity and

Earth System
Dynamics
Discussions

1   acclimatization (Pal and Eltahir 2015, Sherwood and Huber, 2010). Here, we use an empirical equation

2   developed by Stull (2011) to measure the wet-bulb temperature [°C].

3

4    $$\text{TW}_{max} = \text{T}_{max}\ \text{atan}\ (\alpha_1\sqrt{\text{RH}_{max} + \alpha_2}) + \text{atan}(\text{T}_{max} + \text{RH}_{max}) - \text{atan}(\text{RH}_{max} + \ \alpha_3) +$$

5    $$+ \ \alpha_4(\text{RH}_{max})^{\frac{3}{2}}\text{atan}(\ \alpha_5\text{RH}_{max}) - \alpha_6 \qquad\qquad (1)$$

6

7

8   where TW_{max} is the maximum wet-bulb temperature [°C], T_{max} is the maximum temperature [°C], and RH_{max} is

9   the maximum relative humidity [%]. This relationship is based on an empirical fit, as in Stull (2011), where the

10   coefficient values are α_1 = 0.151977, α_2 = 8.313659, α_3 = -1.676331, α_4 = 0.00391838, α_5 = 0.023101, and

11   α_6 = 4.686035. The Eq. (1) covers a wide range of relative humidity and air temperatures with an accuracy of

12   0.3°C.

13   **2.4 Peak Over Threshold**

14

15   In order to determine return levels (RLs) of extreme maximum temperatures and maximum wet-bulb

16   temperatures in Sindh, the Peak Over Threshold approach (POT) is applied to the meteorological stations, the

17   ERA Interim, and the bias corrected ERA Interim data. In this analysis, extremes are defined as exceedances over

18   threshold distributed according to the Generalized Pareto Distribution (GPD), which is characterized by two

19   parameters, the shape ξ and the scale σ. The GPD for exceedances $x - u$ of a random variable x reads as

20

$$G(x) = 1 - \left[1 + \xi\left(\frac{x - u}{\sigma}\right)\right]^{-\frac{1}{\xi}} \qquad (x > u, \xi \neq 0)\,, \qquad (2)$$

21

22   where u is the threshold. The choice of the threshold u is done in order to ensure that the model in (2) provides a

23   reasonable fit to exceedances of this threshold. The result for the two parameters shape ξ and scale σ depend on

24   the threshold u (Coles, 2001). The shape parameter ξ determines the tail behavior while the scale parameter σ

25   measures the variability. For a negative shape parameter, $\xi < 0$, the distribution is bounded (beta distribution), for

26   vanishing shape parameter, $\xi = 0$, the distribution is exponential, and for a positive shape parameter, $\xi > 0$, the

27   distribution has no upper bound (Pareto distribution).

28

29   In particular, for a negative shape parameters $\xi < 0$ the GPD has an upper bound

30

$$A_{max} = u - {}^{\sigma}\!/_{\xi} \qquad\qquad (3)$$

31

$$G(x) = 0 \qquad\qquad (x > A_{max}, \xi < 0\ )$$

32

33   where A_{max} is an absolute maximum (Lucarini et al., 2014). The choice of the optimal threshold for performing

34   statistical inference from a time series is crucial. A too large value for u would reduce the number of exceedances

35   to a few values, inflating the variance of the estimators and by consequence the analysis would unlikely yield any

36   useful results. On the other hand, a too small value for u would violate the asymptotic nature of the model, with

37   a possible biased estimation and wrong model selection (Coles, 2001).

38

39   The threshold selection is the first step in the application of POT approach, and the stability of the shape

Earth System
Dynamics

Discussions

1   parameters ξ and the scale parameters σ fitting the GPD is assessed with various thresholds. The threshold chosen

2   for each station is the lowest value which stabilizes the estimates shape parameters ξ and the modified scale

3   parameters σ* (see details later in Section 3.1). The shape ξ, the scale σ and the return levels are estimated using

4   the Maximum Likelihood Estimator (MLE) using the R software (R Development core team 2015), which also

5   provides an standard errors of estimates.

6

7   Multi-occurrence is an important characteristic of extreme climatic events and is referred to as clustering. These

8   clusters are consecutive occurrences of above threshold events. It is important to treat the clustered extremes to

9   achieve the independence assumption, which is crucial for the POT model, in order to apply MLE. We treated the

10   clusters using the concept of Extremal Index (EI) (see Newell, 1964, Loynes, 1965, O'Brien, 1974, Leadbetter,

11   1983, Smith, 1989, Davison and Smith, 1990). The Extremal Index θ measures the degree of clustering of

12   extremes. It ranges between 0 and 1, (θ = 0 means strong clustering, θ = 1 absence of clusters). Leadbetter

13   (1983) interprets 1/θ as the mean number of exceedances in a cluster.

14

15   The extremal index θ can be estimated in two separate ways. Here, we apply the 'intervals estimator' automatic

16   declustering by Ferro and Segers (2003). A distinctive property of this method is that it avoids the subjective

17   choice of cluster parameters. The main ingredient is an asymptotic result for times between threshold

18   exceedances. The exceedance times are split into two types, a set of vanishing intra-exceedance times within the

19   clusters, and an exponentially distributed set of inter-exceedance times between clusters. The method is iterative

20   starting with largest return times and stops when a limit for the inter-exceedance times is reached. The standard

21   errors of the estimated parameters is obtained by a bootstrap procedure. In this study, the extremal index value is

22   ≤ 0.5 in all the time series referring to the clusters.

23

24   The primary focus of the study is to estimate N - years return levels (RLs) x_N, which is exceeded on the time

25   scale of N years (Coles, 2001) and reads

26

27

$$x_N = u + \frac{\sigma}{\xi}\left[(Nn_y\zeta_u)^\xi - 1\right], \qquad\qquad (4)$$

28

29   where N represents the return period, n_y is the number of observations per year , ζ_u is the probability of an

30   individual observation exceeding the threshold u, the shape parameter is ξ and the scale parameter is σ.

31

32   **2.5. Bias Correction Method**

33
34   A simple bias correction is applied to each ERA Interim time series through a rescaling that adjust the first two

35   moments (mean and variance) to the sample moments calculated on the corresponding observations. Therefore,

36   the bias correction is applied to the entire time series and it is not tailored to the extreme events only. The bias

37   corrected ERA Interim time series x is expressed as

38

39

40

Earth System
Dynamics

Discussions

$$x = \bar{z} + \frac{y_{ERA} - \bar{y}}{\sigma_y} \cdot \sigma_z$$

1
2   (5)

3   where y_{ERA} is the ERA Interim time series, $\bar{y}$ and σ_y its mean and standard deviation, whereas $\bar{z}$ and σ_z are

4   the mean and standard deviation of the meteorological station temperatures. The bias corrected ERA Interim time

5   series shows better results compared to the original ERA Interim data. The comparison of extremes as detected in

6   the station observations, in the ERA Interim, and in the bias corrected ERA Interim time series is carried out in

7   Section 3.

8   **3. Results and Discussion**

9   **3.1 Threshold Selection**
10

11   The threshold selection is the first step in a POT analysis. It is essential to choose a threshold that is high enough

12   to be in the asymptotic limit of the distribution of exceedances, but low enough to have ample data for the fit. The

13   threshold selection is performed using diagnostic plots of the modified scale parameter σ* (σ* = σu – ξu) and the

14   shape parameter ξ of the observed, ERA Interim, the bias corrected ERA Interim T_{max}, and TW_{max} in all stations.

15   In GPD, the excesses above a high threshold have same shape but shifted scale. In order to deal with this problem

16   the modified scale σ* is used, because its estimate remains constant above a sufficiently high threshold

17   guaranteeing that the asymptotic properties are obeyed (Sacrrott and MacDonald, 2012).We observe both the

18   modified scale parameter and the shape parameter ξ stability plots carefully. The threshold u is selected as the

19   lowest value where the two parameters are invariant in order to reach the asymptotic limit (Coles, 2001 and

20   Furrer et al., 2010). Figure 2 shows the parameter stability plots of the station observed T_{max} for Karachi only, as

21   an example to explain the threshold selection procedure. We observe that the 90% quantile is an appropriate

22   threshold for all the station observed, the ERA Interim, the bias corrected ERA Interim T_{max}, and TW_{max}.

23

24   In addition to diagnostic plots of the modified scale parameter σ* and the shape parameter ξ, the mean residual

25   life plot is used to select the appropriate threshold for the POT analysis. The mean residual life plot is initiated by

26   Davison and Smith, (1990), according to them lowest value of the threshold should be selected when the

27   threshold based mean excesses are consistent. Hence, the threshold is selected when the plot is approximately

28   linear, like in case of Karachi the station observed T_{max} plot appears to be linear and stable at u = 36, indicating u

29   = 36 as the most suitable threshold for Karachi (Figure 3).

30   **3.2 GPD Fit**
31

32   The goodness of fit is evaluated by means of Quantile-Quantile (Q-Q) plots and hypothesis testing. The Q-Q plot

33   analysis is performed for the stations observed, the ERA Interim, the bias corrected ERA Interim daily T_{max} and

34   TW_{max}. The Q-Q plots of the observed T_{max} show that the GPD fits well in most of the stations. However, in a

35   few stations the empirical values show slight deviation from the modeled values like Jacobabad, Mohenjo-daro,

36   Padidan and Chhor. In spite of minor deviations at some stations, still most of the exceedances have a good fit

37   with the model. The Q-Q plots of the observed TW_{max} also show good GPD fits in all stations.

38

1   The Q-Q plots of the ERA Interim T_{max} indicates that the GPD fits are not good. The empirical values of the

2   higher quantiles are deviating from the theoretical quantiles in all stations. However, if the higher quantiles are

3   neglected, then the stations like Jacobabad, Mohenjo-daro, Rohri, Padidan, Nawabshah, Chhor, and Badin shows

4   that the exceedances fit very well. Likewise, the Q-Q plots of the ERA Interim TW_{max} do not show good fits with

5   the GPD model. The Q-Q plots of the bias corrected ERA Interim $T_{max,}$ and TW_{max} show better results than the

6   ERA Interim. We notice that the T_{max} of the ERA Interim and bias corrected ERA Interim fit better than the

7   TW_{max} if the higher quantiles are ignored.

8

9   In order to assess the goodness-of-fit, we apply the Kolmogorov-Smirnov (K-S) test and Anderson-Darling (A-D)

10 test to the data of meteorological stations, ERA Interim, bias corrected ERA Interim T_{max} and TW_{max}. The p-

11 values indicate a good performance of the fit procedure. Table 3 displays the results of the K-S and A-D statistics

12 of the T_{max} and TW_{max} in all the data sets.

13 **3.3 Parameter Estimates**
14

15 Here, we analyze the shape parameter ξ, the scale parameter σ, and threshold u for all considered datasets. The

16 standard errors of the shape ξ and the scale σ parameters are estimated using the Maximum Likelihood

17 Estimation (MLE), and given in Table 4. The spatial distribution of the shape parameter ξ and the scale parameter

18 σ of the GPD in Sindh are shown in Figure 4. The shape parameters ξ are all negative in all datasets at all

19 stations. This is hardly surprising, as meteorological and physical processes make sure that the temperature

20 cannot grow locally without control. Figure 4 displays the bias corrected ERA Interim results only. The observed

21 T_{max} shape parameters ξ are between -0.418 to -0.223, and for TW_{max} within -0.323 to -0.177. The bias corrected

22 ERA Interim T_{max} shape parameters ξ range from -0.305 to -0.002, and TW_{max} are between -0.18 to -0.01.

23

24 The scale parameters σ of the observed T_{max} are from 2.08 to 2.76, and the TW_{max} are in a range 1.86 to 2.76. In

25 the ERA Interim analysis, the scale parameter σ of T_{max} is within 1.00 - 1.95, and for TW_{max} within 0.74 -1.75.

26 We observe a difference in the scale parameters of both the observed, the ERA Interim T_{max} and TW_{max}. We find

27 that the scale parameters of the bias corrected ERA Interim data are much closer to those estimated for T_{max} and

28 TW_{max} using the station data. In the bias corrected ERA Interim T_{max} the scale parameters σ are between 1.50 -

29 2.75, while for TW_{max} are within a range 1.40 – 2.40 (Figure 4).

30 **3.4 Absolute Maxima**
31

32 Once the shape ξ, the scale σ, and the thresholds u are fixed, it is possible to compute the theoretical absolute

33 maxima using Eq. (3) (Section 2.4). Theoretical absolute maxima can be compared with the observed ones for

34 each station to better understand the signals of warming in Sindh. The daily maximum temperature T_{max} and the

35 maximum wet-bulb temperature TW_{max} (station data, the ERA Interim, and the bias corrected ERA Interim) have

36 negative shape parameter ξ in all stations. This means that according to Eq. (2) in section 2.4, the probability

37 distribution function (pdf) is bounded by the maximum values. These maximum values are the theoretical upper

38 limits predicted by the GPD fit. The analysis shows that the observed absolute maxima T_{max} and TW_{max} in all

39 stations of the three data sets are below the theoretical absolute maximum, as expected (Figure 5). This gives us

40 confidence on the quality of our fit. The following piece of information can also be derived. Assume that one

1   observes in the future an extreme event larger than the maximum inferred in the present dataset; this may suggest
2   some non-stationarity in the most recent portion of the dataset.

3   **3.5 Return Levels**
4
5   The return levels (RLs) are computed considering various return periods (2, 5, 10, 20, 50, 100-year). The return
6   level plots of the stations observed, the ERA Interim, the bias corrected ERA Interim daily maximum
7   temperature T_{max} and daily maximum wet–bulb temperature TW_{max} are displayed in Figures 6 and 7. The return
8   levels follow the north-south gradient of the climatic mean temperatures. The northern parts of the Sindh are
9   hotter than the southern parts. Therefore, different stations have different potential for maximum temperature
10 return levels. The stations located in the North are Jacobabad, Mohenjo-daro, Rohri, Padidan, and Nawabshah.
11 While Hyderabad, Chhor, Karachi, and Badin are sited in the South.
12
13 The 2, 5, 10, 20, 50, 100-year RLs estimated in Sindh for station observed T_{max} at time reach over 50°C in
14 Jacobabad, Mohenjo-daro, Padidan, Nawabshah, and over 45°C in Rohri, Hyderabad, Chhor, Karachi, Badin.
15 The ERA Interim T_{max} return levels are at least 3°C to 5°C lower in all stations. However, the ERA Interim T_{max}
16 captures the geographical variability of the field, but cannot estimate the correct magnitude of the events. For
17 example, in Badin the return level of the station T_{max} is 42°C in a 3-year return period, while the ERA Interim
18 show the same value of the return level in a 30-year return period (Figure 6).
19
20 The RLs of TW_{max} are over the 35°C in all meteorological stations. As for the ERA Interim RLs of TW_{max} are
21 greater than 30°C for all the stations except Karachi, which has RLs less than 30°C. Here, we see again that the
22 RLs of the ERA Interim TW_{max} are smaller than the RLs of station TW_{max}. For example, in Badin station, the RLs
23 of the station TW_{max} is 38°C in a 4-years return period whereas, the ERA Interim reaches the same RLs in a 15-
24 year return period (Figure 7).
25
26 It is important to underline that the bias between the station and the ERA Interim data is rather relevant when one
27 wishes to address the impact of hot climatic extremes to the active crop production in the region. The crops are
28 very sensitive to temperature variations, and even a rise of one degree Celsius can cause detrimental changes in
29 the phenological stages of the crops (Hatfield and Preuger, 2015). Every crop has a certain limit to tolerate the
30 temperature. When temperature exceeds this limit, the crop yield is drastically reduced. In summer, the
31 temperature and humidity increase to an extent that there are high chances of a rapid pests spread in the crops.
32 Sindh produces cotton, wheat, rice, mango, banana, and dates, so a correct estimate of temperature extremes is
33 very important in order to avoid the crops failure and the reproduction of pests. Therefore, we apply the standard
34 bias correction on the ERA Interim data to check the alterations in the return levels and return periods of T_{max} and
35 TW_{max}.
36
37 The bias corrected ERA Interim T_{max} and TW_{max}, show improvements in the return levels (RLs), along with a
38 good correspondence in each station. In a maximum temperature T_{max} analysis the RLs of the bias corrected ERA
39 Interim overlap the RLs of the station observations in a range 5-100 years, but do not overlap within a range 2-
40 5years, in the Nawabshah, Hyderabad, Karachi, and Badin. However, the rest of the stations show no overlaps of

Earth System
Dynamics
Discussions

1   the return levels in both the bias corrected ERA Interim and station observations. In a wet-bulb temperature
2   TW_{max} analysis, the RLs of the bias corrected ERA Interim overlap the RLs of the station observations in
3   Mohenjo-daro, Hyderabad, Chhor, and Badin at some intervals. While, no overlapping of the RLs is detected in
4   rest of the stations, while they differ at some intervals (Figures 6 and 7).
5
6   The 2, 5, 10, 20, 50, 100-year RLs of T_{max} for the bias corrected ERA Interim data are greater than 50°C in
7   Jacobabad, Mohenjo-daro, Padidan, Nawabshah, and greater than 45°C in Rohri, Hyderabad, Chhor, Karachi,
8   Badin. As for the TW_{max}, the 2, 5, 10, 20, 50, 100-year RLs of the bias corrected ERA Interim exceed 35°C in all
9   stations. Figures 6 and 7 show that the ERA Interim time series improves a lot after the bias correction, but the
10 two data sets still have some quantitative differences.
11
12 The extremes of daily maximum wet-bulb temperature TW_{max} are estimated as above the human survivability
13 threshold 35°C throughout the region, so the risk of hyperthermia is very high here. The human habitability in
14 such a warm region is already at risk. The most vulnerable people are those who are involve in the everyday
15 outdoor activities like farming, fishing, building construction, athletes, elderly and infants can have heat strokes,
16 dehydration etc. Therefore, an early warning system is necessary in Sindh, to avoid the crop failure, water
17 shortages and casualties due to the heat stress each year.
18
19 We also plot the station and bias corrected ERA Interim T_{max}, and TW_{max} return levels spatially for the 5, 10, 25
20 and 50-year return periods (Figures 8 and 9), as a detailed spatial overview of the temperature extremes in Sindh
21 might be of interest to the policy makers.

22 **4. Summary and Conclusion**
23
24 The main objective of this study is the assessment of the return levels of the extreme daily maximum
25 temperatures T_{max} and wet-bulb temperatures TW_{max} in Southern Pakistan (Sindh). In addition, the performance
26 of the ERA Interim TW_{max} is compared to the weather station TW_{max} to assess the ability to estimating
27 temperature extremes in Sindh. Moreover, a standard bias correction is applied to the ERA Interim data to
28 improve its performance in representing temperature extremes.
29
30 In summary, the Peak Over Threshold (POT) method is applied to the daily T_{max} and TW_{max} data of nine
31 observatories and to the corresponding nearest ERA Interim temperature data. Standard declustering technique is
32 applied to all time series to achieve the independence assumption of extremes. The 90% quantile is the
33 appropriate threshold choice for the weather stations, the ERA Interim and the bias corrected ERA Interim
34 maximum temperature and wet-bulb temperature. A Generalized Pareto Distribution (GPD) is fit to both T_{max} and
35 TW_{max} for all three datasets. The results show that the shape parameter ξ is negative for all stations. The scale
36 parameter σ estimated on weather station temperatures is much closer to the bias corrected ERA Interim
37 estimates than the original ERA Interim data ones. The theoretical absolute maxima of the time series are higher
38 than the observed absolute maxima in all stations. The Q-Q plots are used to assess the GPD fit, which results to

Earth System
Dynamics
Discussions

1 be acceptable for both T_{max} and TW_{max} station data as compared to the ERA Interim data. However, the bias

2 corrected ERA Interim shows improved GPD fits than ERA Interim.

3

4 Return levels (RLs) of T_{max} and TW_{max} are estimated for the 2, 5, 10, 25, 50, 100-year return periods in all

5 datasets. The RLs of T_{max} estimated using the meteorological station temperatures are greater than 50°C in

6 Jacobabad, Mohenjo-daro, Padidan, Nawabshah, and greater than 45°C in Rohri, Hyderabad, Chhor, Karachi and

7 Badin. While the RLs of TW_{max} in station data are larger than 35°C in the entire Sindh, when using ERA Interim

8 temperatures, they are estimated as greater than 45°C in Northern Sindh and greater than 40°C in southern Sindh.

9 The differences in the RLs using the two datasets are between 3°C and 5°C for both shorter and longer return

10 periods due to the minor variations in the shape and scale parameters. Although the ERA-Interim dataset does not

11 capture well the magnitude of the extremes, but it provides a good representation of their spatial fields.

12

13 A simple standard bias correction is applied to the ERA Interim to assess whether the return levels of extremes

14 are better predicted after the rescaling is applied. The bias corrected ERA Interim T_{max} and TW_{max} gives return

15 levels closer to the meteorological stations observed ones than the original ERA Interim return levels at all

16 stations. Although the bias corrected ERA Interim shows a good correspondence with the meteorological station

17 data, some differences remain.

18

19 This paper contains novel and beneficial information regarding the assessment of the temperature extremes (T_{max}

20 and TW_{max}) in Sindh, which would help the local administrations to prioritize the regions in terms of adaptations.

21 This research fills the gaps in the literature providing information on T_{max} and TW_{max} extremes in Sindh, which

22 would benefit both public and private stakeholders.

23

24 **Acknowledgements**

25

32 **References**

33
34 Acero, F. J., García, J. A., Gallego, M. C., Parey, S. and Dacunha-Castelle, D.: Trends in summer extreme
35 temperatures over the Iberian Peninsula using nonurban station data, J. Geophys. Res. Atmos.,
36 doi:10.1002/2013JD020590, 2014.
37
38 Bramati, M.C., Tarragoni, C., Davoli, L., Raffi, R., Extreme Rainfall in Coastal Metropolitan Areas of Central
39 Italy: Rome and Pescara case studies. *Geografia Fisica e Dinamica Quaternaria*, **37**, pp. 3-13, 2014.
40
41
42 Brunetti, M., Maugeri, M., Monti, F. and Nanni, T.: Temperature and precipitation variability in Italy in the last
43 two centuries from homogeneized instrumental time series, J. Climatol., 26(3), 345–381, doi:10.1002/joc.1251,
44 2006.
45

1   Burgueño, A., Lana, X. and Serra, C.: Significant hot and cold events at the Fabra Observatory, Barcelona (NE
2   Spain), Theor. Appl. Climatol., doi:10.1007/s007040200001, 2002.
3
4   Brunetti, M., Maugeri, M., Monti, F. and Nanni, T.: Temperature and precipitation variability in Italy in the last
5   two centuries from homogenized instrumental time series, J. Climatol., 26(3), 345–381, doi:10.1002/joc.1251,
6   2006.
7
8   Brown, S. J., Caesar, J. and Ferro, C. A. T.: Global changes in extreme daily temperature since 1950, J. Geophys.
9   Res. Atmos., doi:10.1029/2006JD008091, 2008.
10
11 Chaudhry, Q.-U.-Z. and Rasul, G.: AGRO-CLIMATIC CLASSIFICATION OF PAKISTAN, Q. Sci. Vis., 9(12),
12 3–4, 2004.
13
14 Chaudhry, Q. Z., Rasul, G., Kamal, A., Ahmad Mangrio, M. and Mahmood, S.: Government of Pakistan Ministry
15 of Climate Change Technical Report on Karachi Heat wave June 2015.
16
17 Choi, G., Collins, D., Ren, G., Trewin, B., Baldi, M., Fukuda, Y., Afzaal, M., Pianmana, T., Gomboluudev, P.,
18 Huong, P. T. T., Lias, N., Kwon, W.-T., Boo, K.-O., Cha, Y.-M. and Zhou, Y.: Changes in means and extreme
19 events of temperature and precipitation in the Asia-Pacific Network region, 1955-2007, Int. J. Climatol., 29(13),
20 1906–1925, doi:10.1002/joc.1979, 2009.
21
22 Christidis, N., Stott, P. A., Brown, S., Hegerl, G. C. and Caesar, J.: Detection of changes in temperature extremes
23 during the second half of the 20th century, Geophys. Res. Lett., doi:10.1029/2005GL023885, 2005.
24
25 Christidis, N., Stott, P. A., Zwiers, F. W., Shiogama, H. and Nozawa, T.: Probabilistic estimates of recent
26 changes in temperature: A multi-scale attribution analysis, Clim. Dyn., doi:10.1007/s00382-009-0615-7, 2010.
27
28 Coles, S.: An Introduction to Statistical Modeling of Extreme Values, Springer London, London., 2001.
29
30 Coelho, C. A. S., Ferro, C. A. T., Stephenson, D. B. and Steinskog, D. J.: Methods for Exploring Spatial and
31 Temporal Variability of Extreme Events in Climate Data, J. Clim., 21(10), 2072–2092,
32 doi:10.1175/2007JCLI1781.1, 2008.
33
34 Davison, A. C. and Smith, R. L.: Models for Exceedances over High Thresholds, J. R. Stat. Soc. Ser. B, 52(3),
35 393–442, doi:10.2307/2345667, 1990.
36
37 Dee, D. P., Uppala, S. M., Simmons, A. J., Berrisford, P., Poli, P., Kobayashi, S., Andrae, U., Balmaseda, M. A.,
38 Balsamo, G., Bauer, P., Bechtold, P., Beljaars, A. C. M., van de Berg, L., Bidlot, J., Bormann, N., Delsol, C.,
39 Dragani, R., Fuentes, M., Geer, A. J., Haimberger, L., Healy, S. B., Hersbach, H., Hólm, E. V., Isaksen, L.,
40 Kållberg, P., Köhler, M., Matricardi, M., Mcnally, A. P., Monge-Sanz, B. M., Morcrette, J. J., Park, B. K.,
41 Peubey, C., de Rosnay, P., Tavolato, C., Thépaut, J. N. and Vitart, F.: The ERA-Interim reanalysis: Configuration
42 and performance of the data assimilation system, Q. J. R. Meteorol. Soc., doi:10.1002/qj.828, 2011.
43
44 Deidda, R. and Puliga, M.: Sensitivity of goodness-of-fit statistics to rainfall data rounding off, Phys. Chem.
45 Earth, doi:10.1016/j.pce.2006.04.041, 2006.
46
47 Dickey, D. A. and Fuller, W. A.: Distribution of the Estimators for Autoregressive Time Series With a Unit Root,
48 J. Am. Stat. Assoc., 74(366), 427, doi:10.2307/2286348, 1979.
49
50 Faranda, D., Lucarini, V., Turchetti, G. and Vaienti, S.: Numerical Convergence of the Block-Maxima Approach
51 to the Generalized Extreme Value Distribution, J. Stat. Phys., doi:10.1007/s10955-011-0234-7, 2011.
52
53 Ferro, C. A. T. and Segers, J.: Inference for clusters of extreme values, J. R. Stat. Soc. B, 65(2), 545–556, 2003.
54
55 Frich, P., Alexander, L. V., Della-Marta, P., Gleason, B., Haylock, M., Tank Klein, A. M. G. and Peterson, T.:
56 Observed coherent changes in climatic extremes during the second half of the twentieth century, Clim. Res.,
57 doi:10.3354/cr019193, 2002.
58
59 Furrer, E., Katz, R., Walter, M. and Furrer, R.: Statistical modeling of hot spells and heat waves, Clim. Res.,
60 43(3), 191–205, doi:10.3354/cr00924, 2010.
61
62 Ghil, M., Yiou, P., Hallegatte, S., Malamud, B. D., Naveau, P., Soloviev, A., Friederichs, P., Keilis-Borok, V.,
63 Kondrashov, D., Kossobokov, V., Mestre, O., Nicolis, C., Rust, H. W., Shebalin, P., Vrac, M., Witt, A. and
64 Zaliapin, I.: Extreme events: Dynamics, statistics and prediction, Nonlinear Process. Geophys., doi:10.5194/npg-
65 18-295-2011, 2011.
66
67 Hatfield, J. L. and Prueger, J. H.: Temperature extremes: Effect on plant growth and development, Weather Clim.
68 Extrem., doi:10.1016/j.wace.2015.08.001, 2015.
69
70 Imtiaz S, Rehman, ZU. 2015. June 25. Death Toll From Heat Wave in Karachi, Pakistan, Hits 1,000. *The New
71 York Times* retrieved from http://www.nytimes.com/2015/06/26/world/asia/karachi-pakistan-heat-wave-
72 deaths.html?_r=0

Acknowledgements

Eidesstattliche Versicherung
Declaration on Oath

Hiermit erkläre ich an Eides statt, dass ich die vorliegende Dissertationsschrift selbst verfasst und keine anderen als die angegebenen Quellen und Hilfsmittel benutzt habe.

I hereby declare, on oath, that I have written the present dissertation by myself and have not used other than the acknowledged resources and aids.

Maida Zahid

Hamburg, den September, 26th, 2017